THE ROLE OF THE Wnt FAMILY OF SECRETED PROTEINS IN OVAL "STEM" CELL BASED LIVER REGENERATION

By

JENNIFER MARIE WILLIAMS

A DISSERTATION PRESENTED TO THE GRADUATE SCHOOL
OF THE UNIVERSITY OF FLORIDA IN PARTIAL FULFILLMENT
OF THE REQUIREMENTS FOR THE DEGREE OF
DOCTOR OF PHILOSOPHY

UNIVERSITY OF FLORIDA

2007

To the rock that steadies me, my husband Matthew.

ACKNOWLEDGMENTS

I thank my principle investigator Bryon E. Petersen for the scientific knowledge and ideals of perseverance that he has favored me. He has graciously humbled me and rewarded me when I was deserving. My mentor in college, Dr. Jerry Goldstein also provided me with the desire to understand the unknown and for that I am truly grateful. I would also like to thank the other members of my committee: drs. James M. Crawford, W. Stratford May, Jr., Naohiro Terada, and Barry J. Byrne for pushing me to evolve into the scientist I am now. Without their continued support and scientific dialogue I would not be prepared for the scientific world outside graduate school.

I cannot explain the importance of friends and family. Never once have my parents or family told me I could not achieve any goal toward which I set my mind. My lab mates and my dearest friends, Kara Hrdlicka, Lisa Stilling, and Emma Westermann-Clark, have seen me through thick and thin. Never have I been without a shoulder to cry on during the tough times or without a hand to squeeze during the exciting ones. For their time and devotion I can only send them smiles in return.

Lastly, I could never have survived the last few years without someone to maintain my sanity and keep me on track. My husband has given me everything I have ever needed and more. I love him and can never tell him enough how much he means to me.

TABLE OF CONTENTS

page

LIST OF TABLES

LIST OF FIGURES

LIST OF ABBREVIATIONS

2-AAF	2-acetoaminofluorene
AFP	α-fetoprotein
APS	Ammonium persulfate
bp	Base pair
CK	Cytokeratin
DAPM	Methylene dianaline
DNA	Deoxyribonucleic acid
ECM	Extracellular matrix
FBS	Fetal bovine serum
FRP	Frizzled Related Protein
Fzd	Frizzled
GFP	Green Fluorescent Protein
HGF	Hepatocyte Growth Factor
HSC	Hematopoietic stem cells
IHC	Immunohistochemistry
i.p.	Intraperitoneal
LRP	Low density lipoprotein receptor-Related Protein
NRL	Normal rat liver
nt	Nucleotide
OCT	Optimal cutting temperature
OLT	Orthotopic liver transplant
O/N	Overnight
PBS	Phosphate buffered saline

PCR	Polymerase chain reaction
PHx	Partial hepatectomy
RNA	Ribonucleic acid
RPM	Revolutions per minute
RT	Room temperature
rtPCR	reverse transcription PCR
RT-PCR	Real Time PCR
SCRsi	Scrambled shRNA
shRNA	small interfering RNA
shRNA	small hairpin RNA
TEMED	Tetramethylethylenediamine
TGF-α	Transforming Growth Factor α
TGF-β	Transforming Growth Factor β
Wnt1si	Wnt1 shRNA

Abstract of Dissertation Presented to the Graduate School
of the University of Florida in Partial Fulfillment of the
Requirements for the Degree of Doctor of Philosophy

THE ROLE OF THE Wnt FAMILY OF SECRETED PROTEINS IN
OVAL "STEM" CELL BASED LIVER REGENERATION

By

Jennifer M. Williams

December 2007

Chair: Bryon E. Petersen
Major: Medical Sciences--Molecular Cell Biology

The Wnt/β-catenin pathway has been shown to be essential in embryogenesis and has been implicated in carcinogenesis. The current study reports novel findings in the Wnt pathway during the rat liver oval "stem" cell induction protocol of 2-acetylaminofluorene (2AAF) and 70% partial hepatectomy (PHx). Western blot analyses, rt-PCR, RT-PCR, and immunohistochemistry (IHC) were utilized to analyze the involvement of the Wnt family in liver injury and oval cell activation.

It was found that Wnt-1, Wnt3, Wnt5a, Frizzled Related Protein 1, Frizzled 5 and Frizzled 7 proteins were predominantly localized in pericentral hepatocytes. Following oval cell proliferation, an increase in Wnt proteins in concordance with the increase in oval cell number was observed. Wnt1 levels message levels peaked during the peak in oval cell numbers, and Wnt1 protein levels as well as β-catenin protein levels peaked after the increase in oval cell numbers. IHC analysis of β-catenin demonstrated oval cells with nuclear translocation of β-catenin throughout the 2AAF/PHx protocol. Hepatic stem cells responded to Wnt3a in culture by exhibiting the same β-catenin translocation visualized by IHC.

Subsequent *in vivo* exposure to an shRNA construct directed toward Wnt1, inhibited the oval cell based liver regeneration. Without the Wnt1 signal oval cells were unable to differentiate

into hepatocytes, lost AFP expression, and underwent atypical ductular hyperplasia that exhibited epithelial metaplasia and mucin production. It is hypothesized that changes in the Wnt pathway during oval cell induction control liver stem cell differentiation through regulation of β-catenin levels, which is known to induce cell proliferation and target gene expression. Furthermore, changes in Wnt1 levels are required for the efficient regeneration of the liver by oval cells during massive hepatic injury.

CHAPTER 1
INTRODUCTION

Uncovering the Role of Wnt in Oval Cells: The discovery of stem cells has led to some of the greatest medical advances of the 20th century. Stem cells, whether adult or embryonic, have differentiation potentials that far exceed initial thought. Cells from practically any organ or tissue can be manipulated toward any cell lineage desired. One day in the not so far future, a simple blood draw could produce the cells needed to grow replacement organs. In conjunction with gene therapy, the therapeutic potential behind these observations is tremendous.

In order to unlock the true capabilities of an adult stem cell one must understand the cell's function in its site of origin. Recognizing an organ specific stem cell through histology and morphology has proven relatively easy; however, thoroughly characterizing the molecular makeup of the same cell has proven more difficult. The use of phenotypical markers has aided the characterization process, but the cellular variations present during routine cellular processes, chemical exposure, and other stresses have made this method of characterization imprecise and difficult to say the least.

Cell labeling techniques have advanced the study of cell differentiation fates, but again this technique has not always provided definitive results. In order to track the differentiation states of progenitors, these cells are frequently labeled with dyes. However, when the cell of interest has been labeled with a dye, after numerous cellular divisions the dye dilutes to undetectable levels. This ultimately makes the determination that a specific cell was directly derived from a distinct progenitor nearly impossible. Another labeling method entails the genetic modification of the cell of interest. The cells contain a gene encoding a fluorescent protein or other protein markers usually under the control of a viral promoter; however, these marker genes have frequently been found to have been silenced *in vivo*, thereby, effectively unlabeling the cell of interest and its

progeny. Although the techniques currently available for the classification of stem cells and their differentiation potentials are not perfect, they can provide a better understanding of stem cell morphology and function, but it is important to note that any observations made by removing a cell from is *in vivo* environment does not adequately describe the cell. Once removed for its site of origin the cell of interest has changed.

Ultimately, scientists must be able to define the characteristics of an organ specific stem/progenitor cell, isolate that cell, and demonstrate *in vivo,* the steps of differentiation which the stem cell undergoes. Once this pathway is clearly defined, the mechanisms controlling these pathways must be elucidated. A thorough understanding of the molecular signals that direct these cells can then be utilized therapeutically.

The identification of an adult liver "stem" cell, the oval cell, has created opportunities for alleviating the shortage of livers available for transplant as well designating a cell for use in gene therapy for the treatment of metabolic disorders. Molecular characterization of the oval cell population has been fruitful, but these cells have still not been completely classified. Oval cells have been manipulated both *in vitro* and *in vivo* toward numerous different cell types of various germ layers, thereby demonstrating their pluripotentiality. Although this is significant for future therapeutics, until the natural functions of oval cells within the liver are understood, the true potential of the oval cell will remain hidden.

This project was designed to further understand the signals that guide an oval cell's differentiation toward a hepatic lineage. Previous works had demonstrated the requirement of Wnt in normal liver development, as well as the role of β-catenin in regulation of liver growth and regeneration. The Wnt family is a known regulator of stem cells that guides self renewal and

differentiation, and, consequently, it was theorized that Wnt could possess some control over oval cell fate during stem cell based liver regeneration.

Through IHC, protein, and RNA analysis a link between the Wnt signaling pathway and oval cell based liver regeneration was established. Inhibition of Wnt1 *in vivo* resulted in an abnormal regenerative process, failure of the oval cells to transdifferentiate into hepatocytes, and extensive atypical ductular hyperplasia.

This project outlined the requirement of Wnt signaling for the differentiation of oval cells toward a hepatic lineage. Without exposure to Wnt, oval cells defaulted to a ductular epithelial state and failed to aid in the regenerative process. This study only begins to elucidate a better understanding of the role of certain signaling proteins in oval cell based regeneration. In addition, the current studies open the door to several other avenues for the classification of the liver stem cell's functions.

CHAPTER 2
BACKGROUND AND SIGNIFICANCE

2.1 The Liver

2.1.1 Anatomy of the Liver

2.1.1.1 Structure of the hepatic organ

In an adult human, the largest parenchymal organ, the liver, weighs approximately 1400 to 1600g. This represents approximately 2% of the total body weight. In the rat, the liver weighs 7 to 8g which accounts for a greater percent of the body weight (approximately 5%).[1] In the human, the liver is comprised of four lobes, whereas, the rat liver contains five lobes.[2]

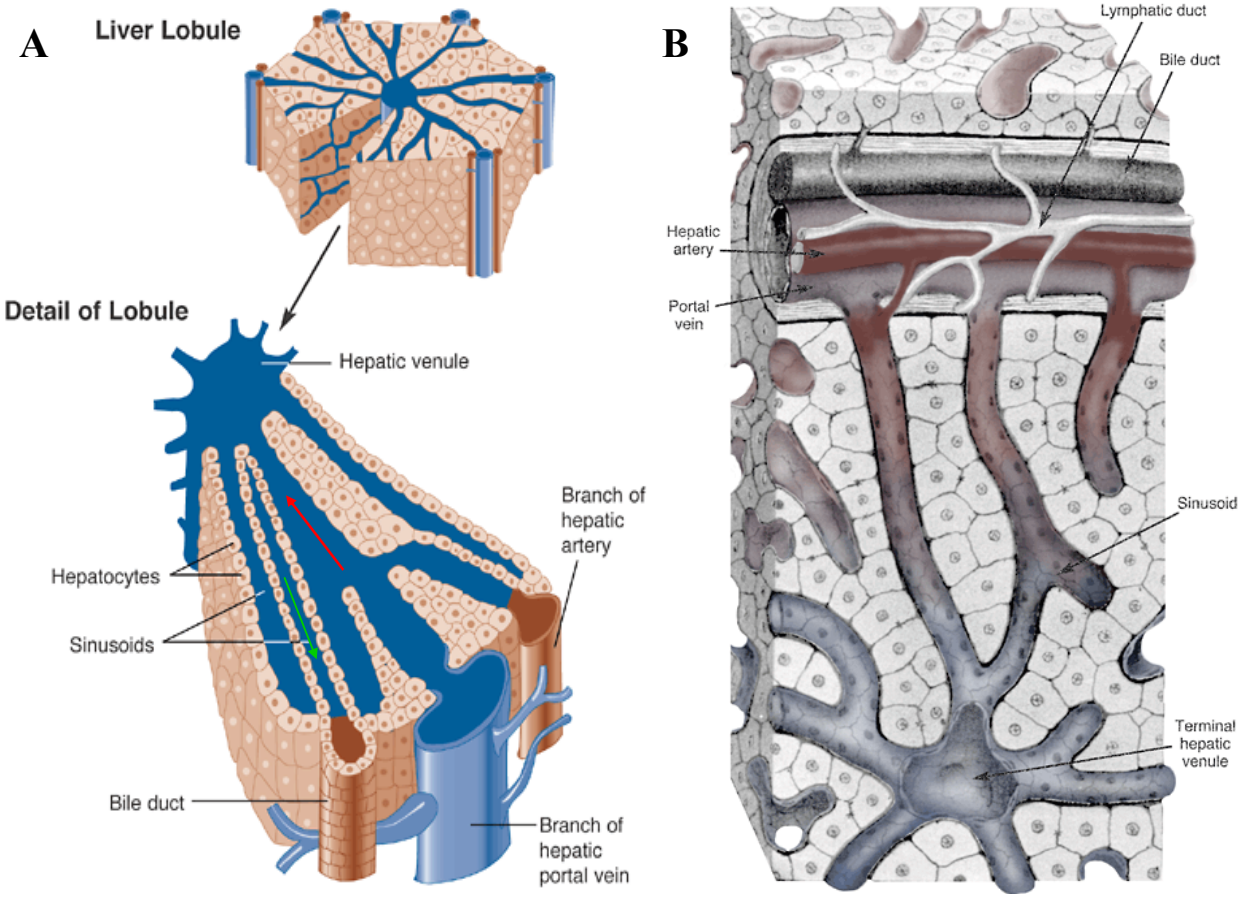

Figure 2-1. Diagrams of hepatic microarchitecture. A. Diagram of a "classic" hepatic lobule. Diagram of hepatic blood flow. *Red arrows* indicate blood flow and *green arrows* indicate the direction of bile flow. B. Hepatic microarchitecture.[3]

The liver has dual afferent blood supplies to maintain its highly vascular parenchyma. The portal vein supplies over 60% of the incoming blood.[1,2] The blood from the portal vein is venous and, therefore, oxygen poor. However, this venous supply is extremely nutrient rich due to the direct drainage of the intestinal epithelium. The hepatic artery provides the remaining 40% of oxygen rich blood to the liver.[1,2] In parallel to the blood vessels but opposing direction of flow, the biliary tree forms excretory ducts that transport bile into the duodenum. The portal vein, hepatic artery and biliary tree form a central vascular bundle termed the portal triad.[2]

2.1.1.2 Microarchitecture of the liver

The liver is divided into hepatic lobules surrounding terminal hepatic venules (central veins) and outlined by portal triads. A hexagonal column of hepatocytes arranged in cords radiating from the central vein toward the portal triad forms the structure of the hepatic lobule (Figure 2-1A).[4] Sinusoids composed of endothelial cells line each cord of hepatocytes and enclose the micro-vascular circulatory system of the liver.[2-4] Essentially, blood enters the liver through the portal triads and flows through the parenchyma in direct contact with each hepatocyte within a cord and ultimately drains into the central vein. Metabolites produced by the hepatocytes are excreted via the bile canaliculus into the canal of Hering, a terminal portion of the bile network within the portal triad.

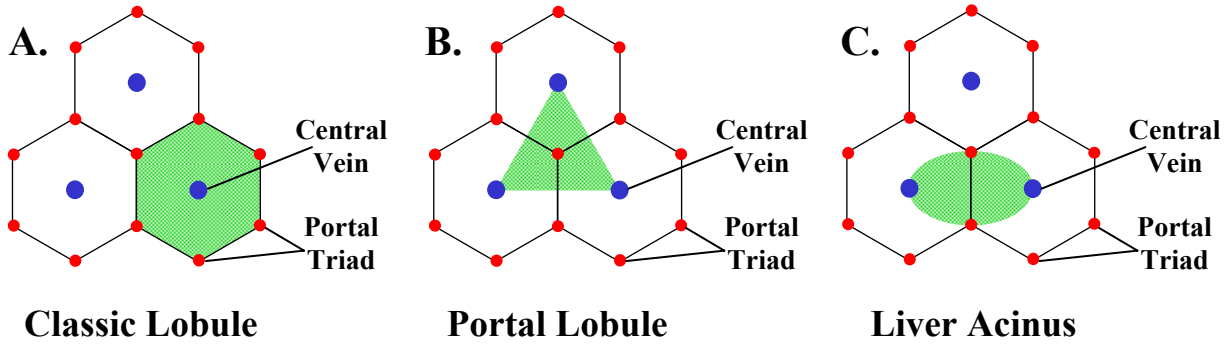

Figure 2-2. Diagrams of the various liver lobules. A. The "classic" lobule. B. The portal lobule. C. The functional unit known as the liver acinus.

The liver parenchyma consists of a various group of cell types including hepatocytes, bile ductular epithelial cells, fat containing stellate cells, sinusoidal and vascular endothelial cells, and liver specific macrophages known as Kupffer cells which rid the liver of debris and aged red blood cells. Hepatocytes encompass 90% of liver weight and carry out the biochemical functions of the liver as well as the production of bile.[2] Hepatocytes are polygonal in shape, large in size (30–40μm), and have a high abundance of smooth and rough endoplasmic reticulum.[4]

The architectural makeup of the liver can be described in three ways. The unit most frequently recognized by histology is the "classic" lobule (Figure 2-2A).[4] This lobule contains portal triad surrounding hepatic cords radiating out from a single central vein. The portal lobule depicts blood flow from one portal triad to its surrounding central veins (Figure 2-2B).[4] Lastly, although the "classic" lobule can be most easily recognized, the liver acinus is the functional unit of the liver (Figure 2-2C).[4]

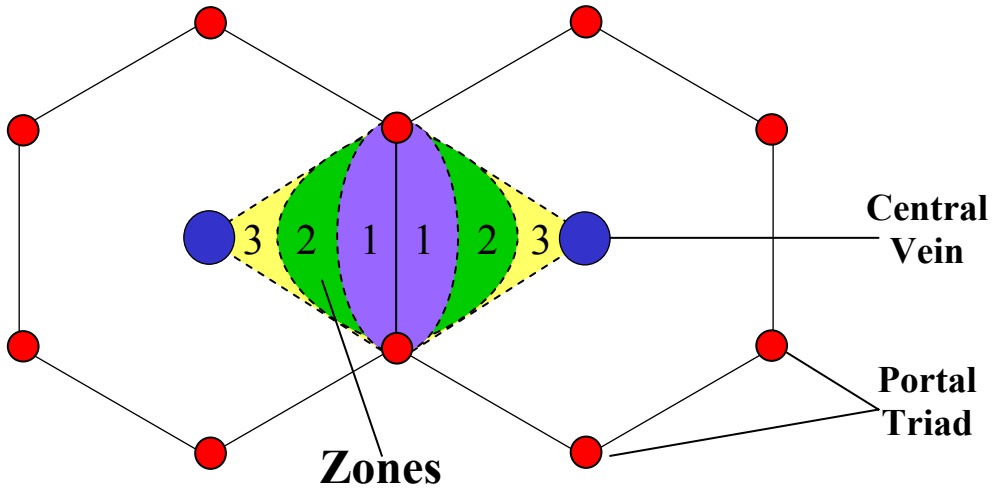

Figure 2-3. The liver acinus. Diagram of the liver acinus including the three zones radiating toward the central veins.

The hepatocytes that extend from one central vein to another can be divided into three zones. Zone 1 includes hepatocytes surrounding the portal triad and receives the greatest concentration of nutrients; Zone 2 is composed of inter-zonal hepatocytes; and Zone 3 consists of

poorly oxygenated hepatocytes nearest to the central vein (Figure 2-3.).[2,4] Within the liver acinus, blood flows through sinusoids from Zone 1 to Zone 3, and the bile moves from Zone 3 to Zone 1. Interestingly, hepatocytes within Zone 3 have an increased DNA content (4N to 16N), predominant bi-nucleation, large size and can undergo centrilobular necrosis. Conversely, hepatocytes within Zone 1 are smaller and usually single nucleated (2N).[5]

It should be noted that the macroarchitecture of the liver seen histologically does not truly elucidate the dynamic functional units of the liver.[6] The liver microarchitecture with regard to the organization of hepatic microcirculation, hepatic venous and arterial systems as well as the biliary tree are much more complex in their functional units than can adequately be described in two dimensions.[6] Three dimensional analysis of these systems via reconstructions complied from modern imaging techniques have begun to unlock the true physiologic hepatic lobule.[6]

2.1.2 Functions of the Liver

2.1.2.1 Homeostasis

As a large parenchymal organ in the body, the liver performs a multitude of functions. To control homeostasis of the body, liver metabolizes amino acids, lipids, and carbohydrates, and serum proteins. For example, by converting glucose into the storage form glycogen during carbohydrate metabolism, the liver effectively decreases blood level of glucose, and conversely, by metabolizing glycogen into glucose, the liver increases blood glucose levels. One of the main sites of glycogen storage is the liver. The liver also maintains the colloid osmotic pressure of the blood by producing the most abundant protein in the plasma, albumin. The liver also produces other important plasma proteins such as lipoproteins glycoproteins including prothrombin and fibrinogen, and the nonimmune α- and β-globulins. Additionally, the liver plays a role in amino acid metabolism through the deamination of amino acids and the formation of urea.[4]

2.1.2.2 Storage

The liver stores and converts several important vitamins taken up from the blood stream. Stellate cells stores vitamin A within their lipid pools. Without the liver, vitamin D metabolism would not be completed. Then the circulating form of vitamin D (25-hydroxycholecaliferol) would never be subsequently converted by the kidney to its active form which would result in rickets and failures in bone mineralization. Lastly, the liver utilizes vitamin K for the production of clotting factors. Decreases in hepatic vitamin K utilization have strong implications in clotting and/or bleeding disorders.[4]

Due to the liver's intricate vasculature and large size, a large volume of blood is located within it at any given time; thus making the liver the largest blood storage organ in the body. An adult human liver can hold about 1500ml of blood which equates to approximately 25% of cardiac output perminute.[4] Also the liver is the main site for iron storage. Homeostasis of blood iron levels depends directly on the ability of the liver to store and metabolize iron. Iron overload results in hemochromatosis which can result in severe liver damage.

2.1.2.3 Drug and toxin detoxification

Processing large volumes of blood induces the liver to function as a detoxifying organ. Liver enzymes, such as alcohol dehydrogenase (ADH), cytochrome-P (CYP) and isoforms of uridine diphosphoglucuronate glucuronosyltransferase (UGT) allow for the alteration of chemical composition of many xenobiotics and their subsequent removal.[2] The liver's conversion of nonhydrophilic drugs to a more water soluble form aids in their excretion by the kidneys.

2.1.2.4 Liver endocrine functions

Although the liver does not actively produce hormones, it modifies the actions of hormones released by other organs. The liver specifically modifies Vitamin D and thyroxin

through metabolism, but it releases growth hormone-releasing hormone to regulate the pituitary's release of growth hormone. Lastly, the liver is one of the main sites for insulin and glucagon degradation which further controls blood glucose levels.[2]

2.1.2.5 Liver exocrine function

The most important function of liver is the production of bile. Bile is important for intestinal absorption of nutrients and elimination of cholesterol. Bile, mostly comprised of conjugated bilirubin, is collected in the liver biliary tree, stored in the gall bladder and eventually drained into the duodenum to act as a detergent.[2]

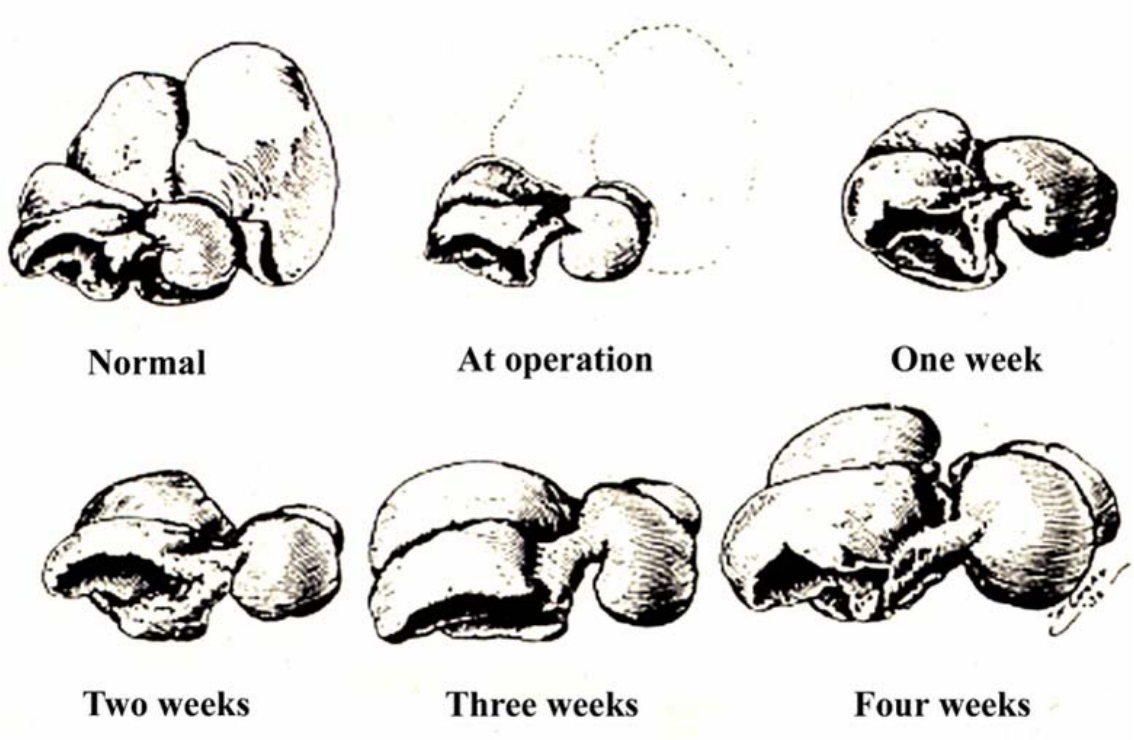

Figure 2-4. Graphic representation of growth of remaining three liver lobes after ⅔ partial hepatecomy in the rat. Compensatory hyperplasia results in the liver regaining original tissue mass in approximately 10 to 14 days.[6] ©1931 American Medical Association. All Rights Reserved.

2.1.3 Liver Regeneration

Compensatory hyperplasia of the liver, most often referred to as liver regeneration, takes place in response to mild to severe liver injury resulting from surgical resection of a portion of

the liver or exposure to destructive agents such as hepato-toxins or hepatotropic viruses. Under normal conditions, hepatocytes exhibit minimal replicative activity; only 1 in every 20,000 hepatocytes undergoes mitotic division at any one given time point, but hepatocyte division is the major driving force behind liver regeneration.[7] Figure 2-4 represents a drawing by Higgins and Anderson of the growth of the residual lobes of the liver after ⅔ partial hepatectomy.[8]

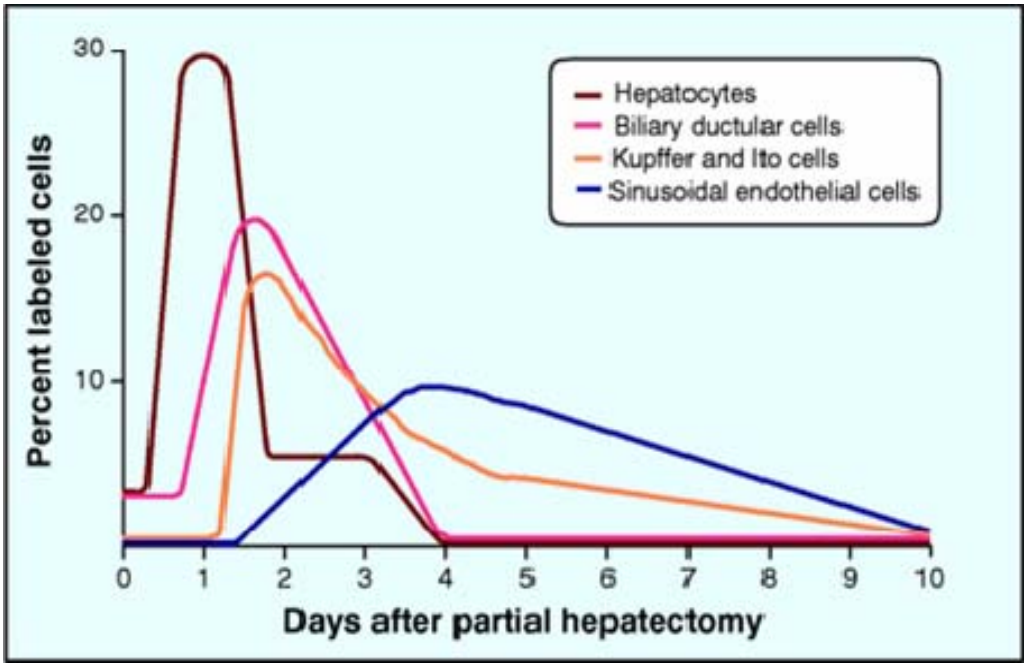

Figure 2-5. Graph of the amount of various resident hepatic cells within the cell cycle during the time following ⅔ partial hepatectomy. Hepatocytes represent the prolifereative driving source behind liver regeneration.[11] ©1997 AAAS. All Rights Reserved.

In the rat, hepatocytes move from the G0 resting phase of the cell cycle into G1, as mediated by the cyclin D1 pathway within 15 hours of partial hepatectomy (PHx).[9,10] Peri-portal hepatocytes are the first to undergo DNA synthesis and proliferation gradually spreads to include the hepatocytes located around the central vein.[7,11] A large peak of DNA synthesis is observed at about 24-hrs post PHx, and a second, yet smaller peak arises at 48 hrs. The smaller peak reflects DNA synthesis occurring in non-parenchymal cells (NPC) and pericentral hepatocytes. Unlike hepatocytes, which display a wave of DNA synthesis from periportal to pericentral, NPCs across

the lobule exhibit simultaneous DNA synthesis.[9] The original liver mass is usually restored within 10 days of the hepatectomy.[12] Figure 2-5 is a graph by Michalopoulos and DeFrances, 1997, representing the percent of individual hepatic cell types dividing at various time points during hepatic regeneration induced by ⅔ PHx.[13]

Several animal models of chemical hepatotoxicity have been developed to study the mechanisms regulating the proliferative response to liver injury. Among the most extensively utilized chemical agents are carbon tetrachloride (CCl_4), which causes necrosis of the centrilobular regions of the liver, and allyl alcohol (AA), which causes periportal necrosis.[14-17] In both models, regeneration of the necrotic region is mediated by proliferation of mature hepatocytes elsewhere in the liver lobule, and the oval cell response is not activated to a degree of importance, if at all.

The liver has an enormous capacity to regenerate, as demonstrated by the ⅔ partial hepatectomy model in rodents. In addition, the liver has a stem cell compartment acting as a backup regenerative system. Activation of the stem cell compartment only occurs when the hepatocytes are unable to divide, functionally compromised, or both. In stem cell-aided liver regeneration, progeny of the stem cells multiply in an amplification compartment composed of the hepatic oval cells. The origins of oval cells remain controversial and several key questions regarding the molecular cues that initiate oval cell proliferation and direct lineage specific differentiation still remain.

2.1.4 Hepatocyte Transplantation for the Treatment of Liver Diseases

The most commonly used and currently most effective treatment for the majority of liver diseases, metabolic and environmental, is the orthotopic liver transplant (OLT). Although extremely effective, OLT is expensive, the numbers of donors does not currently meet the need,

and the post surgical immune suppression has severe side effects. Other potential treatments are currently being developed including hepatocyte transplantation.

Due to the multiple functions of the hepatocyte, transplantation of "normal" hepatocytes in the case of inborn errors in metabolism seems logical. In addition to this, successes in "curing" animal models of these diseases have been intriguing, but in actuality, the clinical application of hepatocyte transplantation still lacks the advances seen in animal models. As of 2006, only 78 hepatocyte transplants have been performed worldwide.[18] Of those transplants, only twenty-one were performed in patients with inherited metabolic disorders.[18] Twenty patients suffered from chronic liver diseases, and the remaining transplants were delivered to acute liver failure patients.[18] The history of hepatocyte transplantation gives insight into the struggles seen in the clinical application of this seemingly simple solution to the worldwide epidemic of liver diseases.

In 1976, Matas *et al.* reported that a portal infusion of hepatocytes resulted in the reduction of plasma bilirubin levels in the rat Crigler-Nijjar model (the Gunn rat).[19] The success of this rat model promoted hope for the future of treatments in patients with inherited and acquired metabolic disorders and liver diseases. The first human trial of hepatocyte transplantation was not achieved until 1992 when Mito *et al*. performed a partial hepatectomy on a series of patients with chronic cirrhotic liver failure.[20] After isolation of hepatocytes from the resected liver, they were autologously implanted via intrasplenic injection. Transplanted, labeled cells were present in the spleen up to six months post transplant, however, the only clinical relevance of these transplants was the demonstration of engraftment.[20]

After successful decreases in serum cholesterol in the Watanabe Heritable Hyperlipidemic rabbit were obtained following transplantation of genetically modified hepatocytes, the first

human inborn error in metabolism was chosen for human trials.[21] Five patients with homozygous familial hypercholesterolemia underwent left lateral segment resection. Hepatocytes were isolated and transduced with the LDL receptor and reimplanted via the liver portal vein three days post resection.[21] This trial demonstrated safety from tumor and infection with over a two year follow up. Nonetheless, the less than 5% transgene expression four months post transplantation ended further hepatocyte transduction and implantation therapy.[18]

Conversely, successful treatment for inherited metabolic disorders has been achieved. Intraportal transplantation of allogeneic mature hepatocytes into four children with Crigler-Nijjar Syndrome type 1 has reproducibly reduced serum billirubin levels by 30 to 50% for greater than three years.[22-25] Of the sixteen humans receiving allogeneic hepatocyte transplants, most saw a decrease in the serum indicators of their diseases, however, the decreases were not significant to prevent orthotopic liver transplantation (OLT).[18] Also the level of donor cell engraftment varied drastically. This factor, in conjunction with the efficacy of whole organ transplant, has inhibited the advances in the treatment of metabolic liver diseases by somatic cell therapy.[18]

Chronic liver disease and acute liver failure present an alternative use for hepatocyte transplantation. Ten patients with chronic liver disease receiving autologous hepatocyte transplantation had hepatocytes present at the injection site (the spleen) up to six months post transplant, but encephalopathy resolution (a clinical indicator of hepatic disease regression) was not attributed to the transplants.[20] Of the seven adults receiving allotransplants, only one recipient's liver demonstrated histologic evidence of hepatocytes forming cord like structures, and only one showed any significant clinical benefit but still underwent OLT.[18] Interestingly, two of three pediatric patients who received a single allotransplant of hepatocytes to treat chronic liver failure fully recovered and the third was successfully bridged to OLT.[26,27]

Acute liver failure has by far had the most patients receiving hepatocyte transplantations, but out of thirty-seven patients treated, only two children and four adults had achieved full recovery with hepatocyte transplant alone. The remainder exhibited varying levels of metabolic improvement as measured by improved encephalopathy and decreased ammonia levels. However, in these cases hepatocyte transplant only functioned as a bridge to OLT.[18]

As seen in hepatocyte transplantation, the possibility of curing human metabolic diseases with somatic cell therapy has great potential. Nonetheless, the current treatment strategies have not proven as effective as the animal models for the same diseases. Furthermore, availability of donor hepatocytes is extremely limited. This fact, compounded by the lack of significant success with autologous cell manipulation and reimplantation, has severely inhibited the current treatment strategies of somatic cell therapy for metabolic diseases. These difficulties have led researchers to determine alternative treatment strategies which might utilize different cell populations.

2.1.5 Hepatocellular and Cholangiocellular Carcinomas

Despite extensive research into its treatment and prevention, HCC remains one of the most frequent malignant diseases worldwide. It is the 4th most common cancer comprising 5.4% of all new cases, and over 437,000 new cases are reported each year.[28] Although rates are much lower in the Northern Hemisphere, the disease is endemic in China, Taiwan, Korea, and Sub-Saharan Africa. This is most likely due in part to the extensive levels of aflatoxin exposure in this region of the world, as well as the endemic rates of viral hepatitis.[29] In these countries, HCC leads the list of causes of death due to a devastating average 5-year survival rate of less than 3%.[29]

Although less prevalent than HCC, cholangiocarcinoma (CCC) accounts for 3% of all gastrointestinal cancers worldwide.[30] In the US alone, approximately 5000 new cases are reported each year. There has also been a three-fold increase in the number of CCC cases within

the US between 1975 and 1999 with no apparent cause.[30] As with HCC, the survival rate of CCC is devastatingly small with a 5-year survival rate of <5% for intrahepatic CCC and 10-15% for extrahepatic CCC.[30]

Cellular morphology of CCC differs from HCC in that the tumor cells are most often arranged in tubules and gland like structures; whereas, HCC cells tends to display a more trabecular or pseudoglandular morphology.[30] Also CCC tends to display a fibrous stroma that HCC lacks.[30] Important to this research, CCC frequently contains mucin positive cells and/or glandular lumens.[30] A more thorough understanding of the cellular origins of HCC and CCC could provide more avenues of attack in the treatment of these endemic diseases while increasing the number of strategies that exist for hepatic cancer prevention.

2.2 Stem Cells and Their Therapeutic Potential

Almost one hundred years ago, Alexander Maximov theorized that within the peripheral blood lymphocytes there exists a population of common circulating stem cells (*gemeinsame Stammzellen*) that possessed pluripotency or could regain this potential.[31] Maximov was the first to believe in the capacity of adult cells to differentiate into one of many cell types. Unbeknownst to Maximov, it would take almost fifty years before his theories could be put into clinical practice, and another forty before a single cell was shown to repopulate bone marrow long term.[32,33] Incidentally, his theories are the basis for the current research boom in the field of somatic cell therapy. The progress therein has the potential to answer three major questions: i) What are the differential and self-renewal capabilities of the various types of somatic cells within the body? ii) Are end organ "stem cells" truly lineage committed? And iii) Can stem cells be utilized to treat cancer, autoimmune disorders, and aberrant genetics in an organ specific manner? Each of these poignant questions has opened a door within the field of medicine currently classified as "Somatic Cell Therapy". Although somatic cell therapy currently has little

clinical utilization aside from bone marrow transplants, somatic cell therapy has limitless potential for the treatment of diseases when utilized in conjunction with gene therapy.

2.2.1 Pluripotenitality of Stem Cells

Stem cells are defined as cells that have the capacity for self renewal and are multipotent, meaning they have the ability to differentiate into cells of various germ layers. Stem cells can be found within the adult somatic tissue as well as the embryo. At this time, the only truly totipotent cell in existence is found in the fertilized egg although current research has revealed the truly multipotent nature of both the adult and embryonic stem cells. However, the true differentiation capacity of these cells has not been fully recognized.

2.2.1.1 Embryonic stem cells

The concept of cell differentiation has been in existence since the 1850's, well before Pappenheim first described the premise of the stem cell in 1919.[34] However, it wasn't until the early 1980's that the clonogenicity and totipotential nature of the embryonic stem cell was finally elucidated.[35]

Murine embryonic stem cells were discovered over twenty years ago. This breakthrough in cell biology enabled a revolution in experimental medicine by establishing an *in vitro* model for early mammalian development, as well as a new source of cells for replacement therapies. Embryonic stem (ES) cells are pluripotent cells derived from the inner cell mass of blastocyst stage embryos.[36-38] ES cells have been manipulated in culture and *in vivo* via directed differentiation into each of the three germ cell layers of ectoderm, mesoderm, and endoderm.[37,39] Specifically, ES cells can be easily directed toward mesoderm specific cell types such as hematopoetic,[40-43] hemangioblast,[44-47] vascular,[48-51] cardiac,[52-54] skeletal muscle, chondrogenic, osteogenic, and adipogenic lineages.[55-58] With more effort, endodermal lineages, most specifically of pancreatic and hepatic origin, can be developed.[59-61] Lastly, the neuronal

differentiation of ES cells has provided a vast amount of research that some suggest indicates that a ES cells may be the revolutionary treatment needed for diseases such as Alzheimer's and Parkinson's.[62] Much research has gone into the pluripotential nature of embryonic stem cells, however, with the current ethical issues and evidence of teratoma formation, use of these cells for somatic cell therapy has many hurdles to overcome before the advantages of this cell type can come to clinical fruition.

2.2.1.2 Adult stem cells

In recent years there has been an increasing body of evidence that adult stem cells have a far greater degree of plasticity than once thought. Bone marrow derived stem cells have been found to naturally produce (or can be manipulated towards producing) practically all endothelial, mesenchymal and epithelial lineages found in the body.[63-65] Neuronal stem cells have been shown to be capable of differentiating into a hematopoietic line and then back to a neuronal lineage.[66] In addition, stem cells isolated from the brain have been shown to generate an entire mammalian organism, more specifically a mouse.[67] Although these studies have only been conducted in rodent models, they do suggest that adult mammalian stem cells may be utilized to treat cellular dysfunction within any organ system of the body. Theise *et al*. (2000) and Alison *et al*. (2000) reported that human adult bone marrow stem cells could differentiate into mature hepatocytes, thereby providing the first link from animal studies to human studies and proof of concept.[68-70] This data has the potential to develop into clinical applications within the very near future.

Over one hundred years after the conception of the "stem cell", the first single cell transplant to successfully rescue a lethally irradiated mouse was published. To address the pluripotentiality of the adult stem cells, specifically the hematopoietic stem cells (HSC), Krause *et al*. performed a transplant of single cell HSC combined with short term repopulating cells. The

single cell transplanted was a lineage negative, PKH26 labeled cell transplanted into lethally irradiated mice.[71] These cells demonstrated multi-lineage engraftment as seen by donor cells present that had differentiated into epithelial cells of the lung alveoli, GI tract, cholangiocytes and hair follicles eleven months post transplant.[71] However, the technique used for this and other similar experiments was a very simple feet up or feet down (animals either lived or died) and, thus, the extension of single cell transplantation to human clinical trials has been and will be very nearly impossible.

Bone marrow stem cells have also been shown to posses the ability to differentiate into liver, intestine, skin, skeletal muscle, heart muscle, pancreas, and central nervous system both in mouse models and human recipients of bone marrow or organ transplants.[69,72-74] Mesenchymal stem cells (MSC) from the bone marrow also exhibit a similar pluripotentiality.[75] Bone marrow stem cells (HSC or MSC) have been shown to give rise to endothelial cells of the vascular system and muscle as well as hepatocytes *in vivo*.[76] In addition, bone marrow stem cells have been shown to participate in neural development and vice versa.[76-78] Stem cells *in vitro* have have been shown to produce bone, connective tissue, and cartilage.[76-78] Lastly, neural stem cells from the adult mouse brain can contribute to the formation of chimeric chick and mouse embryos, and give rise to cells of all germ layers.[67] Other adult stem cells are currently being evaluated for their pluripotential nature, but none to date have been as successful as the HSC. Results from these studies demonstrate that adult stem cells have a very broad developmental and differentiation capacity.

2.2.2 Stem Cell Therapeutics

Clinical uses of stem cells for the repair of tissues such as heart and nervous system have been attempted with clinical trials.[79,80] Transplantation of stem cells into the heart after myocardial infarction has improved revascularization and has aided in healing; however, the

clinical trials have failed to demonstrate that the cells have truly differentiated into cardiac myocytes.[81] As with other somatic cell therapies, clinical relevance of these procedures has yet to be demonstrated even though success has again been seen in animal models.

Another avenue for the clinical use of stem cells presents itself with the advent of bioengineered organs and/or tissues. The development of tissue scaffolds for the seeding of stem cells has immense potential, but until recently the clinical applications of these scaffolds have been limited. The most clinically relevant engineered tissue has been cartilage.[82] The injection of tissue engineered cartilage into osteoarthritic as well as nonarthritic knees and other joints been reported to have greatly improved joint stability and motion.[83] However, further long-term studies must be made to determine the stability and long term effects of these grafts.[83] The growth of autologous cells on decellularized human heart valves and subsequent implantation of these valves has also been clinically worthwhile.[84] Another engineered tissue that had been evaluated in a clinical study was the bladder. Here, patients received bladders engineered with autologous urothelial and muscle cells.[85] Up to five years post implantation these patients demonstrated clinical benefit from the implanted tissue.[85] The successes seen with bladders, heart valves and cartilage demonstrate the endless possibilities for the clinical use of stem cells.

The combination of tissue engineering in conjunction with autologous stem cells could revolutionize the organ transplant field. However, the ability to grow a patient another kidney from a stem cell isolated from their blood is still a dream that is yet to be fully realized. Someday, adult and/or embryonic stem cells may be used in a variety of ways for the treatment of different human diseases. Nevertheless, until the scientific community is able to reproduce successes seen in animal models, the huge clinical potential of the stem cell will remain locked within the Petri dish.

2.3 Liver Oval "Stem" Cell

2.3.1 Oval Cell Biology

2.3.1.1 Hepatic oval cell compartment

There is a strong interest in characterizing hepatic stem cells with respect to their origin, mechanism of activation, and their final lineage destination. Oval cells are the primary candidates for the title of liver stem cell. Adequate data has been gathered demonstrating oval cells existence within the regenerating liver, but their place of origin and their role in liver development, regeneration, and carcinogenesis remains enigmatic. Oval cells dramatically increase in number when hepatocyte proliferation is suppressed. 2-Acetoaminofluorene (2-AAF) given prior to hepatic injury induced by ⅔ partial hepatectomy (PHx) results in suppression of hepatocyte proliferation through inhibition of Cyclin D as well as DNA adduct formation.[86] Oval cells of undetermined origin then arise in the portal zones of the liver. Morphologically, oval cells are small in size (approximately 10μm), with a large nuclear to cytoplasmic ratio, and contain an oval shaped nucleus, hence the name "oval cell" (Figure 2-6).[5,87]

Figure 2-7 shows the oval cell migration and infiltration of the liver during the 2AAF/PHx protocol. Beginning about 3 days after PHx, oval cells are visible within the portal region of the liver. They proliferate and peak in number 9 days post PHX. They then differentiate into small, basophilic hepatocytes and eventually mature hepatocytes. After 21 days, little evidence of oval cell infiltration remains and hepatic architecture has returned to normal.

Oval cells have similarities to bile ductular epithelial cells in their distinct isoenzyme profiles, expressing certain cytokeratins (e.g. CK-19), gamma-glutamyl transpeptidase (γGT), and may also express high levels of alpha-fetoprotein (AFP).[88,89] Several monoclonal antibodies including A6 for mouse and OV6, OC.2, and BD1 for rat have been developed to aid in their identification and characterization within various species including humans.[88-102]

Within the rat model, Evarts *et al.* (1987 and 1989) revealed extensive activation of the oval cell compartment within the 2-AAF/PHx model, a variant of the Solt-Farber protocol.[103,104] In additional studies, the same investigators illustrated that proliferation of oval cells and their subsequent differentiation into hepatocytes during the early stages of carcinogenesis were closely associated with an activation of stellate cells. It was then suggested that perisinusoidal stellate cells may regulate the developmental fate of the progenitor cells, either directly by secreting growth factors, such as hepatocyte growth factor (HGF) and transforming growth factors alpha (TGF-α) and beta (TGF-β), or indirectly via effects of extracellular matrix (ECM) components induced by urokinase up-regulation.[105] Progenitor cell proliferation and differentiation may also be regulated by autocrine production of TGF-β, acidic fibroblast growth factor, and insulin-like growth factor II, which are factors that oval cells have been shown to produce.[5] Hence, hepatic injury-induced changes in cytokines and growth factors appear to modulate *in situ* oval cell proliferation/differentiation within the liver. Further study of the growth factors, such as Wnt, that are involved in these processes will lead to great advances in liver therapeutics.

Oval cells in the liver represent an alternative source of proliferating cells in the regenerating liver. Proliferating oval cells in both the rat and murine models appear to radiate from the periportal region, forming primitive ductular structures with poorly defined lumena.[106] The origin of oval cells remains unclear. Due to their involvement in periportal repair, some data suggests that oval cells exist in very small numbers in the periportal region of the liver lobule, and that they emerge from this niche in response to severe hepatic injury.[107,108] Though oval cells do not normally participate in the regenerative response to PHx or CCl_4 injury, they can be induced to do so through suppressing mature hepatocyte proliferation. Administration of 2-AAF prior to and during hepatic injury induced by PHx or CCl_4, blocks the proliferation of

hepatocytes by interfering with their ability to divide. As with allyl alcohol induced injury, oval cell proliferation in these models begins in the periportal region before arborizing into the mid-zone as regeneration progresses. Oval cell proliferation can thus be stimulated in these otherwise non-oval cell aided regenerating models.[109]

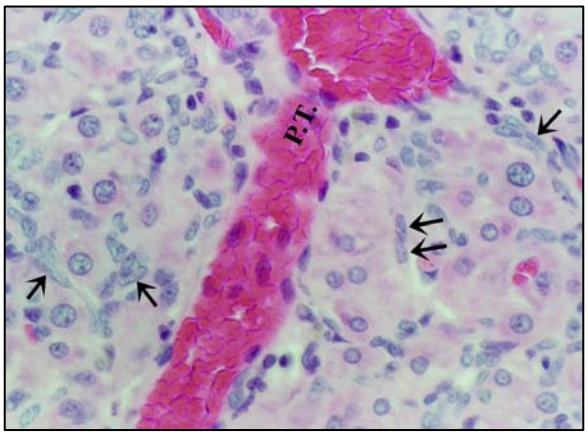

Figure 2-6. H and E of rat liver from day 11 of the 2-AAF/CCl_4 protocol. The small oval cells (arrows) are situated between the larger hepatocytes surrounding a portal triad (P.T.). Magnification 20X.

Lemire and Fausto (1991) showed that a very small number of cells localized in the canals of Hering of adult normal rat liver expressed the fetal form of AFP mRNA, suggesting that this may be the compartment where unactive oval cells reside.[110] Conversely, in 1992 Marceau *et al.* suggested that bile ductular cells expressing the fetal form of AFP in the adult liver are unlikely to be the putative stem cells, because they lacked other markers stem cell markers, and in contrast to hepatoblasts, they do not react with the monoclonal antibody BPC5.[111]

Petersen *et. al* exposed rats to methylene dianaline (DAPM) 24 hrs prior to hepatic damage (2-AAF/hepatic injury, PHx or CCl_4).[112] Under these circumstances the bile ductular epithelium was destroyed and the oval cell response was severely inhibited.[112] This study was the first to elucidate a direct association between the requirement of an intact bile ductular epithelium and the ability to mount an oval cell response. This data, however, does not prove that oval cells arise

from bile ductular cells because the DAPM could have elicited either a direct or indirect toxic effect upon the oval cells, which may have resulted in the inhibition of their activation. This study does support the idea that oval cells arise from the periportal zone, specifically from the canals of Hering.[112]

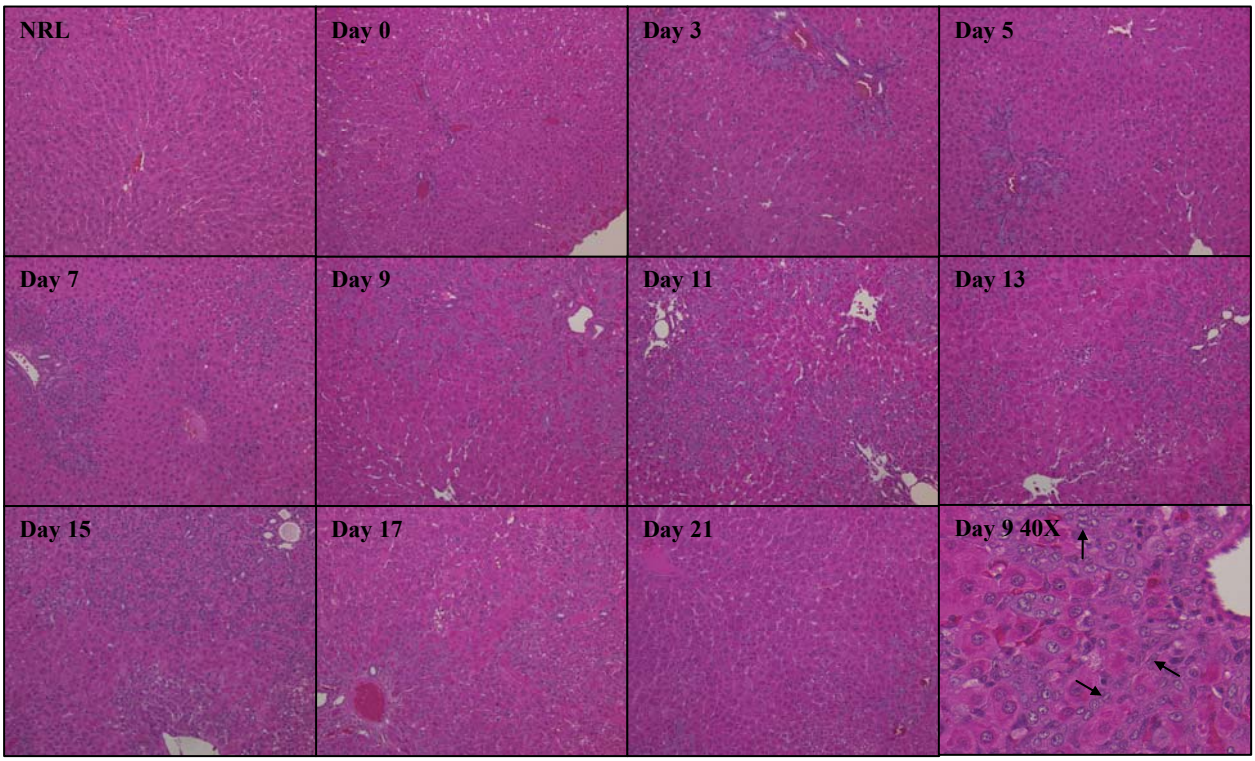

Figure 2-7. H and E of livers from the 2AAF/PHx protocol. Oval cell infiltration can be visualized across the 2AAF/PHx time course. Oval cells appear within portal regions of the liver rapidly following PHx. Peak oval cell production occurs after 9 days. Arrows within the 40 X magnification of Day 9 indicate the oval cells migrating toward the central vein. 13 days post PHx small, basophilic hepatocytes emerge as the oval cells differentiate. After 21 days the hepatic microarchitecture has returned to normal. Magnification 20X.

Interestingly, Petersen *et. al* has also shown that a percentage of oval cells may actually arise from an extra-hepatic source within the bone marrow.[65] Several other investigators have confirmed that bone marrow derived cells possess the ability to produce functioning hepatocytes and bile ductular cells. [69,70,113]These recent findings have clouded the clarity as to the origin of oval cells. Although numerous studies suggest that the oval cells reside somewhere within the

hepatic architecture in close association with bile duct epithelium, the exact oval cell niche has yet to be discovered.

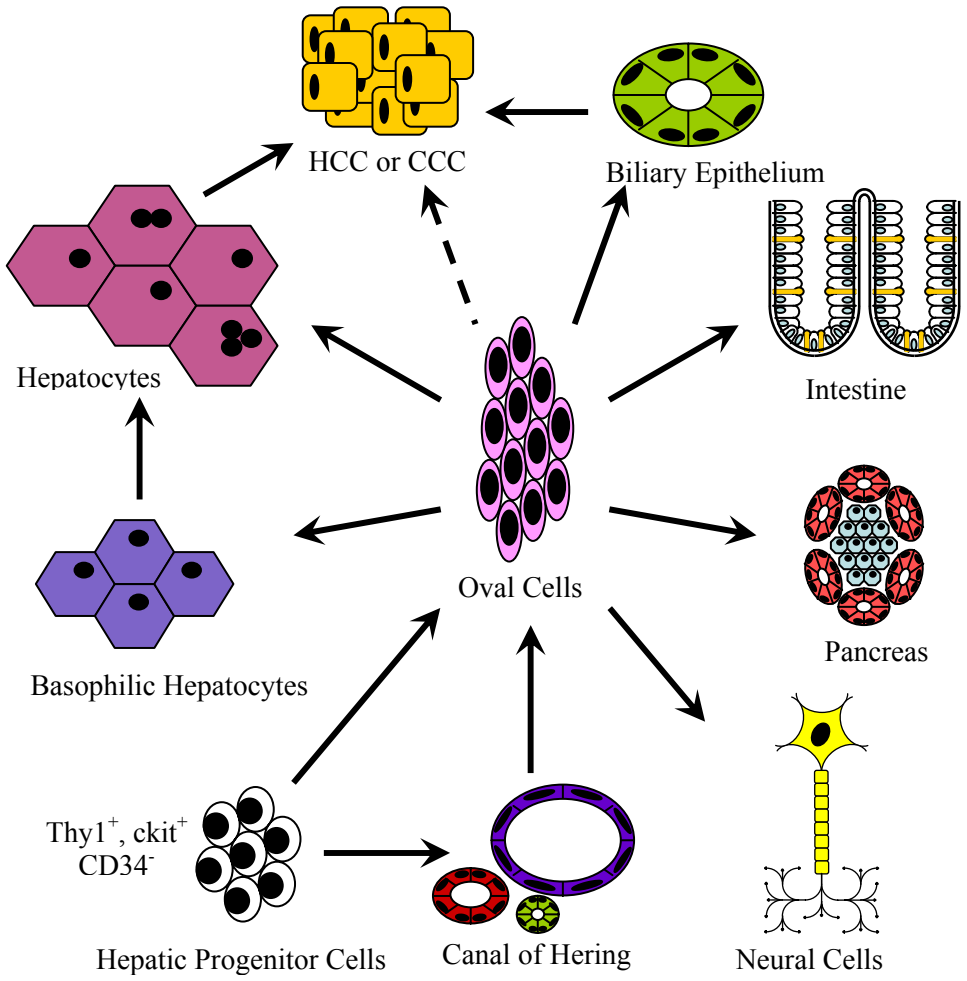

Figure 2-8. Drawing of potential end points of oval cell differentiation. Hepatic progenitors may reside in an extrahepatic site or within the Canal of Hering in the portal regions. Oval cells can differentiate into cells of hepatic, pancreatic, intestinal, and neuronal lineages and they have been implicated in hepatic cancers.

2.3.1.2 Oval cell plasticity

Figure 2-8 represents a schematic diagram of the endpoints and potential endpoints of oval cells according to a review by Lowes et al (2003) and work by Deng *et. al*.[114,115] The hypothesis that oval cells differentiate into hepatocytes is certainly not a novel idea, having been proposed as early as 1937 by Kinosita *et al*.[116] Through the years several investigators have provided

evidence to substantiate this thought to varying degrees.[117-121] The unpredictable success of these earlier studies in demonstrating oval cells differentiating into hepatocytes and bile ductular cells results from the complex problems posed by both the heterogeneous starting population of oval cells used in transplantation studies together with kinetic complexities inherent with tracing tagged DNA. Additionally, the limited types of reagents utilized by these earlier studies may have affected the results obtained. However, it is generally accepted that oval cells possess the ability to become both hepatocytes and bile ductular cells.

Scientists have found that HSCs obtained from adult peripheral blood retain a tremendous developmental "plasticity". Environment has become a key factor in determining the developmental proclivity of a stem cell. HSCs have been shown to give rise to the oval cells and within the liver, oval cells retain many hematopoietic stem cell markers including Sca-1 (mouse) and Thy-1 (rat) but gain expression of liver specific markers such as AFP.[77,88,89,122] Taken together these data suggest that either these HSCs and oval cells share a common developmental origin or they are both derived directly from the same stem cell.

Regardless of origin, all stem cells execute their developmental program by regulating gene expression. Determining which signals internal or external that induce differentiation, maintenance of pluripotentiality, or self renewal could prove very therapeutically relevant. Understanding both an oval cell's potential plasticity as well as the control of that plasticity will lead to a better understanding of the biology of oval cell as a whole.

2.3.1.3 Oval cells in therapeutics

With the increasing interest in characterizing oval cells with respect to their origin, questions arise regarding the mechanism of their recruitment and their differentiation potential. Investigators hope that some day these cells can be used therapeutically in the restoration of

human livers damaged by chemicals and infectious disease, as well as inherited metabolic disorders.

Two distinct obstacles must be overcome for oval cells to be considered for clinical application. Maintenance of oval cells in an undifferentiated state in culture has surfaced as the first major hurdle. Developing this technique is critical, because any therapeutic use of these cells will require the expansion of a small population of cells *ex vivo* prior to transplantation. The second impediment has been selectively directing the differentiation of oval cells down a hepatocyte or bile duct epithelial committed pathways as needed. It is anticipated that the signals mediating these differentiation processes will be sufficiently complicated as to disallow their exact replication *in vitro*. Factors governing oval cell differentiation may include contact with other cell types, contact with the ECM, or exposure to soluble signaling proteins in the serum such as the Wnt family of proteins. To circumvent the need for overcoming this second hurdle, cells could be transplanted in their precursor form and the natural microenvironment of the liver used to dictate their differentiation, but this theory has yet to be validated.

2.4 Stem Cells and Cancer

2.4.1 Theories of Cancer Development

2.4.1.1 Cellular origins of cancer

To accurately determine the cellular origin of any cancer, one must identify the individual cell type that initiates the cascade of events ultimately resulting in tumor development. The linear progression from that initial cell through the multistep process of tumor initiation, promotion, and progression must be clearly defined. The use of phenotypic cellular markers to indicate distinct cellular origins of a cancer has proven highly unreliable due to cellular variations present during routine cellular processes, chemical exposure and other stresses.

Although certain cell types consistently exhibit specific cellular markers, the presence of those markers is not definitive of a cell's origin or differentiation potential.

The similar histologic appearance and growth characteristics linking embryonic tissues and cancer have led the pioneers of pathology to conceptualize a stem cell origin of cancer. Research linking the resident organ specific stem cells and the development of cancer has been observed in numerous malignancies in the skin, liver, as well exocrine glands such as breast and prostate, and the hematopoietic system. Regardless of their origin, transformation of cells to a malignant phenotype requires a series of epigenetic changes and genetic mutations.

2.4.1.2 Stem cell theory of cancer

In the late 1800's, Conheim and Durante hypothesized that cancer developed from rudimentary embryonic tissues present in mature organs.[123] These tissues resulted from excessive proliferation of embryonic tissue that lay dormant in mature organs and later underwent oncogenesis. This theory became known as the "embryonal rest hypothesis."[123] Later, the theory of anaplasia based on the dedifferentiation of mature tissues induced by chemical or viral exposure replaced the embryonal rest theory.[123] The most recent theory of carcinogenesis involves the maturation arrest of resident tissue stem cells. The more primitive arrested stem cell results in a tumor with a less differentiated phenotype.[123] Currently, the scientific community hotly debates whether the dedifferentiation theory or the maturation arrest theory correctly defines neoplastic development.

2.4.2 Oval Cells and Liver Cancers

2.4.2.1 History of oval cell theory of hepatic carcinogenesis

The liver should be viewed as an organ that contains two distinct cellular pools: the unipotential hepatocytes and the multipotential oval "stem" cell. Tumors may arise by either the dedifferentiation of an adult mature hepatocyte or by the maturation arrest of a liver stem cell.

The immature state of a stem cell does imply an increased potential for self-renewal and differentiation, and the ability to undergo numerous and rapid divisions indicates a higher likelihood of DNA damage and malignant transformation in the presence of a carcinogen. Conversely, the minute number of oval cells within a normal liver in comparison with the multitudes of hepatocytes causes one to question the theory that only hepatic stem cells are sufficiently damaged during chemical carcinogenesis. It seems reasonable to expect that both cellular pools could provide progenitors cells for neoplastic development. As it stands, these two proposed origins of hepatic cancers have support in the literature demonstrating their cell of origin in both HCC and CCC development, and yet the debate still continues.

Genesis of liver tumors most likely occurs via multiple molecular mechanisms, which depend on both the nature of the carcinogen and the lesion it induces. In reality, researchers may never determine that only one cell type can undergo neoplastic changes, but the most long-standing theory of the dedifferentiation of the hepatocyte has numerous studies behind it. In 1992, Farber stated that rare, original mature hepatocytes in all three zones of the adult liver appear after initiation with genotoxic carcinogens, and he stated that foci or islands of altered hepatocytes and nodules derived from these rare, original mature hepatocytes.[124]

The concept of the liver stem cell playing a role in chemically induced carcinogenesis can be traced back as far as the early 1930s.[8] These studies demonstrated that hyperplasia of small round cells in the periportal region of the liver preceded the development of hepatocellular carcinoma.[8] The hepatic oval "stem" cell is currently believed to play an essential role in the etiology of liver development, growth, and regeneration, and they are also still being implicated in the progression of hepatocellular carcinogenesis. With this premise, the stem cell origin of

liver cancer is either the resident facultative "oval" stem cell, the progeny of such a cell, or the transitional duct cell.[125]

2.4.2.2 Evidence for oval cell theory of hepatic cancers

In 1956 Farber *et. al* initially theorized the participation of oval cells in the formation of hepatic cancers due to their morphological changes during early chemical carcinogenesis.[117] The exposure of the liver to ethionine, 2-acetylaminofluorene (2-AAF) and 3'-methyl-4-dimethylaminoazobenzene (Me-DAB), result in: 1) oval cell proliferation which progressively involved the entire liver lobule, 2) degenerative and hypertrophic changes in the hepatocytes next to proliferating oval cells and 3) nodular regenerative hyperplasia of liver cells.[117] There were, however, some important differences observed in the three models involving the time course of the appearance of oval cells and the fate of these cells after stimulation by the chemicals. In the ethionine and 2-AAF models the oval cells appeared at days 7 and 14 days post-exposure, respectively. In contrast, the Me-DAB model produced oval cells significantly later, 21 days post-exposure. More importantly, the fate of the oval cells in the Me-DAB model was different from those induced by ethionine and 2-AAF. At the earlier time points oval cells derived from all three models appear similar in morphology. However, at later time points, areas of apparent transition between oval cells and hepatocytes were more numerous in the Me-DAB animals but almost absent in those animals that received either ethionine or 2-AAF.[117]

The above observation raises an important issue. If the morphological transition from oval cell to hepatocyte can be observed after Me-DAB exposure, then the theory that oval cells have the capacity to differentiate into hepatocytes can be verified. The fact that ethionine or 2-AAF did not produce the same results suggests that the compounds capable of inducing oval cell proliferation may greatly affect both the rate and extent of oval cell differentiation into hepatocytes. That a large percentage of oval cells are in the cell cycle during the early stages of

chemical carcinogenesis indicates these cells have the capacity to differentiate into hepatocytes. This suggests that at least a percentage of HCCs can be derived from an oval cell lineage. Also CCCs are thought to be derived from a bile ductular type of stem cell that has lost the capacity to generate hepatocytes.

Interestingly, there has been increasing experimental evidence to support of the notion of stem cell derived HCC. Hixson and colleagues employed a battery of monoclonal antibodies specific for antigens associated with bile duct cells, oval cells, and fetal, adult and neoplastic hepatocytes to analyze the phenotypic relationship between oval cells, foci, nodules and HCC during chemical hepatocarcinogenesis.[102] They determined that oval cells, γ-GT-positive hepatocellular foci, persistent hepatocyte nodules, and primary HCCs all express both oval cell and hepatocyte antigens, suggesting a precursor-product relationship between oval cells and carcinomas. Similar results were obtained by Dunsford *et al.* (1989) using different monoclonal antibodies raised against oval cells.[126,127] These lineage relationships between oval cells and HCC also exist in other models of liver carcinogenesis. For example, animals on a choline deficient diet supplemented with ethionine (CDE) diet display markers for oval cells in a significant percentage of nodules and HCC.[102]

Evidence for oval or ductal cells as progenitors for HCC is not restricted to experimental rodent models of chemical hepatocarcinogenesis. Results from Van Eyken *et al.* (1988) on CK expression in 34 "classical" human HCCs using monospecific anti-cytokeratin antibodies showed that all HCCs were positive for CK-8 and CK-18.[128] However, in 17 cases, a variable number of tumor cells were positive for CK-7 and CK-19, both known to be bile ductular epithelium markers.[128] The authors also reported that only 3 of 11 well-differentiated tumors displayed this "unexpected" pattern of immuno-reactivity as opposed to 7 out of 7 poorly

differentiated tumors.[128] This is important in light of earlier findings by Denk et al. (1982) that CKs continue to be expressed when hepatocytes become neoplastic.[129] These observations become particularly significant in light of Hsia *et al*. (1992) and Vandersteenhoven *et al*. (1990) who demonstrated immunohistochemically the presence of oval type cells with characteristics of both bile ducts and hepatocytes in the liver of patients with end stage cirrhosis and/or tumors in patients with hepatitis B infection.[130,131] Although this molecular evidence does suggest that these tumors are derived from the oval cell compartment, they do not eliminate the possibility that these tumors developed via dedifferentiation of hepatocytes.

A recent paper documented evidence of oval cells and/or rat liver epithelial (RLE) cells capable of progressing to HCC and CCC from the *in vitro* transformation of these cell types. Spontaneous transformation of RLE or transformation of oval cells with chemical carcinogens resulted in the tumors displaying a wide range of phenotypes including well-differentiated HCCs, CCCs, hepatoblastomas and poorly differentiated or anaplastic tumors.[132-134] While these findings are interesting from the point of view of what might happen, theoretically, these *in vitro* studies have been of limited value in clarifying what really happens *in vivo*. To date, no reported study on *in vitro* neoplastic transformation of oval cells has been able to match up, step-by-step with what occurs *in vivo* with the exception of morphologic and immunohistochemical similarities between these *in vitro* tumors and some *in vivo* cancers. As stated earlier, cancer may arise from the phenotypic change in a rare cell, both *in vivo* and *in vitro*, but it becomes almost impossible *in vivo* to identify the cell of origin.

Currently, there is no direct evidence that any cell type among the hepatocytes, proliferating ductal epithelial cells and/or oval cells is the cell of origin for foci, nodules and HCC or CCC development. Thus the basis for oval cell participation in hepatic cancer

development is all circumstantial, speculative and indirect, albeit strong, it is still not conclusive. Within these complex animal carcinogenesis models, conclusions concerning whether original hepatocytes, altered hepatocytes, or proliferating oval cells are the likely cells of origin for evolution to cancer has not been feasible to date.

2.5 Wnt Family of Proteins

2.5.1 Wnt Pathway

2.5.1.1 History of the Wnt pathway

The Wnt family of highly conserved growth factors has an active role in the *in vivo* regulation of developmental and homeostatic processes across the animal kingdom. Interestingly, membership within this class of proteins is not based on functionality but instead relies on amino acid sequence homology. This method of classification has created a large group of proteins with various functions associated with often contradictory activities and numerous mechanisms of downstream signaling. The implied involvement of Wnt pathways in a wide variety of developmental events as well as numerous human diseases ranging from deformities to cancer has caused a drastic increase in the interest in unraveling the actions of this complex protein family.

Wnt protein sequences are highly conserved across species and there are a large number of proteins included in the family. Mammals have 19 Wnt genes which can be classified into twelve distinct subfamilies.[135] Of these twelve subfamilies, eleven are found in the Cnidarian genome. The family of Wnt receptors, proteins known as Frizzled, also has a large number of members (10) which are also highly conserved across species.[135] This cross phylum conservation of these gene families indicates the developmental role of Wnts was initiated over 650 million years ago and very early in the evolution of metazoans.[135]

2.5.1.2 Wnt proteins and signaling

The Wnt proteins are characterized by a highly conserved series of cysteine residues, and although they have an N-terminal signaling sequence, they are highly insoluble. This insolubility has been one of the most difficult obstacles to the understanding of concentration dependent morphogenic nature of the Wnt proteins. Discovering the palmitolated state of Wnt3a by Willert *et. al* alleviated some of the problems associated with their notoriously difficult purification.[136] The discovery of this lipid modification resulted in the first ever isolation of a biologically active form of a Wnt protein. The palmitolation occurs exclusively on the highly conserved cyteine residues and facilitate secretion of the protein and probably the formation of the gradients that determine the morphogenic activity of the Wnt proteins.[137]

The Wnt family has several downstream signaling pathways including the Wnt/β-catenin cascade, the noncanonical planar cell polarity pathway, and the Wnt/Ca^{++} pathway; however, the majority of research has focused on the β-catenin dependent signaling cascade. Although the Wnt1 gene (initially termed int-1) was initially discovered in 1982 by Nusse and Varmus, the link between Wnt and β-catenin was not discovered for nearly ten years when Wnt-1 was definitively shown to regulate cell adhesion β-catenin levels.[138,139] Since that time the signaling pathway that is termed the "canonical" pathway has been fairly well defined.

In cells not exposed to Wnt, β-catenin is phosphorylated by Axin and GSK-3β within the destruction complex. This phosphorylation signals β-catenin for ubiquination and degradation. Concurrently, Wnt target genes are repressed by the association of TCF with Groucho. While complexed with Groucho, TCF activates the transcription of genes not regulated by the canonical Wnt pathway and represses the activation of Wnt responsive genes.

The canonical Wnt signaling pathway begins with Wnt binding to its receptor Frizzled and the coreceptor LRP5/6. This binding allows for the phosphorylation of LRP and the recruitment

of Axin from the destruction complex to the membrane. Disheveled (Dsh) is also phosphorylated by an unknown mechanism. The removal of Axin and the phosphorylation of Dsh inhibit the function of the destruction complex which results in a cytoplasmic accumulation of β-catenin. Whether actively transported or simply due to excess cytoplasmic β-catenin concentration, β-catenin translocates to the nucleus and replaces Groucho in order to associate with TCF. β-catenin in complex with TCF acts as a transcriptional activator for Wnt responsive genes. Figure 2-9 is a diagrammatic representation of the canonical Wnt signaling pathway.

2.5.2 Functions of the Wnt Family

2.5.2.1 Role of Wnt in differentiation and development

The Wnt family of proteins and their in depth "canonical" signaling pathway (Figure 2-9) has been implicated in a variety of regulatory aspects of cellular differentiation and embryonic development.[135,140,141] This family been described as a requirment for differentiation and development of the brain, cartilage, mesenchymal tissues arising from somites, and limb bud formation.[142-151] Individual Wnt proteins and their downstream signals are also instrumental in the directing the differentiation of progenitor cells.[136,149,152] It should be noted that some of these studies illustrate a Wnt involved in the differentiation of progenitors, while others implicate different Wnt family members responsible for the maintenance of progenitors undifferentiated state.[136,152-154]

The best example of Wnt control on differentiation was exhibited by Weismann's lab at Stanford. He demonstrated Wnt signaling resulted in the expansion of hematopoietic stem cells (HSCs) that lacked discernable lineage specific markers, and when transplanted these cells generated B, T, and myeloid cells.[154] This pioneering paper, demonstrated Wnt's role in inducing a stem cell's self-renewal without altering the stem cell's original lineage potential. Wnt has also been acknowledged as being responsible for the expansion of progenitors possessing predefined

fates such as the self-renewing crypts of the intestine, cardiac neural crest cells, and cells of the anterior pituitary.[155-157]

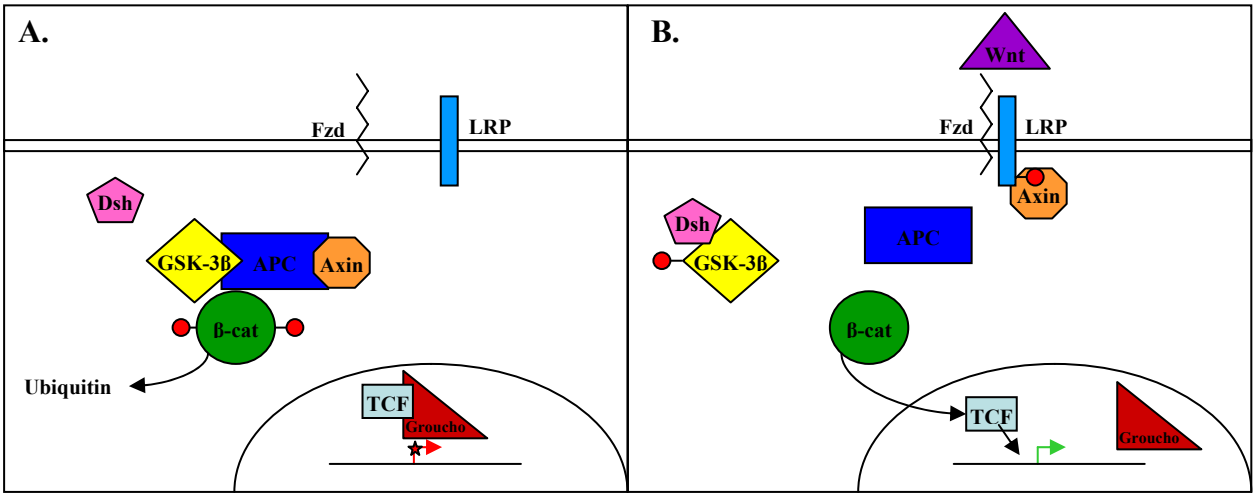

Figure 2-9. Representation of the "cononical" Wnt pathway. A. In the absence of Wnt, β-catenin is dually phosphorylated by GSK-3β and Axin within the destruction complex. This phosphorylation initiates the ubiquitination and degradation of β-catenin. B. When Wnt binds to Frizzled and its co-receptor LRP5/6, LRP is phosphorylated which draws Axin to the membrane and away from the destruction complex. Disheveld (Dsh) is also activated in an unknown manner and facilitates the phosphorylation of GSK-3β. Phosphorylated GSK-3β cannot phosphorylated β-catenin. The unphosphorylated and, therefore, unubiquitinated β-catenin accumulates in the cytoplasm and is shuttled into the nucleus. Within the nucleus, β-catenin displaces Groucho from its complex with TCF, thereby, changing TCF from a repressor into an activator of Wnt responsive genes.

2.5.2.2 Wnt family and disease

Although no documentation of any mutation or amplification of genes encoding Wnt ligands or receptors has been linked to human cancer to date, several components of the Wnt pathway have been implicated in carcinogenesis, especially TCF, APC and beta-catenin.[158] The member of the destruction complex known as adenomatous polyposis coli (APC) was first discovered as the tumor suppressor that undergoes a loss of function in Familial adenomatous polyposis (FAP) and >80% sporadic colorectal cancer.[159] Mutations in other downstream signals within the Wnt pathway have been specifically connected to the formation of HCC, CCC,

sporadic medulloblastomas, and esophageal squamous cell cancinomas.[159] Cancers containing mutations resulting in the disregulation of the downstream Wnt signaling molecules include cancers of the colon, liver, breast, prostate, and brain.[158]

The various functions of the Wnt proteins, their receptors, and downstream signals can readily be seen in the variety of human diseases linked to these genes. A large portion of the diseases are associated with bone and connective tissue morphogenesis and include Familial tooth agenesis, osteoporosis pseudoglioma syndrome, and Dupuytren skin disease.[159] Interestingly, a homozygous mutation in the human Wnt3 gene results in the drastic phenotype of tetra-amelia.[159,160] This single mutation indicates the intense developmental requirement of the Wnt proteins in limb bud formation. Neurologic requirements for Wnts are more generalized as they have been implicated in Alzheimer's disease and schizophrenia.[159] Within the heart, Frizzled receptors have been implicated in cardiac hypertrophy and myocardial infarctions. Lastly, Wnt4 mutations result in Mullerian-duct regression and virilization, an intersex phenotype, and errors in kidney development.[159] The vast actions of this family and its cross species developmental requirements can readily be observed in the various human diseases directly linked to Wnt and its downstream signals.

2.5.3 Wnts and the Liver

2.5.3.1 Wnts and liver regeneration

The Wnt family has strong ties to the process of regeneration. Wnt knockouts inhibit regeneration of limbs.[151,160] Mutations in Wnt3 result in a complete failure in limb bud formation. Also, the evident rise in Wnt and its downstream signals immediately following partial PHx deeply implies the involvement of Wnt in the regenerative processes of the liver.[161] Through the study the expression of Wnt and its downstream mediators throughout oval cell

differentiation along the hepatic lineage as well as during the oval cell response to injury, the role of the Wnt family in the liver can be fully elucidated.

2.5.3.2 Wnts and liver development and liver zonation

β-catenin has a dual role in regulating hepatocyte adherens junctions and transcription of Wnt regulated genes. The regulation of β-catenin by both the Wnt family and the HGF have been implicated in the control of hepatocyte division and liver growth.[162] Mice that over express β-catenin have a three to four fold increase in hepatic size due to increased hepatocyte proliferation.[163,164] This clearly indicates the dramatic role β-catenin has in liver growth and development. Also changes in APC levels across the liver functional lobule have been recognized as contributing to the zonation of the lobule. APC levels are high in pericentral hepatocyte which correlates to low levels of β-catenin activation.[165,166] Conversely, in periportal hepatocytes, β-catenin activation is high whereas APC levels are low. Knocking out APC resulted in Zone 3 hepatocytes with gene expression profiles similar to those of Zone 1.[165] Clearly Wnt signaling has critical roles within the liver.

2.5.3.3 Wnts and liver diseases

Although Wnt family members are not as clearly associated with liver diseases as their down stream signals, these signaling molecules have severe implications in liver disease processes. Most significant are the roles that these molecules play in liver tumors both benign and cancerous. Nuclear localization of β-catenin has been reported in 90-100% of hepatoblastomas and a significant but small percentage of hepatic adenomas.[162] Also interesting was that in those adenomas that had nuclear translocation of β-catenin, 46% progressed to HCC. β-catenin translocation is present in a very high percentage of HCC.[162] Although the mechanisms controlling that translocation vary, the influence of the Wnt signaling cascade is very apparent in HCC development.[162] Lastly, within CCC, a decrease in adherens β-catenin and E-cadherin in

conjunction with nuclear β-catenin localization has been observed. Although no mutations in Wnt genes have been found in tumors, their down stream molecules are actively implicated in carcinogenesis and other disease processes, therefore, understanding the role Wnt family members have in normal tissues can greatly increase our understanding of disease processes.

CHAPTER 3
SPECIFIC AIMS

In 1956 E. Farber recognized the same cell type appearing in the liver after several different chemical injury models. He classified these small cells with high nuclear to cytoplasmic ratios as oval cells. Although debate continues as to the site of origin of these cells, they are universally considered to be the resident hepatic stem cell. Some suggest that oval cells arise in the Canal of Hering; while others believe they arise form an extra hepatic source. *In situ* oval cells are bipotential in nature. When they are present in the liver they differentiate toward both hepatic and bile ductular epithelial lineages.

The Wnt family of secreted proteins controls various differentiation pathways during numerous stages of embryogenesis, including hepatic development. Wnts have been shown to maintain stem cells in an undifferentiated state while increasing self renewal, and they have been shown to direct progenitor differentiation. They have also been implicated in hepatocyte based liver regeneration after partial hepatectomy. With known Wnt involvement in hepatic organogenesis and regeneration, investigating the role of this family during stem cell directed liver regeneration seemed logical.

Based upon the involvement of Wnt family members in hepatic organogenesis, it is hypothesized that Wnt1 is a critical molecule required for the differentiation of oval cells toward mature hepatocytes. In order to test this hypothesis, two specific aims were designed. They are as follows:

- **Specific Aim #1:** To determine if the Wnt signaling pathway plays a role in hepatic stem cell based liver regeneration
- **Specific Aim #2:** To determine whether Wnt1 is required for directing oval cells to differentiate toward hepatic lineage during stem cell based liver regeneration.

Specific Aim #1: To fully understand the signals which direct oval cell differentiation the 2AAF/PHx model was employed. Briefly, animals received an implant of a 28 day time release 2AAF pellet. Hepatocytes are inhibited from their normal replication by 2AAF. Seven days after 2AAF implantation animals underwent a ⅔ partial hepatectomy. As early as 3 days after partial hepatectomy oval cells begin to migrate out from the portal region and infiltrate the hepatic lobule, radiating toward the central vein. Oval cell numbers peak at approximately 9 days after partial hepatectomy. Oval cells begin to differentiate into basophilic small hepatocytes roughly 13 days post PHx. By 21 days after PHx the liver has regained its normal architecture and little evidence of the oval cell infiltrate remains.

Initially, livers obtained from the peak of oval cell production were analyzed for the presence of members of the Wnt signaling pathway. Immunohistochemistry was performed for the Wnt receptors Frizzled numbers 7 and 5; Frizzled related protein 1 (Frp1), a known inhibitor of the Wnt pathway; low density lipoprotein receptor-related protein 5 (LRP5), the coreceptor for Wnt; three individual Wnts (Wnt5a, Wnt3, and Wnt1), and the downstream signaling molecule β-catenin. After determining that the Wnt pathway was activated during oval cell induction, western blot, rt-PCR and IHC were utilized to asses the pattern of Wnt activation throughout the 2AAF/PHx model.

Cells isolated from perfused livers were separated by density with a Nycodenz fractionation gradient. The resulting four fractions contained immune cells and stellate cells (F1), oval cells (F2), small hepatocytes and Kupffer cells (F3) and hepatocytes (F4). Isolated cell fractions from normal liver and the peak of oval cell proliferation were compared for Wnt1 levels and β-catenin levels. As an indicator of active Wnt signaling, changes in the phosphorylation status of β-catenin were also examined.

The observation that hepatocytes expressed high levels of Wnt proteins and oval cells demonstrated evidence of β-catenin translocation and decreased phosphorylation levels indicated an active response to Wnt signaling by oval cells. This response was further evaluated by exposing a hepatic stem cell line, designated WB-F344, to purified Wnt3a protein. After 48 hours of incubation with Wnt3a, β-catenin translocation was visualized.

Specific Aim #2: The *in vitro* protein and RNA data supported a role for the Wnt pathway in oval cell based liver regeneration, however, as no definitive link between Wnt1 and oval cell differentiation had been established, a short hairpin Wnt1 siRNA construct was designed. To test the efficiency of the shRNA construct to knockdown Wnt1 protein levels, stably transfected PC12/Wnt1 cells were transiently transfected with Wnt1 or scrambled (SCR) shRNA vectors containing green fluorescent protein (GFP). GFP expression was utilized to determine transfection efficiencies. Wnt1 levels were then assessed by western blot.

The construct was deemed successful enough for *in vivo* knockdown of Wnt1 signaling during oval cell activation. Animals underwent 2AAF implantation and PHx. Venous injections of shRNA vectors complexed with the cationic lipid vector JetPEI were performed 3 and 6 days after PHx. Animals were sacrificed at 9, 11, 13, 15, and 21 days after PHx. Tissue was collected for paraffin sections, frozen sectioning, protein analysis and RNA analysis, and liver and body weights measured.

GFP expression was evaluated in every organ collected from the animals in order to ascertain the sites of shRNA vector uptake. Histology and morphology of livers were then analyzed for deviations from normal oval cell based liver regeneration. Immunohistochemistry, western blot, and rtPCR were performed to detect changes in Wnt protein levels as compared to standard 2AAF/PHx animals.

CHAPTER 4
MATERIALS AND METHODS

4.1 Animals Studies

The 2-AAF/PHx model was utilized to accurately assess the activation and fundamental biology of the liver stem cell. This model provided the basis for understanding oval cell biology with respect to growth, proliferation and differentiation, as well as in response to extrinsic interventions. The assessment of oval cell differentiation states *in vitro* can be informational; however, *in vivo* evaluation holds greater value in the analysis of the liver stem cell's inherent functions. To date, no substitute has been found that adequately replaces an animal model in examining the fate of oval cells.

4.1.1 Animals and Animal Housing Facilities

All animals utilized in this study were under approved animal protocols submitted to the University of Florida IACUC committee. All animals utilized in this study were Fisher 344 male rats obtained from Charles River Laboratories, Inc. (Wilmington, MA). Animals were housed in a barrier facility under sterile conditions at the Animal Care Services Facility in the Medical Science/ Communicore Building. The Animal Care Services is a state of the art animal facility that provides a pathogen-free barrier environment. The animal care program is accredited by AAALAC. The facility is supervised by veterinarians, which are always present at the facility or on call. Animals are checked several times per day, and a veterinarian is always available for consultation, particularly if decisions need to be made regarding euthanizing an animal prior to the sacrifice date. The University of Florida meets National Institutes of Health standards as set forth in the DHHS publication #NIH 86-23 and accepts as mandatory the PHS "Policy on Humane Care and Use of Laboratory Animals by Awardee Institutions" and the National Institutes of Health "Principles for the Utilization and Care of Vertebrate Animals Used in

Testing, Research and Training." The University of Florida has on file with the Office for Protection Form Research Risks an approved Assurance of Compliance.

4.1.2 Animal Sacrifice and Tissue Collection

All animals utilized for tissue collection were euthanized by administration of an overdose (150 mg/kg) of Nembutal Sodium Solution (OVATION Pharmaceuticals, Inc., Deerfield, IL) This is consistent with the recommendations of the panel on euthanasia of the American Veterinary Medical Association and the Guide for the Use and Care of Laboratory Animals (U.S. Department of Health and Human Services/NIH Publication #86-23).

After euthanasia, tissue from brain, heart, lung, liver, pancreas, spleen, kidney, and intestine was collected for paraffin embedding, frozen sectioning, and RNA and protein collection. Samples for protein and RNA were snap frozen in a histobath containing 2-methylbutane and kept at -80ºC until isolation was performed. Tissues for paraffin embedding were fixed O/N in 10% Neutral Buffered Formalin (Richard-Allan Scientific, Kalamazoo, MI). The formalin was then exchanged for PBS and the tissue submitted for embedding by the University of Florida Molecular Pathology Core Facility. Tissue collected for frozen sectioning was immediately placed in Tissue-Tek O.C.T. Compound (Sakura Finetek U.S.A., Inc., Torrance, CA), snap frozen in a histobath containing 2-methylbutane, and stored at -80ºC until sectioning. All paraffin and frozen sections were cut to a 5μm thickness.

4.1.3 Oval Cell Induction in the Rat

4.1.3.1 2-AAF pellet implantation

Continuous administration of 2-AAF was used to suppress proliferation of mature hepatocytes prior to partial hepatectomy. Utilization of a 2-AAF time release pellet alleviated undue stress to the animals associated with multiple 2-AAF oral gavage and reduced the amount of human exposure to the 2-AAF.

Briefly, the animals were anesthetized with isoflorane. The abdomen was shaved and scrubbed three times in a circular pattern emanating from the center outward with ethanol and three times with Betadine (Purdue Pharma L.P., Stamford, CT). The animal was then draped with a Steri-Drape (3M, St. Paul, MN) with only the incision site exposed. Then a very small, approximately 1/4 inch, incision was made in the lower right quadrant of the animal's abdomen. A midline incision would not suffice because the pellet must be placed distal to the liver in order to prevent adherence of the pellet to the body of the liver. The fibrosis associated with adherence would complicate the subsequent partial hepatectomy.

After opening the abdominal wall, a small incision was made within the abdominal muscle to facilitate entry to the peritoneal cavity. A 70 mg/28 day release (2.5 mg/day) 2-AAF time release pellet (Innovative Research Inc., Sarasota, Fl) was carefully introduced through the incision into the peritoneal cavity. The muscle tissue was then closed using 1-2 sutures of 3-0 Vicryl (Ethicon, Inc., Cornelia, GA). The skin was closed with the Autoclip Wound Closing System (Braintree Scientific, Inc., Braintree, MA). Rats were then placed in a warmed cage and monitored for complete recovery. This procedure yielded a survival rate of greater than 95%.

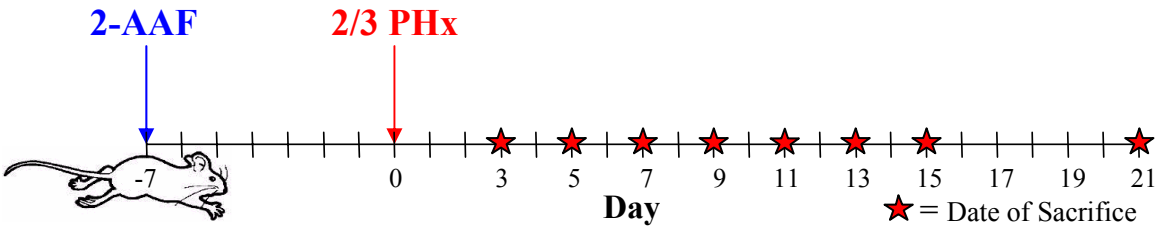

Figure 4-1. Oval cell induction in the rat. Diagrammatic representation of oval cell induction model in the rat including 2-AAF pellet implantation, partial hepatectomy, and dates of sacrifice.

In successful procedures, hypothermia and dehydration were not an issue during recovery, and in the event of excessive blood loss during surgery, animals were injected i.p. with 1-3ml

sterile saline. The animals were checked every six hours until fully recovered. The stainless steel staples were removed after 10 days.

4.1.3.2 Two-thirds partial hepatectomy

The removal of 66% of the liver was originally described by Higgins and Anderson.[8] Figure 4-1 represents a diagrammatic representation of the 2-AAF/PHx oval cell induction model in the rat. The animals were anesthetized with isoflorane. The abdomen was shaved and scrubbed three times in a circular pattern emanating from the center outward with ethanol and three times with Betadine (Purdue Pharma L.P.). The animal was then draped with a Steri-Drape (3M) with only the incision site exposed. A 1.5 cm longitudinal incision was made in the skin just below the xyphoid process. The incision was continued through the midline of the abdominal muscle, exposing the liver. The tip of the xyphoid process was excised to facilitate removal of the liver and limit liver injury during extrusion. Next the left medial, right medial and the left lobe of the liver were gently extruded through the incision. The lobes were then tied off with a silk suture. The exposed lobes were excised and the remaining stump examined for excessive bleeding prior replacement within the peritoneal cavity. Bleeding from the stump indicated incorrect tying off of the excised lobes. If bleeding occurred and was unable to be controlled the animal was euthanized. The muscle tissue was then closed using 4-5 sutures of 3-0 Vicryl (Ethicon, Inc.). The skin was closed with the Autoclip Wound Closing System (Braintree Scientific, Inc.). The stainless steel staples were removed after 10 days. Rats were then placed in a warmed cage and monitored for complete recovery.

This procedure yielded a survival rate of greater than 90%. The 10% death rate was usually associated with the aforementioned bleeding from the incorrectly tied liver stump. The difficult in obtaining the correct the tension on the ligating suture should be noted. A ligature tied too tightly causes the liver proximal to the knot to tear and this situation is practically impossible to

resolve. Conversely, insufficient tension on the ligature results in the inability to staunch the blood flow to the stump and subsequent bleeding.

In successful procedures, hypothermia and dehydration were not an issue during recovery. In the event that any blood was lost during surgery, animals were injected i.p. with 1-3ml sterile saline. The animals were checked every six hours until fully recovered. The stainless steel staples were removed after 10 days. Animals were sacrificed at days 3, 5, 7, 9, 11, 13, 15, 17, and 21 days post-PHx. Tissue collected was analyzed by IHC, rtPCR, and western blot.

4.1.4 Density-Based Separation of the Liver

4.1.4.1 Perfusion of the liver

In order to isolate intact hepatocytes and oval cells from the whole liver a perfusion was performed. Following an i.p. injection of 60 mg/kg sodium pentobarbital, complete anesthesia was determined by pinching the back feet and absence of a leg and/or abdominal muscle contraction. The animal's four appendages were then secured to the surgical table with tape. The abdomen was shaved and then sterilized with 95% ethanol. A midline incision was made to expose the peritoneum. The incision was then expanded laterally distal to the ribcage as well as proximal to the iliac crest. These lateral incisions create abdominal flaps that can then be secured to the table and creates greater access to the abdominal organs. The abdominal viscera were displaced toward the rat's lower right quadrant in order to expose the inferior vena cava. The inferior vena cava was cannulated with a 20 gauge catheter and the hepatic artery ligated. The thoracic cavity was then opened, and the superior vena cava occluded with a hemostat. The liver was then perfused with 1X S and M solution followed by an 80mg of collagenase in 1X $CaCl_2$ modified 1X S and M. The entire liver was then harvested and placed in 1X PBS for subsequent oval cell and hepatocyte isolation. The procedure resulted in the complete exsanguination of the animal.

4.1.4.2 Density gradient separation of liver cells

The suspension was filtered through a 125μm nylon mesh and centrifuged at 500 rpm for 5min to pellet the majority of hepatocytes. Two Nycodenz stock solutions at 30% (wt./vol.) were prepared, one with cyanol FF, one without. The stock solutions were subsequently serially diluted to 26, 19 (blue), 15 and 13% (blue) in 1X PBS (Gibco) and sequentially layered (volume of 1.5ml each). The cells of the pellet were resuspended in 11% Nycodenz solution and loaded on the top of the gradient. Centrifugation was then performed at 8,000 × g for 30min. Cells were located at the four gradient interphases F1-4 starting at the top. Fraction 1 contained stellate cells and immunologic cells. Fraction 2 contained mostly oval cells. Fraction 3 was small hepatocytes and Kupfer cells. The final fraction contains mature hepatocytes. Cells from the interphases were collected and finally washed in 1X PBS and then utilized for protein or RNA isolation.

4.2 Liver Stem Cell Response to Wnt

4.2.1 *In vitro* Response of Rat Liver Epithelial cells to Wnt3A

In order to verify that oval cells do respond to Wnt signaling, WB-F344 a rat liver epithelial cell was exposed to Wnt3a. WB-F344 cells were derived from the liver of an adult Fisher 344 rat.[167] WB-F344 cells are considered to be liver stem cell like and are accepted as a substitute for primary oval cell culture as oval cells are notoriously difficult to grow in culture.[167-173]

4.2.1.1 Maintenance of liver stem-like cells, WB-F344

WB-F344 cells were graciously provided by Lijun Yang, M.D. The cells were maintained in DMEM (GIBCO) media containing 10% fetal bovine serum, 10 I.U. Penicillin/ml, and 10μg/ml Streptomycin in a 37°C humidified incubator containing 5% CO2 and 95% air, and passaged using 0.25% trypsin plus 0.02% EDTA treatment. The culture medium was changed every other day.

4.2.1.2 Exposure of liver stem-like cells to Wnt3A

WB-F344 cells were plated at approximately 20-25% confluency on collagen coated coverslips within a 6 well dish. 24 hours after plating, the media was replaced with 1.0ml of media supplemented with 250ng/ml Wnt3A (R and D Systems,minneapolis, MN). 48 hours after exposure to Wnt3A, the media was removed and the cells washed twice with 1X PBS. The cells were then fixed with ice cold methanol for 10min. Immunofluorescence staining for β-catenin was performed as described below to determine the response of rat liver epithelial cells to Wnt3a exposure.

4.3 Wnt shRNA Model in Rat

In order to confirm that oval cells require Wnt signaling in order to differentiate into hepatocytes, Wnt1 protein expression was inhibited with shRNA technology. Transiently blocking the production of Wnt1 RNA effectively impeded Wnt1 protein production. Due to the lack of Wnt1 stimulation, oval cells could not differentiate toward a hepatic lineage. As a result, oval cells underwent atypical ductular hyperplasia.

4.3.1 Wnt shRNA Plasmid

4.3.1.1 Design of Wnt shRNA vector

A shRNA hairpin to the rat Wnt gene was constructed with shRNA Wizard (InvivoGen, San Diego, CA). A custom-made psiTNA-H1gz-Wnt1 plasmid was then created by InvivoGen. As a control, a vector containing a scrambled shRNA construct that is not complimentary to any known gene was utilized. The vector contained a 21nt sequence incorporated into a hairpin with a 7nt spacer region. Once the shRNA was transcribed in a mammalian cell, the hairpin was cleaved resulting in a 21bp double stranded RNA that served to bind to and knockdown the production of the Wnt mRNA through the dicer pathway.

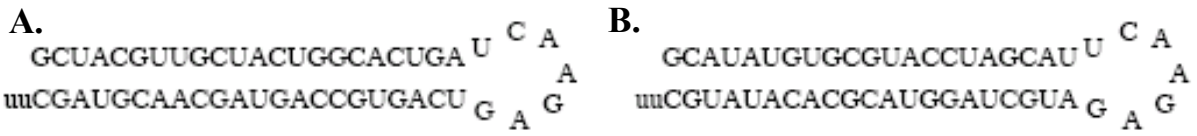

Figure 4-2. shRNA hairpin structures. Diagram of the (A) Wnt1 and (B) SCR shRNA hairpins.

The shRNA hairpin construct was under the control of the H1 promoter. The H1 promoter drove the expression of the unique gene encoding the H1 RNA, the RNA component of the human RNase P complex. The pshRNA vector also contained a CMV-HTLV promoter controlling the expression of a GFP::zeo fusion gene. The GFP::zeo fusion gene produced the GFP protein and Zeocin resistance in mammalian cells. A bacterial origin of replication and EC2K promoter allowed *E. coli* to produce the vector and express Zeocin resistance. Lastly, the β-Glo pAN site within the vector contained the human beta-globin 3' untranslated region and polyadenylation sequence which allows for sufficient arrest of the GFP::zeo transgene transcription. Figure 4-2 is a diagrammatic representation of the Wnt1 and SCR shRNA hairpins. Figure 4-3 is a diagrammatic representation of the pshRNA-Wnt1 vector. Figure 4-4 is the sequence of the pshRNA-Wnt1 vector and the relevant restriction enzyme sites, gene sites, and orientations of open reading frames.

4.3.1.2 Wnt shRNA plasmid amplification

The lyophilized pshRNA vector was resuspended in 20µl of molecular grade H_2O to obtain a plasmid solution at 1µg/µl. The pshRNA vector was transformed into LyComp GT116 *E. coli* (InvivoGen). GT116 is a strain that contains a *sbcCD* deletion mutant that helps the bacteria to better handle hairpin DNA structures than other strains of *E. coli.* A vial of GT116 was thawed on stored on ice for 5min and then reconstituted with 1ml of reconstitution solution on ice for 5min. The cells were rehydrated for 30min on ice. Then 1µl of 1µg/µl pshRNA was incubated with 100µl of GT116 cells on ice for 30min. The cells were then heat shocked at 42ºC

for 30 sec and placed on ice for 2min. 900µl of SOC medium was then added and the tubes shaken at 250 rpm for 1hr at 37ºC. The cells were then spread on Fast-Media Zeo (InvivoGen) agar plates and incubated O/N at 37ºC.

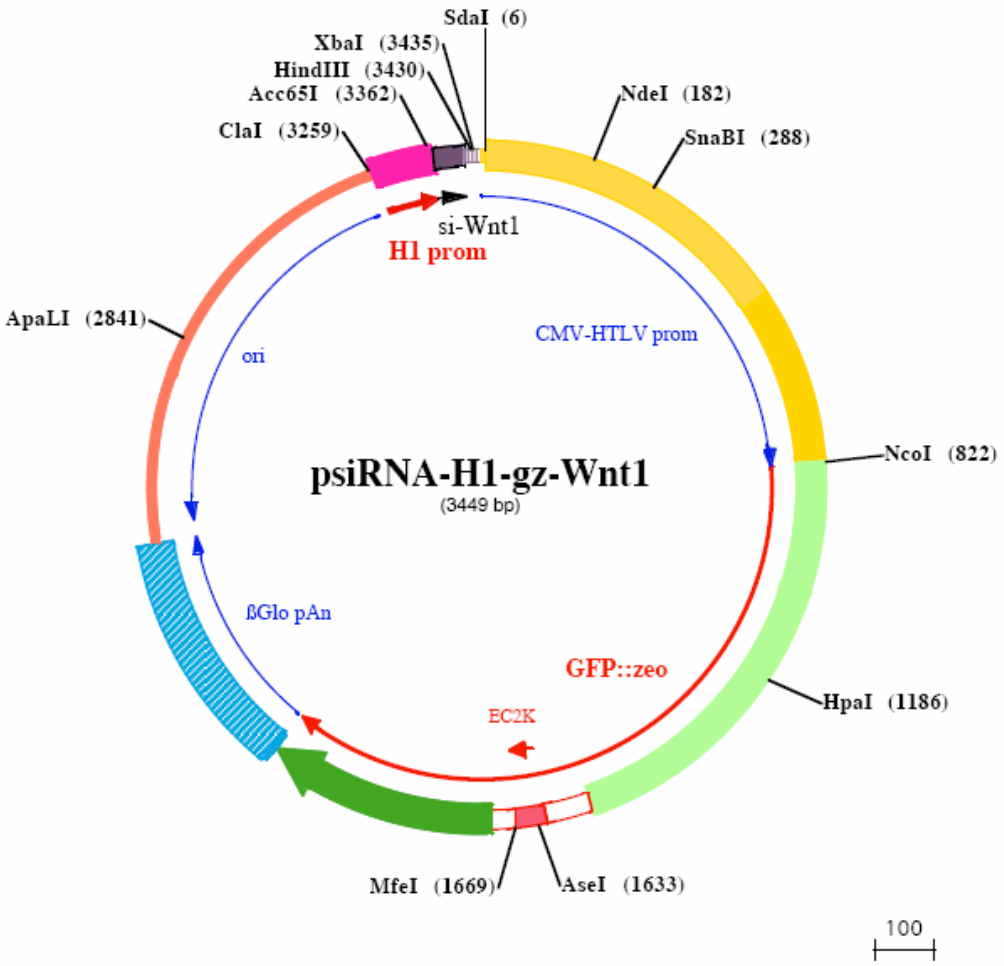

Figure 4-3. Map of the pshRNA-H1-gz-Wnt1 vector.

Colonies were then chosen and grown in volumes of 5ml of Low salt LB (10.0g Tryptone, 5.0g NaCl, 5.0g Yeast Extract) supplemented with 50µg/ml Zeocin (Invitrogen, Carlsbad, CA). Plasmids were isolated from the 5ml cultures with QIAprep Spinminiprep Kit (Qiagen, Valencia, CA) as per manufacturers' specifications. Larger quantities of plasmid were obtained with the with QIAGEN Plasmid Maxi Kit (Qiagen) from 1L low salt LB supplemented with 50µg/ml Zeocin (Invitrogen) cultures of transformed bacteria.

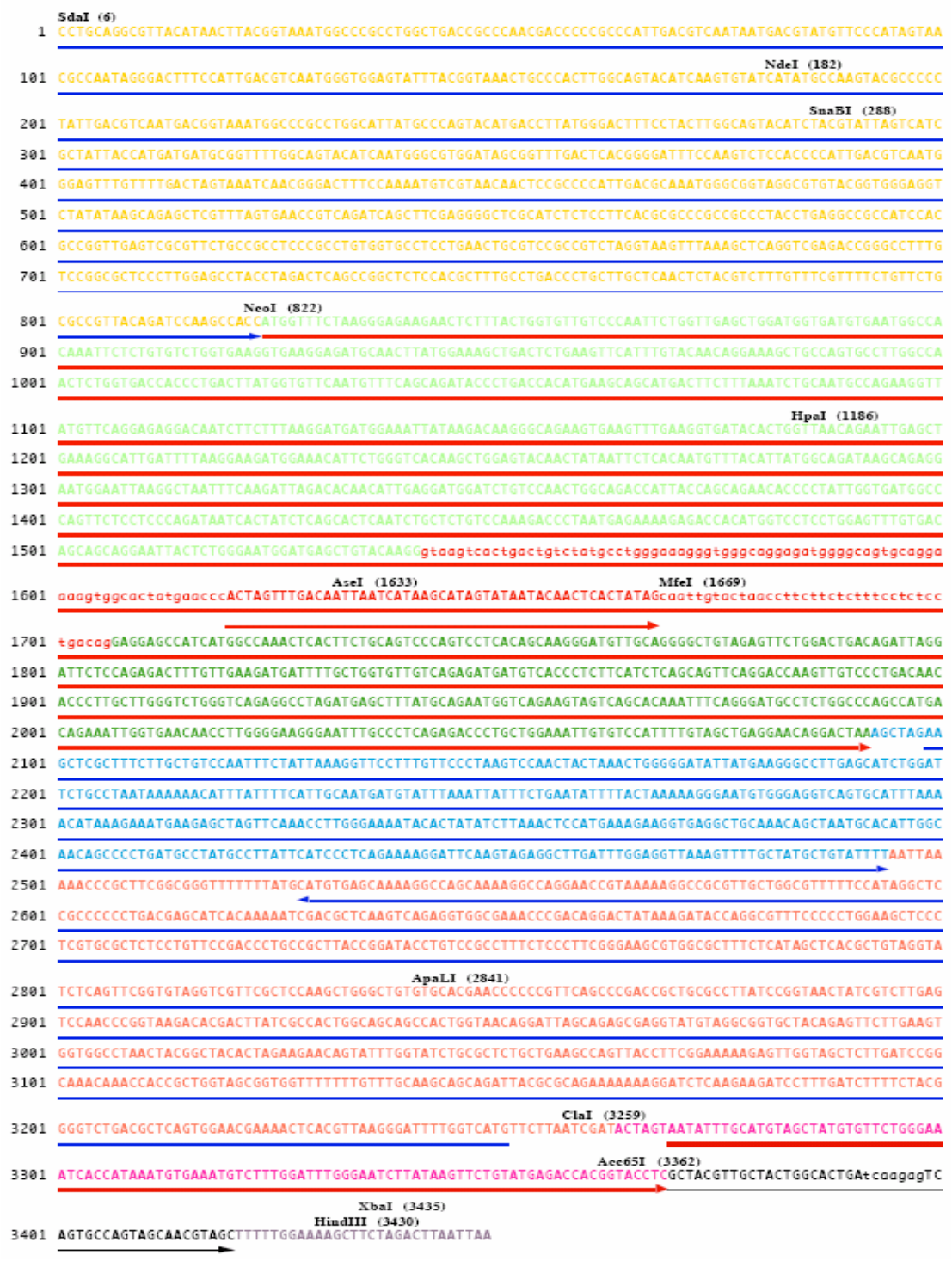

Figure 4-4. The sequence and relevant restriction enzyme sites of the pshRNA-H1-gz-Wnt1 vector.

4.3.1.3 Wnt1 shRNA plasmid analysis

The presence of plasmids isolated from cultures was analyzed by agarose gel electrophoresis. A 30ml mini gel containing 0.7% (w/v) agarose in 0.5X TBE and was heated to dissolve the agarose, and then 0.001% (v/v) ethidium bromide was added. The gel was then allowed to cool in a gel pouring apparatus and a comb with appropriately sized wells was inserted. After hardening, the comb was removed and the gel submerged in 0.5 X TBE in a gel electrophoresis chamber. 0.5µl of 10X Agarose gel loading buffer and 3.5µl of Mill-Q H2O was added to 1µl of each sample and each sample was loaded into the wells along with an appropriate molecular weight ladder (1 Kb, 100 bp, etc.). The gel was then run at 90-110 volts for approximately 1 hr or until desired separation of bands was visible on a UV light box. Pictures of agarose gels were obtained with a GelDoc XR (Bio-Rad, Hercules, CA).

After 0.7% agarose gel electrophoresis confirmed presence of plasmids, the plasmids were further analyzed by restriction enzyme digestion with AseI (New England Biolabs, Ipswich, MA) as per manufactures' recommendations. AseI yielded a linearized 3448 bp plasmid when the shRNA hairpin is present. When absent, AseI digestion of pshRNA yields two bands of 1801 bp and 1647 bp. Also DpnI (NEB) digestion was utilized to distinguish between the SCRsi vector and the Wnt1si vector. DpnI digestion of Wnt1si vector resulted in 8 bands of the following sizes: 1747 bp, 593 bp, 536 bp, 277 bp, 202 bp, 75 bp, 11 bp, and 8bp. Whereas, the DpnI digestion of the SCRsi vector yielded only 7 bands of the following sizes: 1747 bp, 795 bp, 536 bp, 277 bp, 202 bp, 75 bp, 11 bp, and 8 bp.

4.3.2 Verification of Wnt1 shRNA Function

4.3.2.1 Confirmation of Wnt1 knockdown in PC12/Wnt1 cells

Wnt1 stably transfected rat pheochromocytoma cells (PC12/Wnt1) were graciously donated by G.M. Shackleford, PhD from the Division of Hematology-Oncology, The Saban

Research Institute, Children's Hospital Los Angeles, CA. PC12/Wnt1 cells were grown in Ham's F12K medium with 2mM L-glutamine adjusted to contain 1.5 g/L sodium bicarbonate, 15% horse serum, 2.5% bovine calf serum, 10 I.U. penicillin/ml, and 10 µg/ml streptomycin in a 37 °C humidified incubator containing 5% CO2 and 95% air, and passaged using 0.25% trypsin plus 0.02% EDTA treatment. PC12/Wnt1 cells were grown to 80% confluency in a 6 well dish and transfected with 4.0µg of DNA utilizing Lipofectamine 2000 (Invitrogen) as per manufacturer's instructions. After 48 hours Wnt1 mRNA and protein levels were analyzed by rtPCR and western blot.

4.3.3 Inhibition of Wnt1 in the Rat

4.3.3.1 *In vivo* shRNA to Wnt1

Animals underwent 2-AAF implantation and ⅔ PHx as previously described. 250µg of pshRNA vector was complexed with 20µl of *in* vivo JetPEI (Polyplus Transfection, NY, NY) as per manufacturers' recommendations. 400µl was given via the femoral vein to each animal in a solution with a final concentration of 5% glucose. Nine animals received the SCRsi vector and twenty-four received the Wnt1si vector. Animals were sacrificed at days 9, 11, 13, 15, and 21 days post-PHx. Tissue was collected and analyzed by IHC, rtPCR, and western blot. Figure 4-5 represents a diagrammatic representation of the shRNA model in the rat.

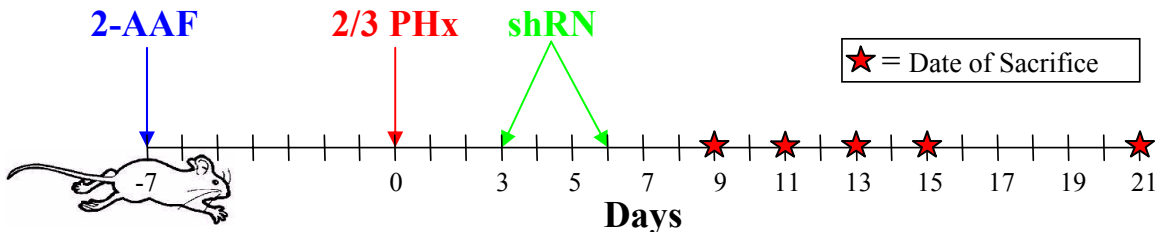

Figure 4-5. Diagrammatic representation of Wnt shRNA model in the rat including 2-AAF pellet implantation, partial hepatectomy, shRNA injections, and dates of sacrifice.

4.3.3.2 Femoral injections of shRNA vector

All shRNA constructs were delivered via the femoral vein. Briefly, after anesthetization by isoflorane, a very small incision was made on the medial aspect of the left thigh. Fascia surrounding the femoral vein, artery, and nerve was carefully excised. A standard butterfly catheter infusion set with a 21 gauge needle was then inserted into the femoral vein. 400µl of the desired solution was then injected. Bleeding was controlled with pressure and the skin closed with a single Autoclip (Braintree Scientific, Inc.). This procedure lasted less than 5minutes and no complications were observed. The stainless steel staple was removed after 10 days.

Days Post Phx	Wnt1 shRNA	SCR shRNA
7	3	0
9	5	2
11	4	2
13	4	2
15	3	1
21	5	2
Total	24	9

Table 4-1. Numbers of animals sacrificed during *in vivo* Wnt1 shRNA inhibition.

4.3.3.3 Animal numbers

Animals were sacrificed at days 9, 11, 13, 15, and 21 days after PHx. Animal numbers at the various time points are described in Table 4-1. Three animals treated with Wnt shRNA died 7 days after PHx which was one day after the second injection. These animals exhibited massive intestinal hemorrhage. Reasons for these deaths have been determined to be linked to possible loss of vascular and/or intestinal epithelial integrity due to decreases in Wnt1 levels. Localized hepatic administration of the shRNA vector could alleviate this problem in the future.

4.4 Histology and Immunohistochemistry

4.4.1 Histological Analysis

4.4.1.1 Hematoxylin and eosin of paraffin embedded tissue

Tissue sections of 5μM in size were cut and placed in a 42ºC water bath. They were then lifted from the bath with a Superfrost Plus (Thermo Fisher Scientific Inc. Waltham, MA) positively charged slide. The slides were air dried O/N at RT. The paraffin was removed and the slides rehydrated by incubating them in Xylene 2 × 5min, 100% Ethanol 2 × 2min, 95% × Ethanol 2 × 1min, and distilled H_2O for 1min. Nucleic acids and other positively charged molecules were then stained with Hematoxylin 7211 (Richard-Allan Scientific) for 2min 15 sec and rinsed with distilled H_2O for 2 ×1min. The blue color of the Hematoxylin was intensified by incubating the slides in Clarifier 1 (Richard-Allan Scientific) for 1min, distilled H_2O for 1min, Bluing Reagent (Richard-Allan Scientific) for 1min, distilled H_2O for 1min, and 80% Ethanol for 1min. Proteins were then stained a pink color with Eosin-Y (Richard-Allan Scientific) for 1min 30 sec. The tissue was then dehydrated for coverslipping with 2 × 1min 95% ethanol, 2 × 1min 100% ethanol, and 3 × 1min xylene. Coverslips were then applied with Cytoseal XYL (Richard-Allan Scientific).

4.4.1.2 Hematoxylin and eosin of frozen sections

Tissue sections of 5μM in size were cut and placed on Superfrost Plus (Thermo Fisher Scientific Inc. Waltham, MA) positively charged slides. The slides were air dried for 5min at RT. The tissues were fixed in Pen-Fix (Richard-Allan Scientific) for 30 sec. The slide was then washed in distilled H_2O for 1min. Nucleic acids and other positively charged molecules were then stained with Hematoxylin 7211 (Richard-Allan Scientific) for 45 sec and rinsed with distilled H_2O for 1min. The blue color of the Hematoxylin was intensified by incubating the slides in Clarifier 1 (Richard-Allan Scientific) for 25 sec, distilled H_2O for 30 sec, Bluing

Reagent (Richard-Allan Scientific) for 30 sec, distilled H_2O for 30 sec, and 80% Ethanol for 30 sec. Proteins were then stained a pink color with Eosin-Y (Richard-Allan Scientific) for 30 sec. The tissue was then dehydrated for coverslipping with 2 × 1min 95% ethanol, 2 × 1min 100% ethanol, and 3 × 1min xylene. Coverslips were then applied with Cytoseal XYL (Richard-Allan Scientific).

4.4.1.3 Periodic Acid-Schiff staining of paraffin embedded tissue

PAS staining was performed to determine the presence or absence of mucin and glycogen in liver tissue sections. All tissue stained with PAS for was performed by the University of Florida, Department of Pathology, Molecular Pathology Core Laboratory.

4.4.2 Immunohistochemistry

4.4.2.1 Chromogen staining

All staining of paraffin and frozen sections was performed with Vector ABC Kits and Dab or Vector Blue Reagent kits (Vector Laboratories, Burlingame, CA). All staining was performed as per manufacturer's instructions. DAB slides were counterstained with Vector Hematoxylin QS (Vector Laboratories) and mounted with Cytoseal XYL (Richard-Allan Scientific). Vector Blues stained slides were counterstained with Nuclear Fast Red (Vector Laboratories) and coverslipped with VectaMount Permanent Mounting Medium (Vector Laboratories). Slides were incubated O/N at 4ºC for primary antibody and 30min for secondary antibodies. Any special retrieval method needed for a specific antibody is listed in 4.4.2.3.

4.4.2.2 Fluorescent staining

All paraffin slides were deparaffinized and rehydrated as in H and E staining. Frozen sections were air dried and fixed for 10min in ice cold methanol unless otherwise stated in Section 3: Antibodies utilized for Immunohistochemistry. Slides were incubated for 5min in 1X TBS plus 0.1% Tween (TBS-T), and then blocked with serum for 20min and incubated with the

primary antibody 1hr at RT or O/N at 4ºC. Slides were then washed for 5min in 1X TBS-T at RT and incubated with a fluorochrome labeled secondary antibody for 30min. Slides were again washed for 5min in TBS-T at RT and then coverslipped with Vectashield Mounting Media with DAPI (Vector Laboratories). Fluorescence was observed and photographed with a fluorescent microscope or a confocal fluorescent miscroscope. The microscope, camera, and software utilized to assess IHC were a BX51 Olympus Fluorescent microscope fitted with cubes for FITC, Texas Red, DAPI and dual pass FITC/Texas Red, an Optromic Digital Cemera with Image Pro 3.1 Software, and Magnafire 3.1. All confocal microscopy was performed by Doug Smith at the University of Florida Stem Cell program on the Leica TCS SP2 AOBS Spectral Confocal Microscope with the LCS (Leica Confocal Software) Version 2.61, Build 1537 software.

4.4.2.3 Antibodies Utilized for Immunohistochemistry

Protein	Animal	Concentration	Retrieval	Company	Cat. #
Wnt1	Goat	1:50	None	Santa Cruz	sc-6280
Wnt3	Goat	1:50	None	Santa Cruz	sc-28824
Wnt5a	Goat	1:50	None	Santa Cruz	sc-30224
B-catenin	Mouse	1:800	Citrate	BD Biosciences	610153
OV6	Mouse	1:150	None	Gift from S. Sell	Albany, NY
CD45	Mouse	1:100	None	BD Biosciences	554875
Ki67	Mouse	1:100	Citrate	BD Biosciences	556003
SDF-1	Goat	1:50	Citrate	Santa Cruz	sc-6193
AFP	Rabbit	1:800	Trilogy	Dako	A0008
GFP	Rabbit	1 ug/ml	Citrate	Abcam	ab6556

Table 4-2. Antibodies utilized for immunohistochemistry.

4.5 Protein Analysis

4.5.1 Protein Isolation and Quantification

4.5.1.1 Protein isolation from tissue or cells

Tissue was placed in desired amount of RIPA buffer with Protease Inhibitor. The tissue was broken up and then sheared with an 18 gauge needle and 3ml syringe. The tissue was pipetted up and down until tissue was thoroughly homogenized. The sample was vortexed for 30

seconds and then spun at 10,000 × g at 4ºC for 10min to remove excess lipids and DNA. The supernatant was collected into 2.0ml screw cap tube and placed in -80ºC until use.

4.5.1.2 Protein quantification with DC Protein Assay

Blank and protein standards were made in 1ml tube as follows:

1. Blank 25 µl RIPA Buffer without Protease Inhibitor
2. Standard #1 1µl + 24µl RIPA Buffer without Protease Inhibitor
3. Standard #2 2µl + 23µl RIPA Buffer without Protease Inhibitor
4. Standard #3 4µl + 21µl RIPA Buffer without Protease Inhibitor
5. Standard #4 8µl + 17µl RIPA Buffer without Protease Inhibitor

Samples were made with 1ul sample and 24µl RIPA Buffer without Protease Inhibitor Solution in 1ml Clear Tube. In another 1ml tube 125µl Reagent A per reaction and 2.5µl Reagent S per reaction from the DC Protein Assay (Bio-Rad, Hercules, CA) were mixed. Note: Reaction number equals "sample number plus five". 125µl of combined solutions A and S was added to each reaction. When ready to measure 1ml Reagent B was added and tubes vortexed. 5-10min after the addition of solution B the OD of the samples were measured in disposable cuvettes in Spectrophotometer set to 750nm.

4.5.2 Western Blot Analysis of Protein Levels

4.5.2.1 Pouring an acrylamide gel

Main gel (10%, 8%, or 6% Acrylamide Gels): All components of gel except TEMED were mixed in a 15ml polypropelene tube. When ready to pour the gel the TEMED was added.

1. H_2O 4.85ml=10%, 5.35ml=8%, 5.85ml=6%
2. 40% Bis-Acrylamide 2.50ml=10%, 2ml=8%, 1.5ml=6%
3. 2.50ml 1.5M Tris-Cl (pH 8.8)
4. 100 µl 10%SDS
5. 33 µl Ammonium Per Sulfate (APS)
6. 7 µl TEMED

The sponge on the gel pouring apparatus was dampened and the plates cleaned with alcohol. The plates were then aligned and secured in gel pouring apparatus. The gels were

poured using electronic or plastic Pasteur pipettes. They were poured to approximately 1-1.25 cm below the top of the plate. Butyl alcohol was added to top of glass to prevent bubbles and smiling of gel. After 30min the remaining solution in the 15ml tube was inverted to determine if gel solidified. The butyl alcohol was removed and the gel rinsed with Milli-Q H_2O.

Stacking gel: All components of gel except Temed were mixed in a 15ml polypropelene tube. When ready to pour the gel the TEMED was added.

1. 1.25ml H_2O
2. 0.50ml 40% Bis-Acrylamide
3. 0.50 0.5M Tris-Cl (pH 6.8)
4. 20µl 10%SDS
5. 15µl Ammonium Per Sulfate (APS)
6. 2µl TEMED

The gels were pored using electronic or plastic Pasteur pipettes to slightly below top of glass and the comb inserted. After 10-15min, the gel was ready to run after gently removing comb and rinsing the wells with Milli-Q H_2O.

4.5.2.2 Protein sample preparation

The amount of protein to be loaded per well was determined based on source of isolation (tissue or cell culture) and the sensitivity of the antibody being used for detection. Samples were added to the appropriate amount of RIPA Buffer to equal 12µl per lane and placed in a screw cap 2.0ml tube. 3µl of 5X Western Loading Buffer per lane was added to each tube. Each sample was boiled for 10min and then incubated at RT for 5min to cool. Each well of 0.75mm gel was loaded with 15µl of sample with dye. The samples were immediately loaded and any remaining solution placed on ice and returned to storage at -80°C.

4.5.2.3 Electrophoresis of the western gel

The gel was loaded in the running apparatus with small plate facing inward. The inner chamber was filled with 1X Running Buffer till full and overflows and the outer chamber was

filled 2.0 inches. 15µl of samples were loaded per well with 10µl of Protein Standard within the first well. Any empty lanes were filled with 15µl of 2X Western Loading Buffer. The gel was run at 60-80 Volts until the loading dye had migrated out of the stacking gel. Then the gel was run at 100 Volts until the loading dye ran the length of the gel.

4.5.2.4 Transferring of a western gel to a PVDF membrane

The upper left corner of the Immun-Blot PVDF (Bio-Rad) membrane was cut and the membrane was labeled with pencil. It was then dipped in methanol, soaked in water for 5 min, and soaked in 1X transfer buffer for 20min. Sponges and filter papers were also soaked transfer buffer. The gel plates were opened and the stacking gel/wells were removed. The gel was submerged in 1X transfer buffer. A sandwich consisting of black assembly tray, sponge, filter paper, gel, PVDF membrane, filter paper, sponge, and red assembly tray along with an ice block and stir bar were placed in the transfer apparatus. The transfer apparatus was filled with 1X transfer buffer and placed on a stir plate. The transfer buffer was stirred continuously while transferring to ensure the apparatus would not overheat. The proteins were transferred at 200 milliamps for 60min for a 0.75mm gel and 90min for a 1.50mm gel.

4.5.2.5 Probing of western membrane

The membrane was blocked for 1-2 hours at RT with a blocking solution consisting of 5g skim milk, 2g glycine, and 100ml 1X PBS-T. The membrane was then probed with the appropriate concentration of primary antibody O/N at 4ºC. The membrane was then rinsed 3x for 5min each with 1X PBS. The appropriate horseradish peroxidase conjugated secondary antibody was applied in 1X PBS for 30min to 1 hr shaking at RT. The membrane was then rinsed again 3X with 1X PBS for 5 min each.

4.5.2.6 Developing of western membrane with ECL Plus

Excess liquid was removed from the membrane and it was placed within a plastic bag. 25ul of Solution A mixed with 1ml of Solution B ECL Plus reagents (GE Healthcare, Piscataway, NJ) was incubated on the membrane for 5min. Excess ECL Plus reagent was removed. Film was exposed to the membrane for 5s to 10min depending on the brightness of the banding pattern. The membrane was then stripped if further probing was necessary.

4.5.2.7 Membrane stripping for reprobing

20ml of 5X stripping solution was diluted to 1X with 80ml water (100ml total). Then 714µl β-Mercaptoethanol was added and membrane placed within the solution. The membranes were incubated in closed Tupperware container at 56ºC for no longer than 30min with intermittent shaking. The membrane was then washed for 5-8 times of 5min each with 1X PBS-T until all residual B-Mercaptoethanol was removed. Membranes were then reblocked with milk and reprobed as normal.

4.5.2.9 Antibodies Utilized in Western blotting

Protein	Animal	Conc.	MW (KDa)	Company	Cat #
Wnt1	Goat	1:1000	40-42	Santa Cruz	sc-6280
B-catenin	Mouse	1:2000	92	BD Biosciences	610153
Phospho-β-catenin	Mouse	1:1000	92	Cell Signaling	9561
B-Actin	Mouse	1:5000	42	Abcam	3280

Table 4-3. Antibodies utilized for western blot analysis.

4.6 RNA analysis

4.6.1 RNA Isolation

4.6.1.1 Homogenization

Tissues: Tissue samples were homogenized in 1ml of RNABee Reagent (Tel-Test, Inc., Friendswood, TX) per 50-100 mg of tissue using a sonic homogenizer.

Cells Grown in Monolayer: Cells were lysed directly in a culture dish by adding 1ml of RNABee Reagent to a 3.5 cm diameter dish, and passing the cell lysate several times through a pipette. The amount of RNABee Reagent added is based on the area of the culture dish (1ml per 10 cm2) and not on the number of cells present. An insufficient amount of RNABee Reagent may result in contamination of the isolated RNA with DNA.

Cells Grown in Suspension: Cells were trypsinized and the trypsin inactivated with media supplemented with FBS. The cells were then pelleted by centrifugation at 500rpm for 5min. The cells were then lysed in RNABee Reagent by repetitive pipetting. 1ml of the RNABee reagent was used per 5-10 × 106 of animal cells.

4.6.1.2 Phenol-chloroform phase separation

The homogenized samples were incubated for 5min at RT to permit the complete dissociation of nucleoprotein complexes. Then 0.2ml of chloroform per 1ml of RNABee Reagent was added and the tubes vortexed for 30s. The samples were then centrifuged at 12,000 × g for 15min at 4°C. Following centrifugation, the mixture separated into a lower blue, phenol-chloroform phase, an interphase, and a colorless upper aqueous phase. RNA remained exclusively in the aqueous phase. The volume of the aqueous phase was about 60% of the volume of RNABee Reagent used for homogenization.

4.6.1.3 Precipitation and redissolving of RNA

RNA Precipitation: The aqueous phase was transferred to a fresh tube, and the RNA precipitated from the aqueous phase by mixing with 600µl isopropyl alcohol per 1ml of RNABee Reagent used for the initial homogenization. The samples were then incubated at RT 10min and centrifuged at 12,000 × g for 10min at 4°C. The RNA precipitate, often invisible before centrifugation, formed a gel-like pellet on the side and bottom of the tube.

RNA Wash: The supernatant was removed and the pellet washed in 1ml of 75% ethanol. The sample was then vortexed and centrifuged at 7,500 × g for 5min at 4ºC.

Redissolving the RNA: The RNA pellet was air-dried for 5-10minutes, but the pellet was not allowed to dry completely, as this would greatly decrease its solubility. The RNA was dissolved in RNase-free water and stored at -80°C.

4.6.1.4 Quantification of RNA by spectrophotometry

In order to accurately determine the concentration of RNA in each sample, 1 µl of RNA sample was diluted in 99 µl of DEPC-treated H_2O. This solution's absorbance was then analyzed at OD of 260nM and 280nM in a spectrophotometer. The purity was determined based on an OD 260/280 of > 1.8. The concentration of RNA was determined using the following formula:

$$\text{RNA (ng/µl)} = OD_{260} \times 40 \text{ ng/µl} \times \text{dilution factor of } 100$$

4.6.2 RT-PCR

4.6.2.1 First-strand cDNA synthesis from total RNA

First strand cDNA was synthesized utilizing SuperScript First-Strand Synthesis System (Invitrogen) as per manufacturer's instructions. Note: For samples collected from the various time points of the oval cell induction model, 10µg of RNA from three individual animals was pooled. 5.0µg of this pooled RNA was then used for cDNA production. 5.0µg of each individual animal that underwent shRNA injections was utilized for cDNA production.

4.6.2.2 PCR amplification of target cDNA

1. 2µl 10X PCR buffer
2. 0.25µl 10mM dNTP Mix
3. 0.5µl 10µM Forward Primer
4. 0.5µl 10µM Reverse Primer
5. 1µl cDNA
6. 15.55µl Milli-Q H2O
7. 0.2µl Taq Polymerase (5 U/µl)

All previously listed components of PCR reaction were combined on ice with *Taq* Polymerase added immediately before samples were placed in a thermocycler. The PCR reaction was run as follows with the annealing temperature adjusted to the individual primer sets:

1. 94°C for 10min
2. 31 cycles of
    a. 94°C for 30 sec
    b. Annealing temp for 30 sec
    c. 72°C for 30 sec
3. 72°C for 10min
4. 4° indefinitely

4.6.2.3 Primers utilized for DNA/cDNA amplification

Primer name	Primer sequence (5'→3')	Annealing temp (°c)	cDNA size (bp)	DNA size (bp)
Wnt1	F= TTC TGC TAC GTT GCT ACT GGC ACT R= CAT TTG CAC TCT TGG CGC ATC TCA	51	626	3214
Wnt3	F= GCC GAC TTC GGG GTG CTG GT R=CTT AAA GAG TGC ATA CTT GG	56	317	1005
Wnt5a	F= TCC TAT GAG AGC GCA CGC AT R= CAG CTT GCC CCG GCT GTT GA	58	224	4028
AFP	F= AGG CTG TAC TCA TCA TTA AAC T R= ATA TTG TCC TGG CAT TTC G	58	485	4139
β-catenin	F= GCC AGT GGA TTC CGT ACT GT R= GAG CTT GCT TTC CTG ATT GC	58	202	202
GapDH	F= TGA GGG AGA TGC TCA GTG TT R= ATC ACT GCC ACT CAG AAG AC	58	577	577

Table 4-4. Primers utilized for PCR, and rtPCR.

4.6.2.4 Agarose gel electrophoresis

A 30ml mini gel containing 0.7% (w/v) agarose in 0.5X TBE and was heated to dissolve the agarose, and then 0.001% (v/v) ethidium bromide was added. The gel was then allowed to cool in a gel pouring apparatus and a comb with appropriately sized wells was inserted. After hardening, the comb was removed and the gel submerged in 0.5 X TBE in a gel electrophoresis chamber. 0.5µl of 10X Agarose gel loading buffer and 3.5µl of Mill-Q H2O was added to 1µl of each sample and each sample was loaded into the wells along with an appropriate molecular

weight ladder (1 Kb, 100 bp, etc.). The gel was then run at 90-110 volts for approximately 1 hr or until desired separation of bands was visible on a UV light box. Pictures of agarose gels were obtained with a GelDoc XR (Bio-Rad, Hercules, CA).

4.6.3 Real-Time PCR analysis of Wnt1 levels

To accurately assess the variations of Wnt1 levels during various time points of the rat oval cell induction model, levels of Wnt1 message were analyzed quantitatively by Real Time PCR. Wnt1 levels were also quantitatively analyzed in all animals that received shRNA injections.

4.6.3.1 Real-Time PCR of Wnt1

For the analysis of Wnt1 message levels, 2µl of cDNA and 1.25µl each of forward and reverse Wnt1 primer were added to 25µl of Power SYBR Green PCR Master Mix (Applied Biosystems, Foster City, CA). The final reaction volume was 50µl. The reaction was performed on an ABI Prism 7700 Sequence Detection System. The thermocycle sequence consisted of 10min at 95ºC and then 40 cycles of 95ºC for 30 sec, 51ºC for 30 sec, and 60ºC for 30 sec.

4.6.3.2 Real-Time PCR of 18S rRNA

As an internal control for quantification purposes QuantumRNA 18S Internal Standards (Ambion, Austin, TX) were used to amplify 18S message. Samples were prepared as with Wnt1 quantification. The ratio of 18S primer: competimer was 3:7 as per manufacturers instructions.

4.6.3.3 Statistical analysis of Real-Time PCR and densitometry

A statistical analysis was performed as a student T-Test to determine the probability that the data occurred merely by chance.

4.7 Solutions

- **10X Agarose Gel Loading Buffer**
    1. 15.0mg bromophenol blue
    2. 15.0mg xylene cyanol
    3. 8.0g sucrose
    4. Milli-Q H2O qs to 10ml

- **10X $CaCl_2$**
    1. 6.36g $CaCl_2$
    2. Milli-Q H_2O *qs* to 1L

- **10X PBS**
    1. 80.0g NaCl
    2. 2.0g KCl
    3. 11.5g $Na_2HPO_4 \times 7H_2O$
    4. 2.0g KH_2PO_4
    5. Milli-Q H_2O *qs* to 1L

- **RIPA Buffer and Protease Inhibitor Solution**

  RIPA Buffer
    1. 1.5ml 1M NaCl
    2. 0.5ml 1M Tris-Cl pH 8.0
    3. 1.0ml 10% NP-40
    4. 1.0ml 10% NaDeoxycholate
    5. 5.4ml Milli-Q H_2O

  Protease Inhibitor Solution (added to RIPA just prior to use)
    1. 100µl 10mg/ml PMSI in isopropanol
    2. 300µl Apoprotonin
    3. 100µl 100mM NaOrthovanadate

  Total = 10.0ml

- **10X S and M Solution**
    1. 500mg KCl
    2. 8.0g NaCl
    3. 2.4g HEPES
    4. 190 mg NaOH
    5. pH to 7.4
    6. Milli-Q H_2O *qs* to 1L and filter

- **5X TBE**
    1. 54.0g Tris base.
    2. 22.5g Boric acid
    3. 4.7g EDTA
    4. Milli-Q H_2O *qs* to 1L

- **10X TBS**
    1. 80.0g NaCl
    2. 2.0g KCl
    3. 30.0g Tris base
    4. 800ml H_20
    5. Milli-Q H_2O *qs* to 1L

  Adjust pH to 7.4 using 1M HCl

- **5X Western Loading Buffer**
    1. 1.5ml 0.5M Tris-HCl
    2. 1.0g 10% SDS
    3. 2.5ml β-mercaptoethanol
    4. 1.5mg Bromophenol Blue
    5. Milli-Q H_2O *qs* to 10ml

- **10X Western Running Buffer**
    1. 144.0g Glycine
    2. 30.0g Tris-Base
    3. 10.0g SDS
    4. Milli-Q H_2O *qs* to 1L

- **5X Western Stripping Solution**
    1. 37.83g Tris-Base
    2. 1g SDS
    3. pH to 6.8
    4. Milli-Q H_2O *qs* to 1L

- **10X Western Transfer Buffer**
    1. 115.0g Glycine
    2. 24.0g Tris-Base
    3. Milli-Q H_2O qs to 800ml

When diluted to 1X, 80ml of 10X Transfer Buffer was added to 720ml Milli-Q H2O and 200ml Methanol.

CHAPTER 5
RESULTS

5.1 Evaluation of the Wnt Family During Oval Cell Induction

During oval cell activation, members of the Wnt family were up regulated. Specifically, by IHC analysis Wnt3, Wnt1, Fzd 7 and Fzd 5 demonstrated increased expression in pericentral hepatocytes (Figure 5-1). Interestingly, Wnt5a and FRP1, known negative regulators of the canonical Wnt pathway, were only expressed in low levels late in the oval cell induction protocol. The most prevalently expressed Wnt during 2AAF/PHx appeared to be the first Wnt discovered, Wnt1. Further analysis of Wnt one expression during oval cell induction revealed an association of Wnt1 expression and liver "stem" cell based regeneration.

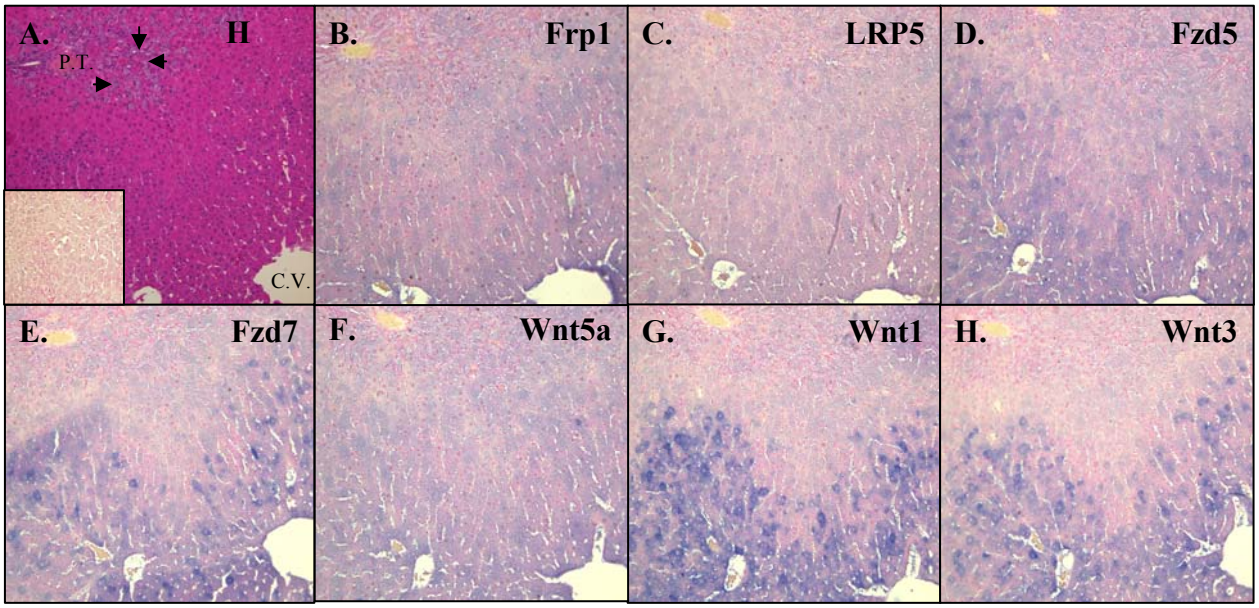

Figure 5-1. 2AAF/PHx 9 Days post PHx versus Wnt Family. Serial sections of 2AAF/PHx Day 9 tissue. A. H and E; A. Insert. IgG Isotype negative control. B. Frizzled Related Protein 1; C. LRP5; D. Frizzled 5; E. Frizzled 7; F. Wnt5a; G. Wnt1; F. Wnt3. C.V.= Central vein; P.T.= Portal triad; Arrows indicate oval cell rich infiltrate surrounding the portal triad and radiating toward the central vein. Wnt family members and their receptors reside within pericentral hepatocytes but not oval cells. Magnification: 10X.

Previously Monga *et al.* demonstrated up regulation of Wnt within hours of PHx.[161] At the time of PHx during the 2AAF/PHx protocol resected livers lobes show low levels of Wnt1

expression (Figure 5-2). Levels of Wnt1 increase during peak oval cell production within the cytoplasm of pericentral and inter zonal hepatocytes. Also hepatocytes surrounded by streaming oval cells migrating toward the central vein activate high levels of Wnt1 expression as visualized by IHC.

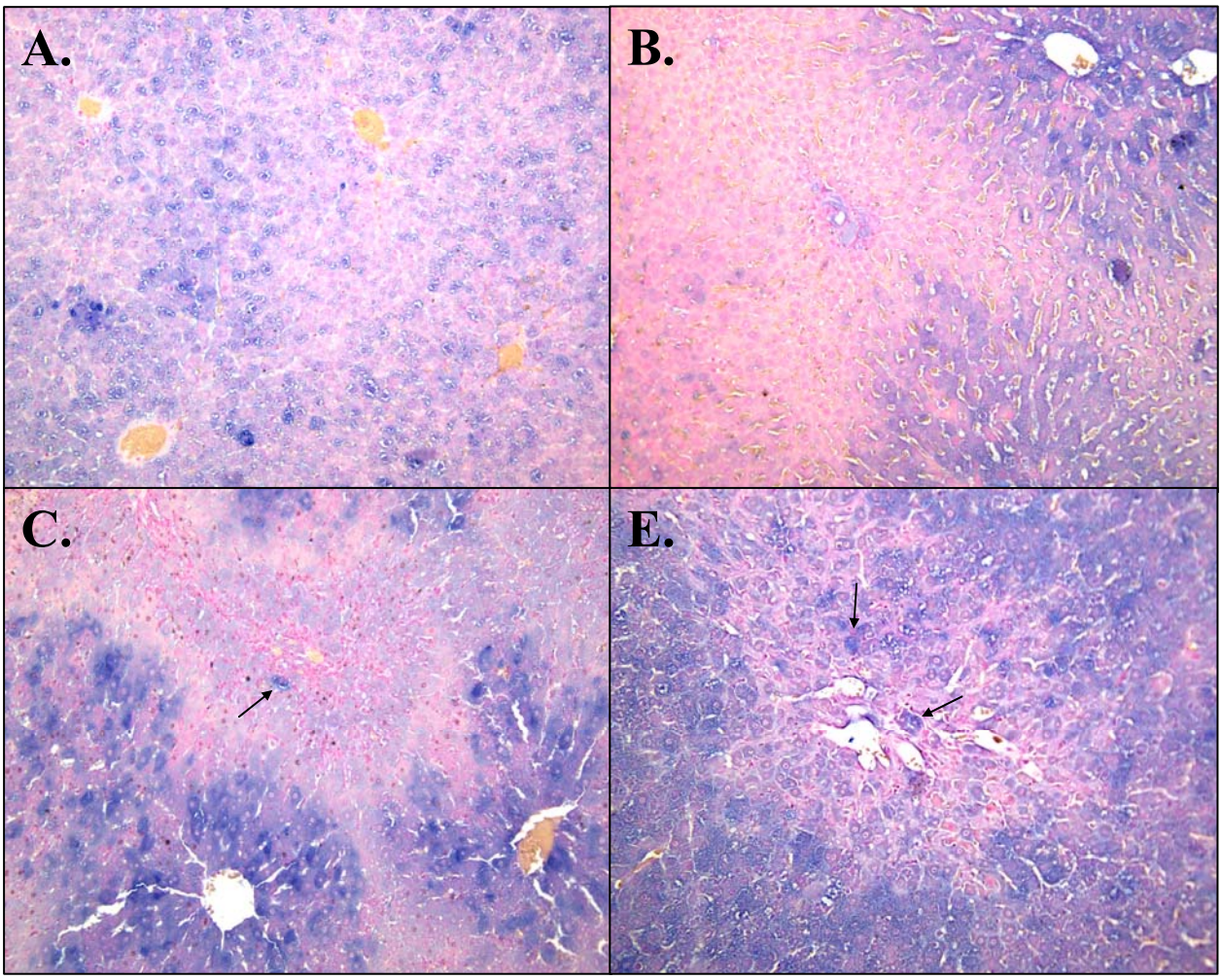

Figure 5-2. Staining of Wnt1 during 2AAF/PHx. A. Day 0; B. Day 3. C. Day 9; D. Day 13. Wnt1 is produced by hepatocytes within hours of PHx as seen in liver obtained at the time of PHx. Pericentral hepatocytes production of Wnt1 can be seen as early as Day 3, and levels increase through out oval cell induction. Hepatocytes engulfed by the migrating oval cells express high levels of Wnt 1 (black arrow). Magnification 20X.

Although Wnt1 expression is not visible within oval cells, they do respond to the Wnt signaling cascade by translocating β-catenin to their nucleus. Dual immunofluorescence for

Wnt1 (red) and β-catenin (blue) of days 9, 13, 15, and 21 days post PHx of the oval cell induction protocol confirms the strict localization of Wnt1 to hepatocytes (Figure 5-3.). β-catenin expression is not confined to adherens junctions within the oval cells. Cytoplasmic and nuclear localization of β-catenin indicates active canonical Wnt signaling pathway.

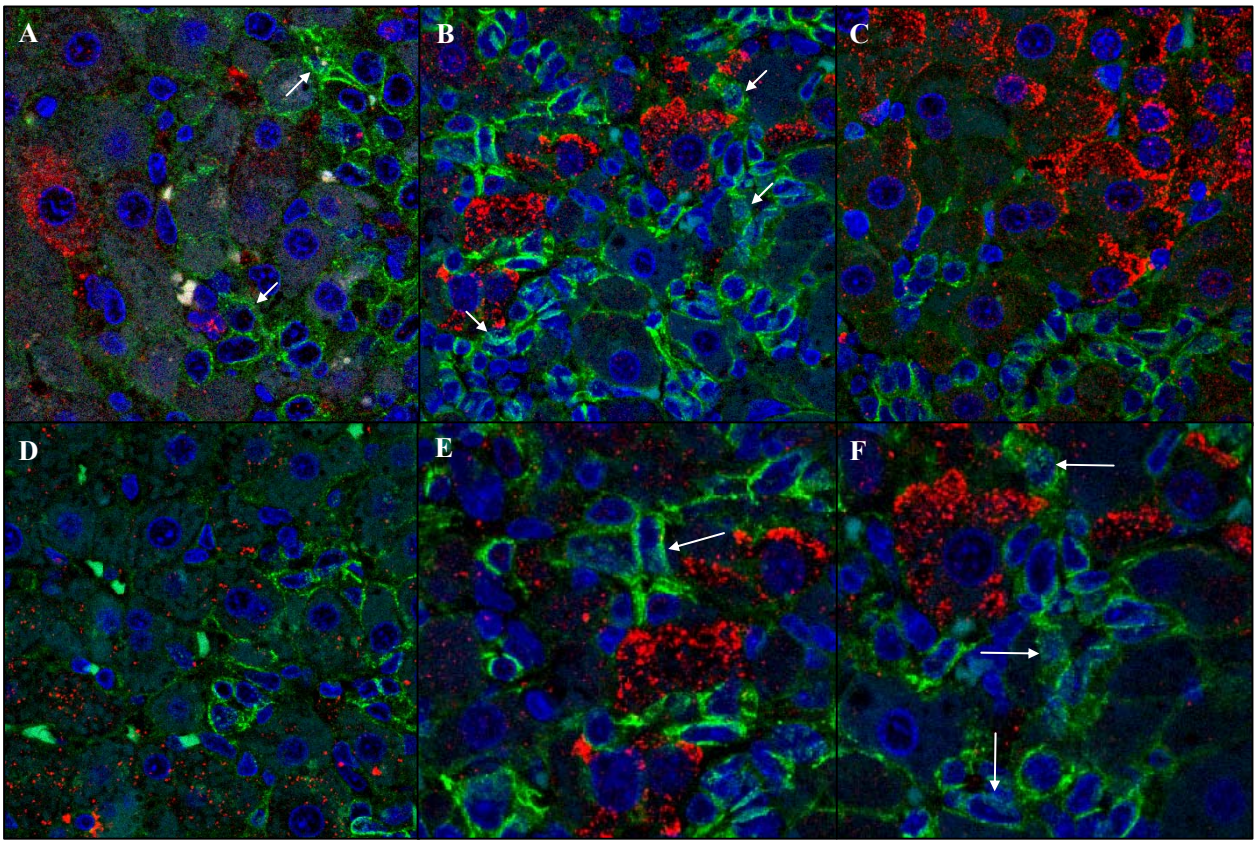

Figure 5-3. Dual Staining of Wnt1 and β-catenin in 2AAF/PHx. A. Day 9; B. Day 13; C. Day 15; D. Day 21; E. and F. Day 13; Pericentral hepatocytes express Wnt1 within their cytoplasm, and oval cells translocate β-catenin to the nucleus in response to Wnt signaling (white arrows). Magnification A.-D. 63X, E. 126X.

Western blot analysis of protein pooled from three individual animals collected from various time points of the oval cell induction protocol further confirmed the Wnt1 expression profile visualized by IHC (Figure 5-4). Both Wnt1 and β-catenin protein levels rapidly increase during the initial stages of oval cell induction and past the peak of oval cell proliferation. This

indicates a role of Wnt1 in not only the activation but more probably in directing the differentiation of oval cells.

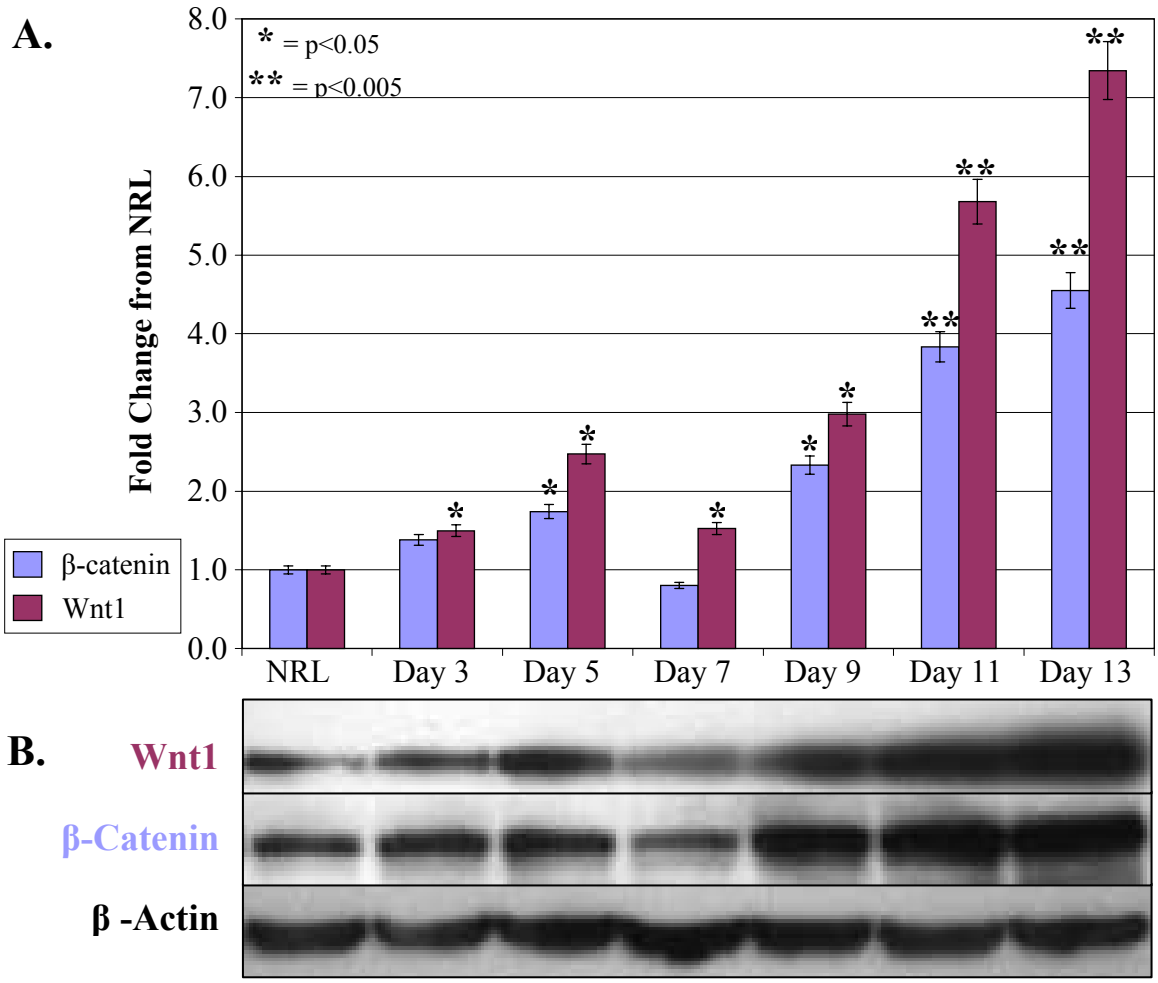

Figure 5-4. Change in β-catenin and Wnt1 protein levels during 2AAF/PHx oval cell induction. A. Densitometric analysis of β-catenin and Wnt1 Western Blots. All data was normalized to β-actin levels and compared to NRL. B. Western blots of various time points after 2AAF implantation and PHx. Both β-catenin and Wnt1 levels increase dramatically after 7 days post PHx.

Fractionation of liver perfusate by Nycodenz gradient centrifugation results in four separate cellular fractions (F1-F4). Fraction 1 mostly includes immunologic cells and stellate cells; Fractions 2 contains oval cells; Fraction 3 holds immature hepatocytes and resident liver macrophages known as Kupffer cells; and Fraction 4 contains mature and multinucleated hepatocytes.

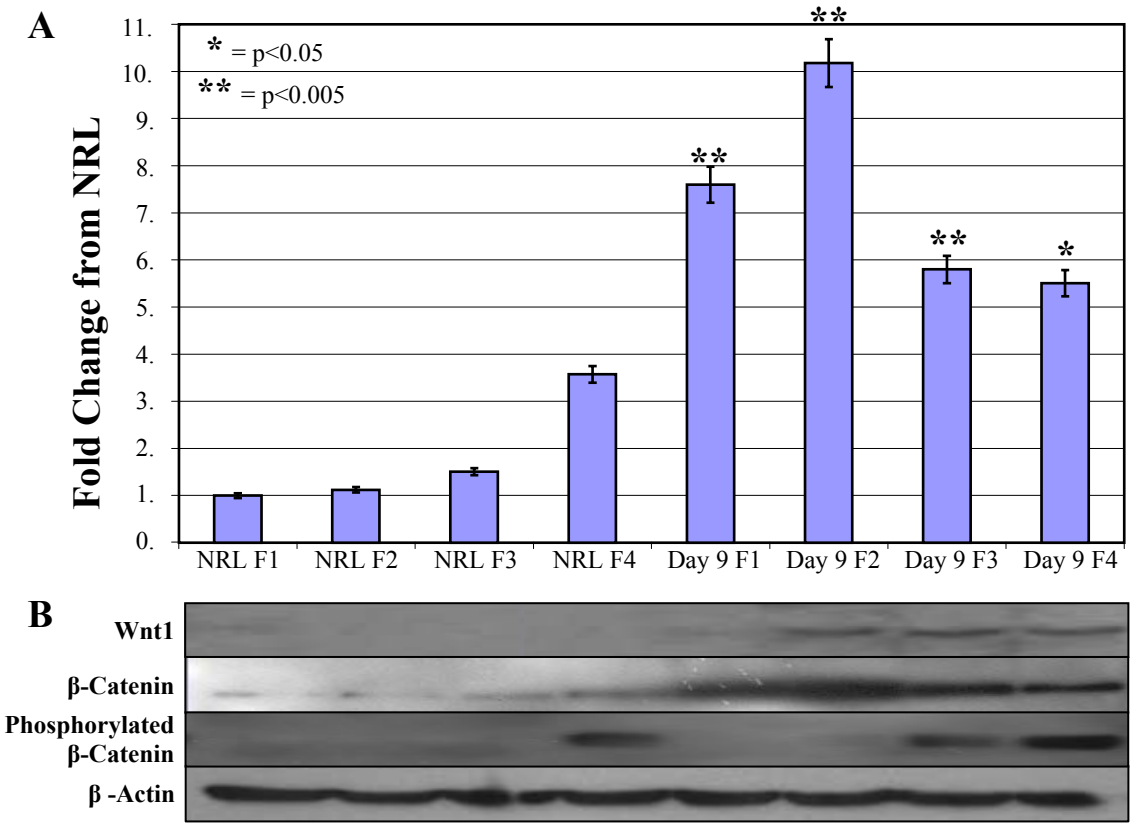

Figure 5-5. β-catenin levels of liver cell fractions. Cells isolated from liver by Nycodenze density based gradient were analyzed by western blot for Wnt1, β-catenin, and phosphorylated β-catenin. A. Densitometric analysis of β-catenin Western Blot. All data was normalized to β-actin levels and compared to NRL F1. B. Western blot of cells isolated by perfusion from normal liver or 9 days post PHx in oval cell induction model. NRL cells fail to express Wnt1, however after oval cell induction, cells within fractions 2 through 4 express Wnt1. β-catenin is considerably increased in cells isolated from Day 9 liver ($p<0.05$ and $p<0.005$). Whereas phosphorylated β-catenin levels are the same in the hepatocyte fraction, increase in the small hepatocyte fraction, and are almost absent from fraction 2 (oval cells) during oval cell induction.

Western blot analysis of protein from these four fractions further confirmed the up regulation of Wnt1 and β-catenin levels in cells from 2AAF day 9 post PHx as compared to NRL (Figure 5-5). More specifically, phosphorylation of β-catenin, an indicator of β-catenin degredation and a lack of Wnt signaling is localized to the hepatocyte fractions. Low levels of phosphorylation is found in the oval cell fraction, but the dramatic 9.08 fold increase in β-catenin

levels in F2 of 2AAF/PHx when compared to the NRL F2 signifies a major decrease in the ubiquitination and destruction of β-catenin in oval cells due to Wnt signaling.

Analysis of the RNA expression of Wnt family members by rt-PCR verified the results seen with IHC and western blot (Figure 5-6). Wnt1 and Wnt3 levels increase over 2AAF/PHx, whereas, low levels of Wnt5a only appears late in oval cell induction. AFP levels indicate the amount of oval cells present within the liver and the expression of AFP peaks at 9 days after PHx. Interestingly, β-catenin message levels remain fairly constant across 2AAF/PHx. This, in conjunction with the drastic protein level increase and the significant lack of phosphorylation in the oval cell fraction, indicates that the increase in β-catenin protein levels is strictly due to a lack of degradation induced by Wnt signaling.

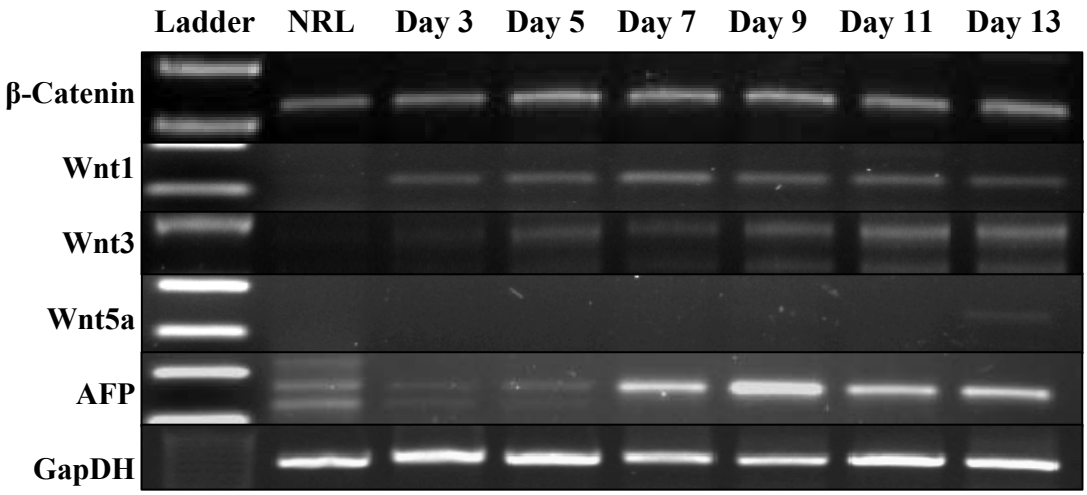

Figure 5-6. Reverse transcription PCR of liver from 2AAF/PHx oval cell induction model. RNA from NRL and 3, 5, 7, 9, 11, and 13 days after PHx in the 2AAF/PHX model. As seen during IHC, levels of Wnt1, Wnt3 and AFP increase during oval cell induction. Wnt5a is not produced until very late in the process, however, β-catenin message levels remain fairly constant.

Real Time PCR of Wnt1 mRNA levels throughout 2AAF/PHx quantitatively demonstrated a statistically relevant increase in Wnt1 message levels prior to and during the peak in oval cell production (Figure 5-7). The Wnt1 mRNA data correlated with the Wnt1 Protein analysis

indicates a strong relationship between Wnt1 and the oval cell induction protocol. The peak in mRNA matches the peak in oval cell proliferation, and the fact that the highest expression of Wnt1 protein occurs after oval cell numbers peak would suggest that Wnt1 more specifically has a role in the oval cell differentiation process.

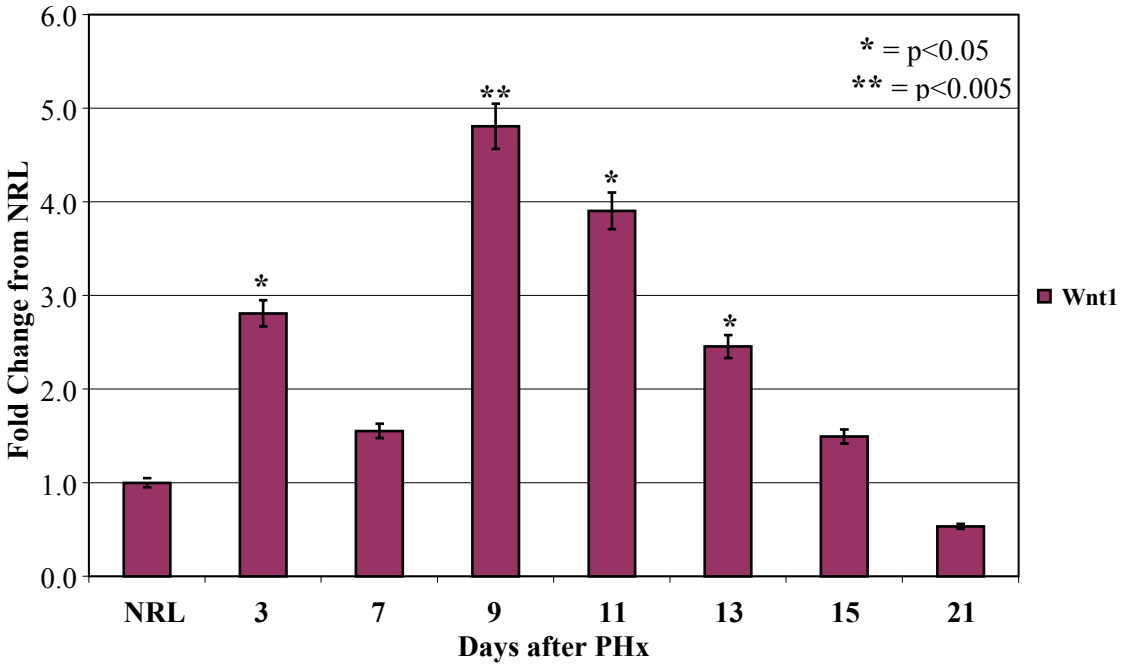

Figure 5-7. Real Time PCR analysis of Wnt1 expression during oval cell induction. Wnt1 mRNA expression increases prior to the peak in oval cell production. The liver contains the greatest Wnt1 message at the height of oval cell production. Significant message levels differences occurs during oval cell induction as compared to NRL.

All data previously collected revealed a correlation between Wnt1 levels and oval cell activation. Although phosphorylation status of β-catenin and imaging of β-catenin nuclear translocation confirm the theory that oval cells respond to Wnt1 signaling, none of this data actually demonstrates a direct oval cell response to Wnt signaling. However, the nuclear translocation of β-catenin by WB-F344 cells, a known hepatic stem cell line, treated with palmitolated Wnt3A definitively links active Wnt signaling and hepatic stem cells (Figure5-8). Untreated WB-F344 cells retain β-catenin within their adherens junctional complexes.

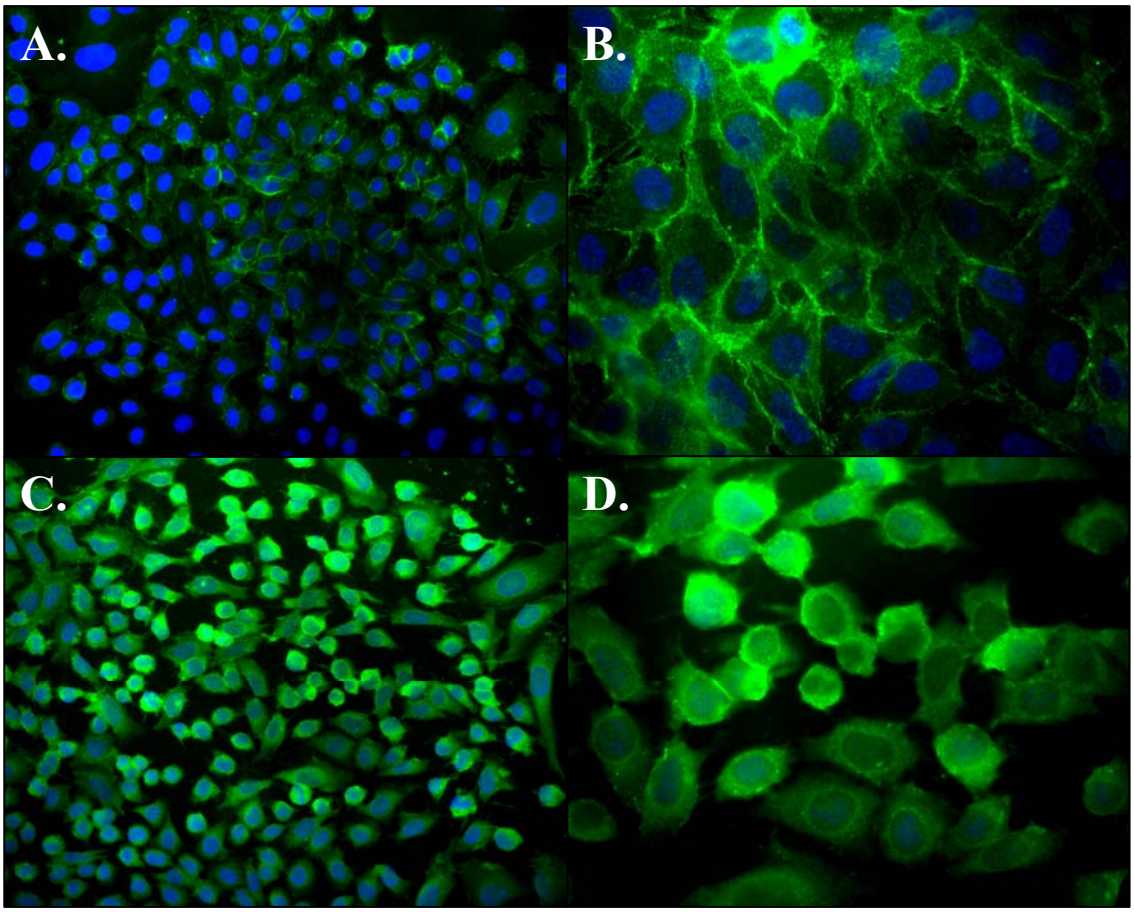

Figure 5-8. Response of WB-F344 cells to Wnt3a stimulation. A. and B.) The β-catenin staining of unstimulated WB cells remains localized to the membrane within adherens junctions. C. and D.) In cells exposed to Wnt3A, β-catenin accumulates in the cytoplasm as well as translocating to the nucleus. Magnification: A. and C. 40X; B. and D. 100X.

5.2 *In vivo* Inhibition of Wnt1 During Oval Cell Induction

To determine the effectiveness of the designed Wnt1 shRNA vector, PC12 cells previously reported to constitutively express murine Wnt1 were transfected with the shRNA in complex with Lipofectamine 2000. Although PC12/Wnt1 cells were highly resistant to the transfection (only approximately 60% transfection efficiency) after 48 hours cells exposed to the shRNA exhibited a 41.8% decrease in cytoplasmic Wnt1 expression (Figure 5-9).

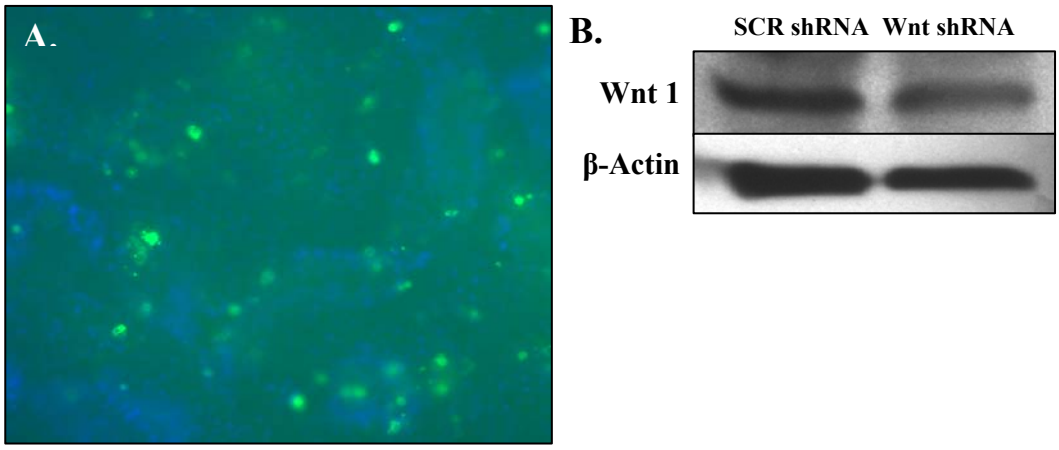

Figure 5-9. Knockdown of Wnt1 in PC12/Wnt1 cells. A. GFP expression in cells 48 hrs after transfection with a Wnt1 shRNA vector containing GFP. B. Western blot of Wnt1 levels in cells treated with Wnt1 shRNA or SCR shRNA. Approximately 60% of PC12/Wnt1 cells expressed GFP 48hrs after transfection. Densitometric analysis showed Wnt1 levels were decreased 41.8% in cells treated with Wnt1 shRNA as compared to SCR shRNA($p<.005$). Magnification 20X.

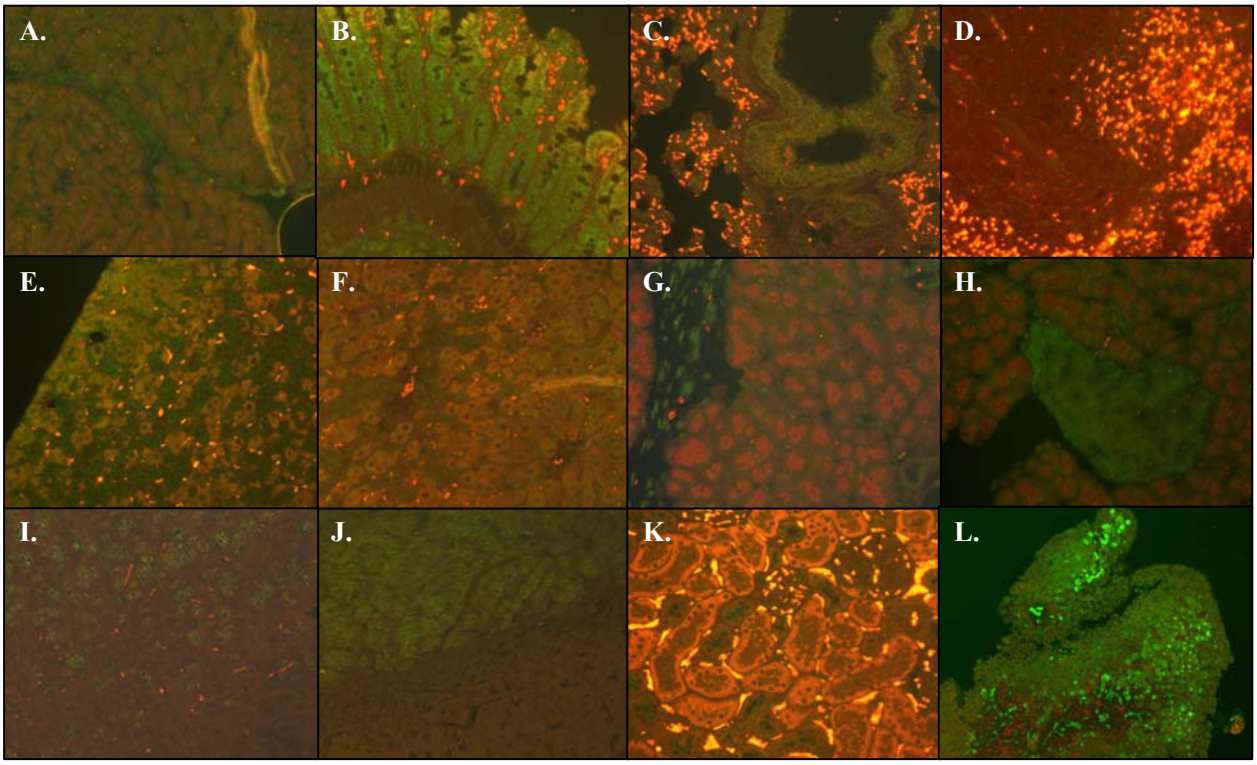

Figure 5-10. GFP expression in shRNA treated animals. A. Heart; B. Intestine; C. Lung; D. Spleen; E. and F. Liver; G. and H. Pancreas; I. Brain, Cortex; J. Brain, Midbrain; K. Kidney; L. Liver from a Control GFP^{+} Mouse. GFP positive cells can be visualized in all tissues sampled, and expression was not limited to vasculature. Magnification 40X.

Analysis of GFP expression through IHC allowed for determination of efficient shRNA vector delivery to target tissues (Figure 5-10). Although expression levels were not uniform across all tissues, GFP expression was found in all tissues analyzed, and expression was not limited to vascular endothelium. Intestinal and bronchial epithelia were distinctly positive. Within the pancreas, islet cells as well as ductular epithelium demonstrated GFP positivity. Interestingly, the brain also expressed high levels of GFP within the cortex and midbrain, demonstrating the cationic lipid delivery mechanism was sufficient to cross the blood-brain barrier. GFP levels were low in spleen and kidney but still visible within the renal tubular epithelium and splenic white pulp.

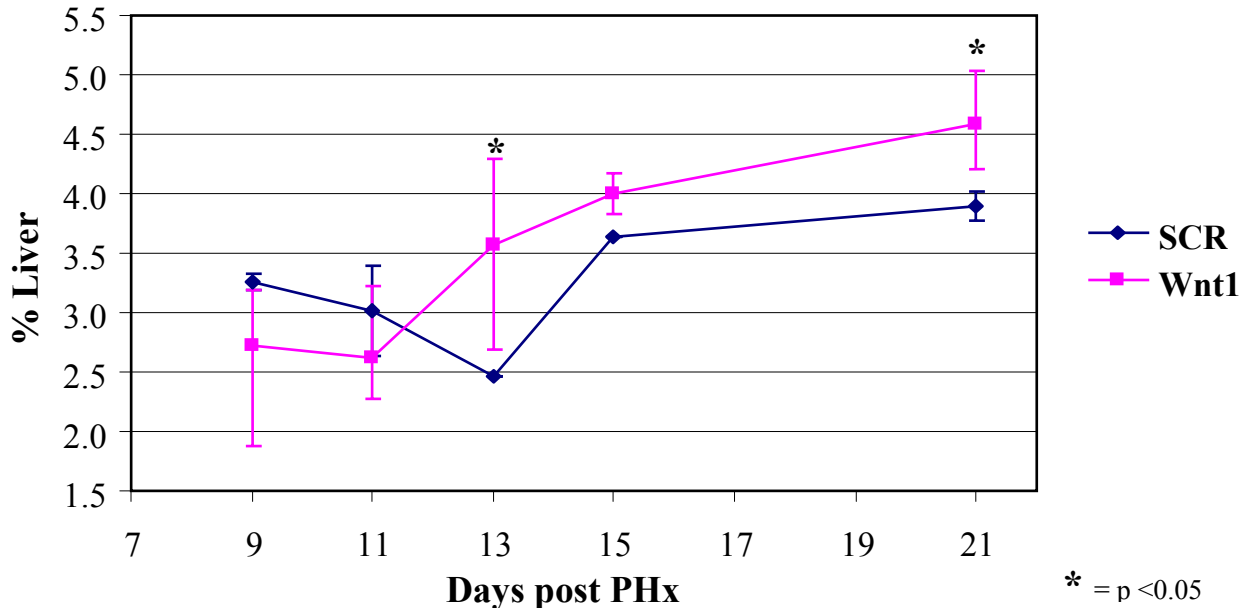

Figure 5-11. Percent liver weights of animals treated with shRNA. The livers of animals treated with shRNA to Wnt1 initially were no larger than those treated with SCR shRNA. However, as time progressed their livers actually surpassed the size of their scrambled counterparts.

Animals and their livers at the time of sacrifice after exposure to shRNA were weighed and the percent of liver weight calculated as liver weight/body weight ×100 (Figure 5-11). Interestingly, Wnt1 shRNA treated animals initially demonstrated no significant difference in

their percent liver weights, however, after what would normally be the peak in oval cell proliferation, Wnt1 shRNA treated animal percent liverweights were on average 0.8% higher than those treated with SCR shRNA ($p < 0.05$). After histological examination, it was possible to conclude this change in percent liver weight was due to both atypical ductular hyperplasia and hepatocyte compensation for the failure of oval cells to function in the regeneration of the liver.

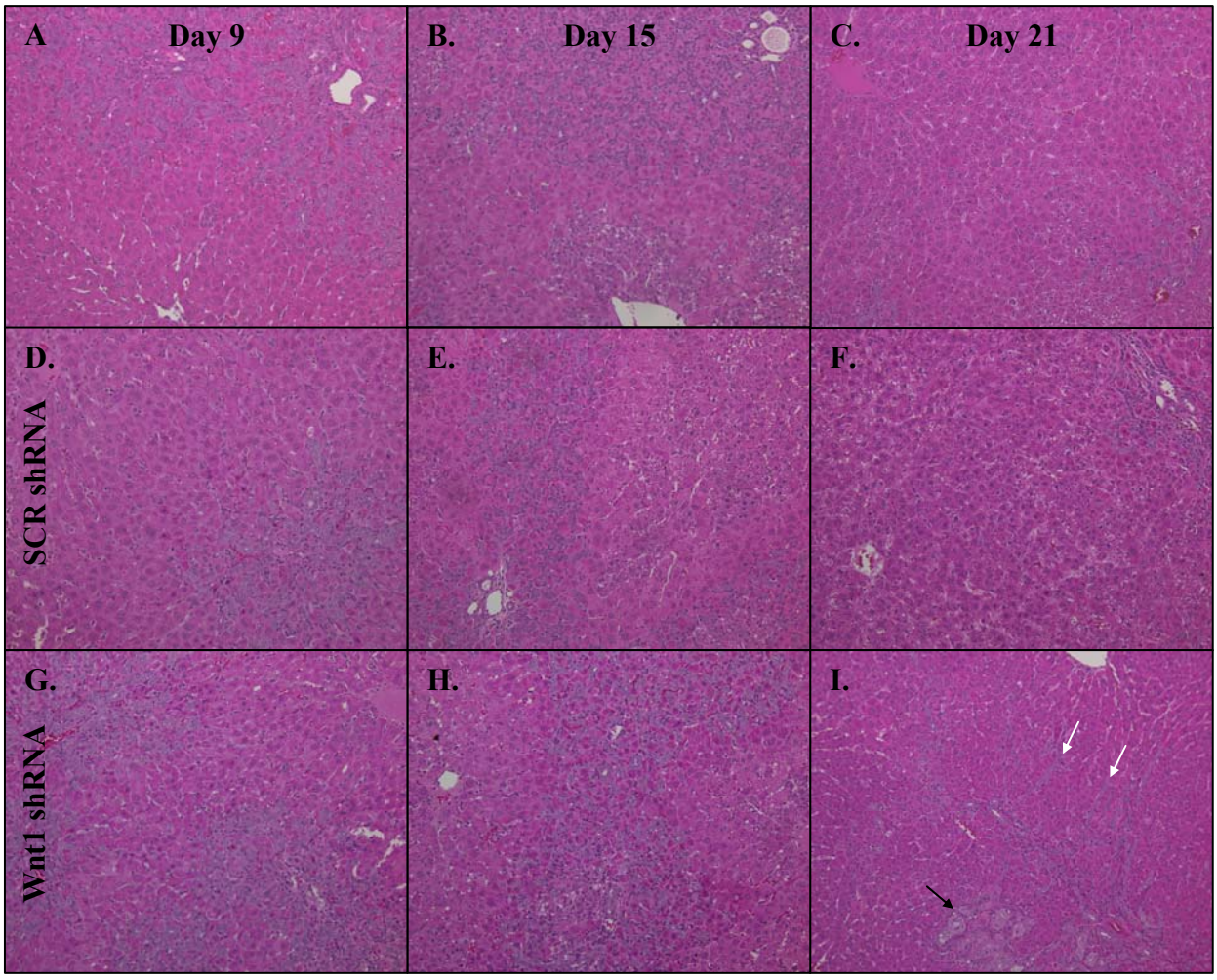

Figure 5-12. H and E of livers from shRNA treated animals. Histologically livers in Wnt shRNA treated animals are similar to nontreated or SCR treated individuals 9 days after PHx. Oval cell infiltrate mimicked the standard reaction. However, as early as 13 to 15 days after PHx atypical ductular hyperplasia appears in Wnt shRNA treated animals. Ultimately, 21 days after PHx, Wnt shRNA treated animals exhibited large sites of atypical ductular hyperplasia (Black arrow) and persistent oval cell streaming from portal triads to other portal triads. (White arrows). SCR shRNA treated animals were unremarkable. Magnification 20X.

Histological analysis of Wnt1 shRNA treated animals revealed morphological changes in oval cell based liver regeneration after Wnt1 shRNA treatment (Figure 5-12). Oval cell morphology appeared unremarkable 9 days after PHx. However, atypical ductular hyperplasia was present in one animal as early as 13 days after PHx. The remaining Wnt1 shRNA treated animals exhibited atypical ductular hyperplasia within 15 days of PHx. As of 21 days after PHx, the atypical ductular hyperplasia appears throughout the liver and oval cells persist in streams extending from portal triads toward other portal triads.

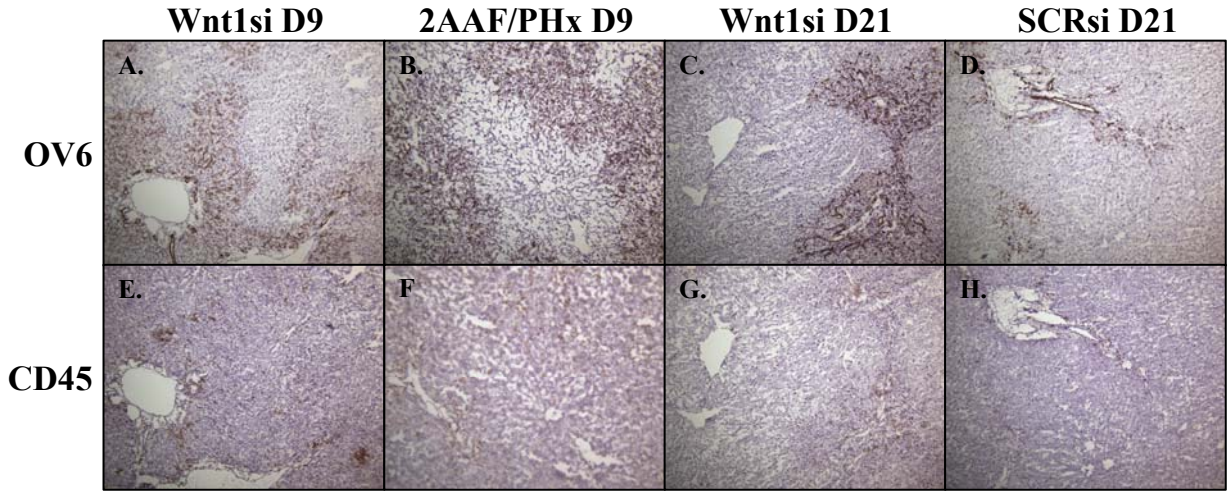

Figure 5-13. OV6 and CD45 staining of serial fresh frozen sections from the livers of shRNA treated animals. A. and E. Wnt1 shRNA treated animal 9 days after PHx; B. and F. 2AAF/PHx animal 9 days after PHx; C. and G. Wnt1 shRNA treated animal 21 days after PHx. D. and H. SCR shRNA treated animal 21 days after PHx. A.-D. OV6 Staining. E.-H. CD45 staining. Although the 2AAF/PHx does induce a slight inflammatory response as seen by infrequent CD45 staining, shRNA treatment does not dramatically increase inflammation. Twenty days post PHx, Wnt shRNA treated animals still posses substantial numbers of oval cells infiltrating the liver, which is not seen in scramble or nontreated animals. Magnification 20X.

Confirmation that the infiltrating cells were in fact oval cells and not inflammatory cells was achieved by staining serial frozen sections for OV6 and CD45 (Figure 5-13). Oval cell numbers in Wnt1 shRNA treated animals approximated those in SCR shRNA treated and nontreated animals 9 days post PHx. Conversely, 21 days post PHx oval cells are virtually

nonexistent in SCR shRNA treated and untreated animals. The cells that compose the atypical ductular hyperplasia as well as the persistent streaming cells exhibit OV6 staining indicating they are of oval cell origin. Minimal CD45 staining in both nontreated and treated animals signify the cells infiltrating the livers are not of an inflammatory origin.

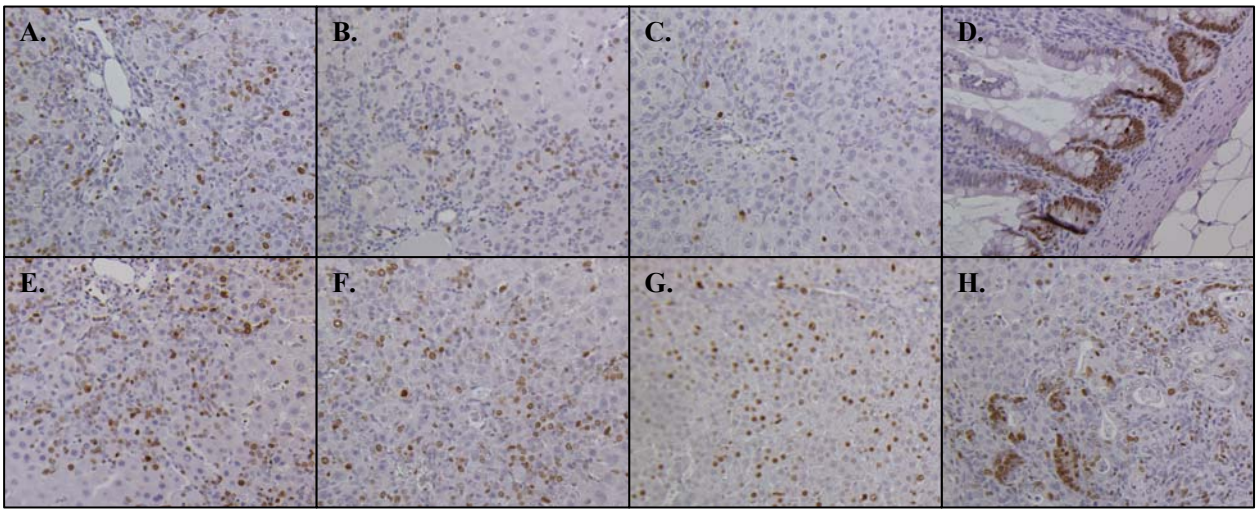

Figure 5-14. Ki67 comparison of 2AAF/Phx versus Wnt1 shRNA treated animals. A. 2AAF/PHx Day 9; B. 2AAF/PHx Day 15; C. 2AAF/PHx Day 21; D. Intestine (Positive control); E. Wnt shRNA Day 9; F. Wnt shRNA Day 15; G. Wnt shRNA Day 21; H. Wnt shRNA Day 21. Proliferation of oval cells 9 days after PHx in shRNA treated animals mimics that observed in 2AAF/PHx alone. In 2AAF/PHx alone, by day 15 proliferation has subsided as oval cells begin differentiating. On the contrary, oval cells in shRNA treated animals continue to proliferate 15 days after PHx. Also, hepatocytes that have begun to recover from the influence of 2AAF exhibit a very high proliferative rate 21 days after PHx. Under normal conditions the liver has completely recovered and division is unnecessary 21 days after PHx. It can also be observed that the sites of atypical ductular hyperplasia are also rapidly dividing 21 days after PHx. Magnification 20X.

The proliferative index of shRNA treated animals was assessed by Ki67 staining (Figure 5-14). Oval cells in Wnt1 shRNA, SCR shRNA treated and standard 2AAF/PHx animals at the day 9 time point were unremarkably similar. However, the oval cells in Wnt shRNA treated animals were still proliferating at an increased rate 15 days post PHx. Interestingly after 21 days the effects of 2AAF upon hepatocytes was diminishing and a significant portion of hepatocytes began dividing in Wnt1 shRNA treated animals. This division along with the ductular

hyperplasia could account for the increased percent liver weights of Wnt1 shRNA treated animals. Also large portions of the hyperplastic foci found in Wnt1 shRNA treated animals 21 days post PHx were also undergoing proliferation as determined by Ki67 staining.

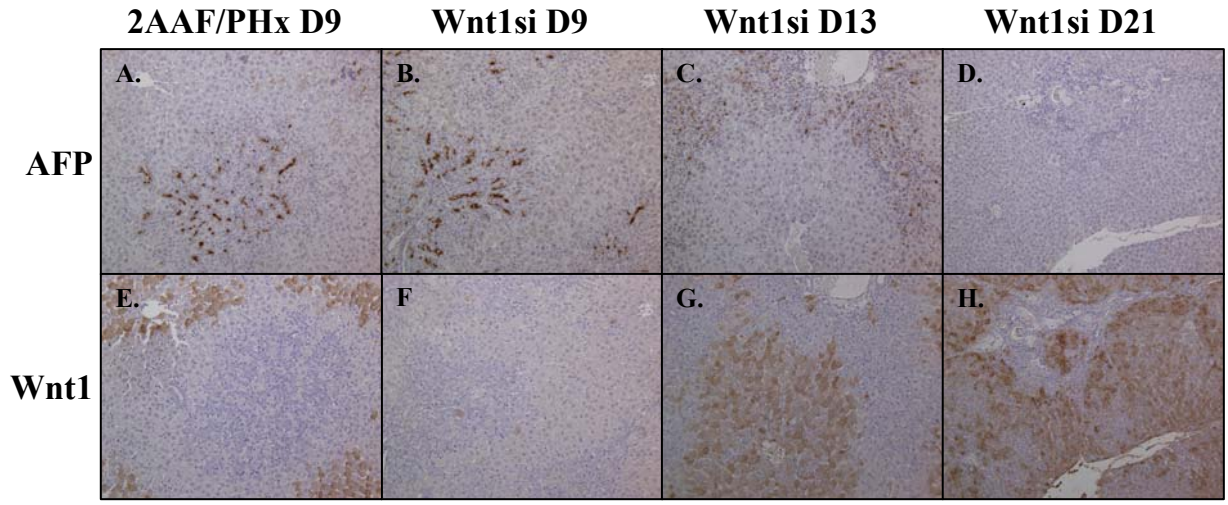

Figure 5-15. AFP and Wnt1 staining of serial sections from Wnt1 shRNA treated animals. A. and E. 2AAF/PHx animal 9 days after PHx after PHx; B. and F. Wnt1 shRNA treated animal 9 days after PHx; C. and G. Wnt1 shRNA treated animal 13 days after PHx. D. and H. Wnt1 shRNA treated animal 21 days after PHx. A.-D. AFP Staining. E.-H. Wnt1 staining. Oval cells from 2AAF/PHx express AFP in high levels, and pericentral hepatocytes express Wnt1. *In vivo* treatment of animals with shRNA to Wnt1 on days 3 and 6 post PHx, inhibits Wnt1 expression until at least day 13 post PHx. After 21 days post PHx, Wnt1 expression returns to inter-zonal and pericentral hepatocytes. The oval cells that infiltrate the liver in shRNA treated animals initially express AFP. After 11 days post PHx, AFP levels decline to negligible 21 days post PHx. Magnification 20X.

As oval cells mature they gain the fetal protein marker known as AFP prior to their differentiation into basophilic, small hepatocytes. Therefore, AFP has been utilized as an oval cell marker. AFP staining of shRNA treated animals further confirmed the previous OV6 staining of the oval cells (Figure 5-15). Nevertheless, although the atypical ductular proliferation maintained OV6 staining, cellular levels of AFP lost intensity beginning 13 days after PHx and were completely lost by 21 days post PHx. Loss of AFP indicates a failure to differentiate toward a hepatic lineage.

Wnt1 levels were also assessed by IHC (Figure 5-15). Although in the standard oval cell induction protocol Wnt1 protein levels are high 9 days post PHx, they were nonexistent by IHC in Wnt1 shRNA treated animals until day 13. Intense expression of Wnt1 appeared in virtually all hepatocytes at this time. On day 21 hepatocytes of Wnt1 shRNA treated animals were still expressing Wnt1, whereas in the SCR shRNA treated or nontreated animals this expression had subsided at this point.

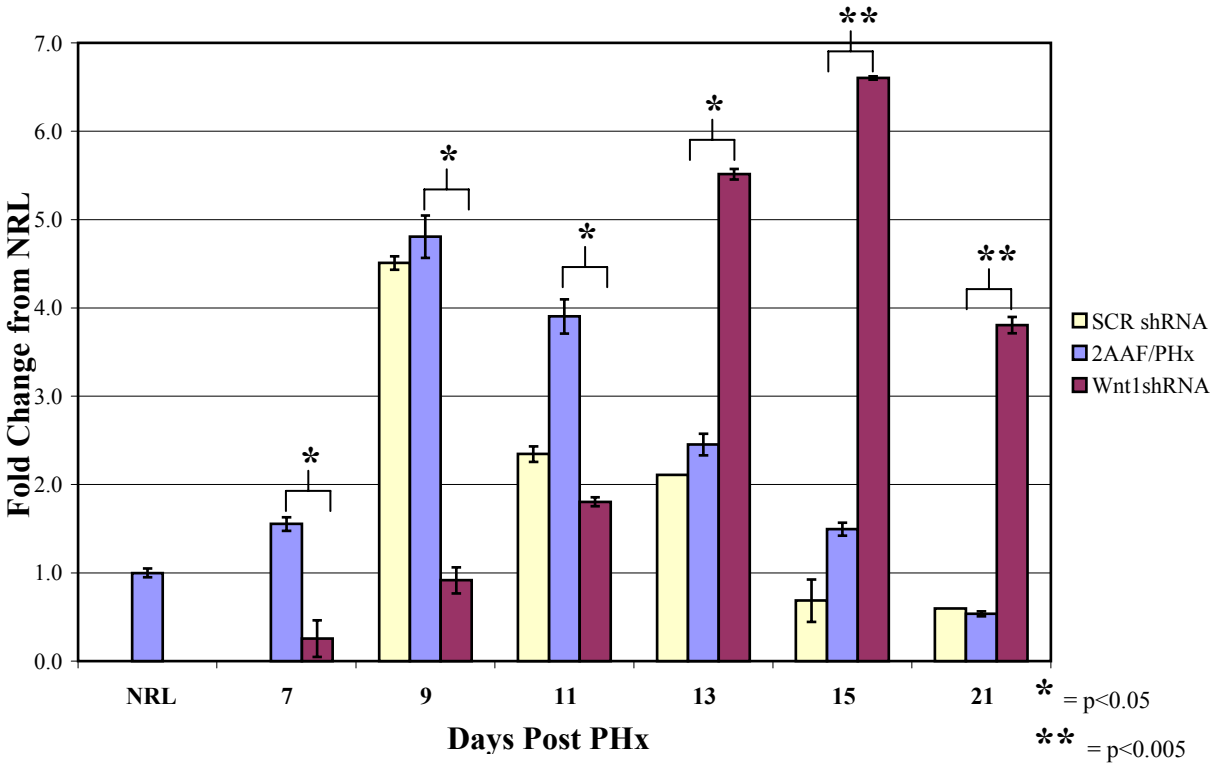

Figure 5-16. Real Time PCR analysis of Wnt1 expression of shRNA treated animals. Wnt1 shRNA treated animals exhibited virtually no Wnt1 message until 13 days after PHx.

Real Time PCR analysis of Wnt1 levels confirmed IHC analysis of Wnt1 levels in shRNA treated animals (Figure 5-16). Animals treated with the scrambled vector demonstrated no appreciable variation in Wnt1 message as compared to 2AAF/PHx control. Wnt1 shRNA treated animals, however, displayed a delayed expression of Wnt1. Wnt1 message was virtually absent

from the animals one day after the last injection with a rapid incline in expression levels 11 days after PHx.

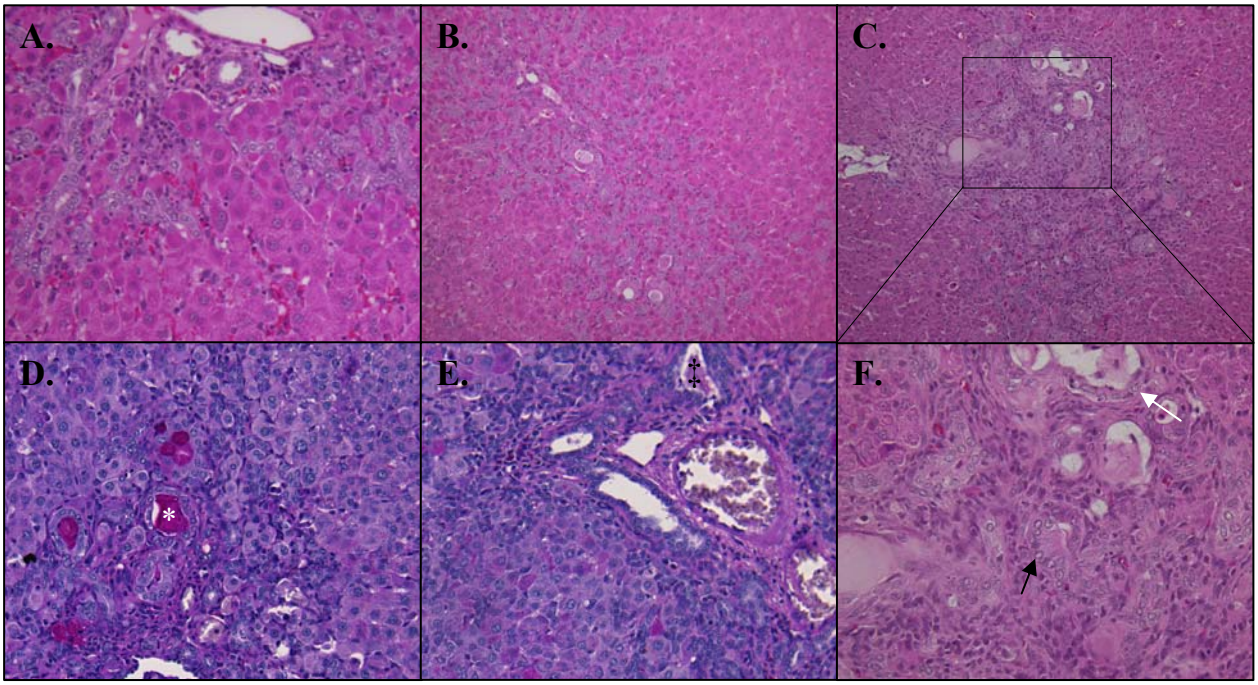

Figure 5-17. Atypical ductular hyperplasia within Wnt shRNA treated animals. A. H and E 9 Days post PHx; B. H and E 13 days post PHx; C. and F. H and E 21 Days post PHx; D. PAS staining of Wnt shRNA treated animal 21 days after PHx; E. PAS staining of day 9 2AAF/PHx. Treatment with shRNA to Wnt1 in the 2AAF/PHx model induces oval cells to undergo differentiation toward a ductular lineage. Ducts remain retain a fairly normal cuboidal morphology until 15-21 days post PHx. At this point, atypical ductular hyperplasia ensues. As seen in D. some ducts undergo transformation into columnar (black arrow) and even squamous (White arrow) phenotypes. The atypical ducts are mucin positive (*), whereas, ducts found in the standard 2AAF/PHx protocol are mucin negative (‡). This indicates the atypical ducts are no longer of a biliary lineage. Magnification A., D., E, and F. 40X; B. and C. 20X.

Further examination of the morphology of the atypical ductular hyperplasia present in Wnt1 shRNA treated animals revealed a potentially preneoplastic state (Figure 5-17). The hyperplastic ducts began appearing 9 days after PHx which is only 3 days after the last Wnt1 shRNA injection. Initially the morphology of the ducts was identical to that of a standard bile duct, small cuboidal cells with a basalar nucleus, but by 15 days post PHx cytology began to change. Not only were the sites of hyperplasia present in nearly all liver lobules, but the cells in

some had undergone metaplasia. Ducts could be visualized with both columnar and squamous metaplasia. Also these hyperplastic ducts were producing mucin which is absent in normal liver or livers from any time during 2AAF/PHx oval cell induction.

CHAPTER 6
DISCUSSION AND FUTURE STUDIES

6.1 Summary of Results

The data presented in this study demonstrated a clear link between Wnt1 signaling and oval cell based liver regeneration. Hepatocytes express and secrete Wnt1 in response to massive hepatic injury (2AAF/PHx). Oval cells invade the liver and respond to Wnt1 signaling by decreasing phosphorylation of β-catenin and translocating it to their nucleus to activate Wnt responsive genes. The message levels of Wnt1 rise during and at the point of peak oval cell production, but protein levels are delayed in reaching their maximum. This clearly indicates that Wnt1 is not responsible for recruiting oval cells to the liver or inducing oval cell proliferation. Instead Wnt1 is essential in guiding oval cells down a hepatic differentiation path.

To provide evidence that Wnt1 is required for oval cell differentiation, an shRNA designed to Wnt1 was utilized *in vivo* during oval cell based liver regeneration. Inhibition of Wnt1 *in vivo* did not delay oval cell migration into the liver. Nevertheless, the oval cells were unable to function normally. Without Wnt1 signaling, oval cells were forced toward a biliary lineage and underwent atypical ductular hyperplasia. It is as if without the Wnt1 signal, oval cells lose AFP expression, and they defaulted to a bile duct phenotype. In compensation, as the effects of 2AAF on hepatocytes wore off, hepatocytes began rapidly dividing to reform the functional liver that the oval cells were unable to generate. Essentially, Wnt1 directs oval cells to differentiate into hepatocytes and without this signal oval cells are unable to differentiate and function normally.

Instead of oval cells simply creating numerous bile ducts, there is morphologic evidence that these cells are potentially going through a preneoplastic process. Within the foci of proliferating ducts, epithelial metaplasia occurred. At the end of the study every animal that was treated with shRNA toward Wnt1 had large areas of atypical ductular hyperplasia, and in about

5-10% of ducts either columnar or squamous metaplasia was present. Chromatin within the metaplastic ducts appeared irregular, but no definitive signs of dysplasia were present. The epithelial metaplasia in conjunction with mucin production is indicative of a preneoplastic process, but no further claims can be made.

Although this study definitively demonstrates a role of Wnt1 in oval cell based liver regeneration and indicates a potentially prenoeplastic state when Wnt1 is absent, it must be repeated and time points collected later than 21 days after PHx. The presence of these atypical ducts is encouraging in regards to indicating an oval cell origin of cholangiocarcinoma, but at this stage no comments can be elicited as to their true purpose. These atypical ducts have two potential paths. They could turn neoplastic or they could regress. Only a longer study could differentiate between these two possible outcomes.

6.2 Interpretation of Results

6.2.1 Wnt Signaling is Required During Oval Cell Based Liver Regeneration

6.2.1.1 Novel findings

No previous study has shown the requirement of the Wnt family in the differentiation of oval cells. Wnts have been implicated in this process but no definitive correlation has been established until now. Also, the mechanism by which Wnt signals are sent and received has only previously been postulated and not truly defined. This research clearly demonstrates a hepatic origin of the Wnt signal and an oval cell response to this signal. When compared to the levels of phosphorylation of β-catenin, the dramatic increase in protein levels of β-catenin without a subsequent increase in β-catenin message can only be explained by Wnt signaling. Also when Wnt1 signaling is absent, oval cell behave distinctly different than when in the presence of Wnt1.

Although much research has been done on β-catenin null and dominant mutant mice and the function of β-catenin in the liver, little has been done with regard to the penultimate upstream signal. Perhaps this is because Wnt is so important and highly regulated.

Mutations in the Wnt family and their receptors are practically nonexistent in the cancer literature. Instead only relative changes in expression levels of certain Wnts can be found. This further implicates the integral role Wnt plays in cellular processes and tumor development. Perhaps changes in the expression of Wnt family members induces so drastic a result the cells are immediately culled to prevent further mishap. If mutations occurred silently in tumors, the expression of these mutations would have some prevalence in the literature but this has not happened.

Conversely, it could be that there are so many Wnts in the family because they are redundant. This redundancy could compensate for any mutations that occur. However, this research tends to negate this theory. Knockdown of a single Wnt protein has induced a drastic phenotype, when other Wnts are known to be expressed throughout the oval cell induction model. This indicates that the evolution of a family of 19 individual Wnts is due to the complex and distinct pathways regulated by these Wnt proteins.

6.2.1.2 Basic science applications

In order for the true nature of oval cells to be understood, their behavior *in situ* has to be monitored, but as Richard Feynman theorized, once you remove something or observe it, the entity has changed due to observation. However, even though the oval cell changes once observed, this is the only mechanism we have to further our understanding of their biology. Therefore, knowing Wnt1 is required for inducing oval cell hepatic differentiation has further defined the role of oval cells in liver regeneration.

Knowledge of the signals necessary to induce oval cells to differentiate into hepatocytes is currently very limited. In culture, the cytokine milieu needed for inducing hepatocyte differentiation is mixed and fairly nonspecific. Also the results are not consistent, not all cytokine mixtures force all oval cells in culture to differentiate. This indicates that either not all the cells are being triggered or there is a heterogeneous population being evaluated. Including Wnt1 in this differentiation media could induce more rapid and more complete differentiation *in vitro.* Also using a known inhibitor of this pathway such as Wif (Wnt inhibitory factor) one could theoretically maintain oval cells in an undifferentiated state in culture.

Investigation of the role of AFP in oval cell differentiation is essential to understanding this process. This research demonstrated AFP expression during the peak in oval cell proliferation. However without Wnt1, AFP expression was lost. This suggests that although some oval cells initially express AFP in the hepatic differentiation path more signals are necessary to complete the differentiation process. Perhaps AFP primes the pump, *i.e*. prepares the oval cells to differentiate into hepatocytes, but Wnt1 actually pushes them over that differentiation hill. If this is the case, determining what induces AFP expression may further allow us to manipulate oval cells in culture and *in vivo.* Also use of Wnt in culture could possibly be utilized to "prime" cells for transplantation.

6.2.1.3 Clinical applications

The demonstration of Wnt1's requirement for oval cell differentiation has strong clinical implications. With the severe shortage of livers to supply the ever increasing need for transplants, clinicians are asking basic scientists to develop alternate methods of organ replacement. Hepatocyte transplant has been performed as previously described, however, the results vary and the number of studies that has been performed is limited. Utilizing stem cells for the facilitation of organ and or functional replacement of tissues has shown great promise. Stem

cells have a much greater capacity for division, differentiation and subsequent repopulation of damaged tissues. Ideally one day we will be able to isolate stem cells from the blood, manipulate them *in vitro*, and implant them into the desired organ.

Oval cells have already been shown to be bone marrow derived, and therefore, theoretically can be isolated from the blood. Oval cells have repeatedly been implanted into livers and donor derivation of regenerated tissue demonstrated. The biggest set back has been the limited numbers of donor derived hepatocytes appearing in the liver. Proving that one can engraft cells into the liver was the first step. Increasing the numbers of donor derived cells is the next step, and perhaps Wnt is the answer. Exposure of oval cells *ex vivo* or *in vivo* to Wnt1 has the potential to increase the differentiation rate of oval cells. Essentially, you could use Wnt exposure to increase the likelihood that the cells you implant will differentiate the way you want them too. If exposure to Wnt1 pushes oval cells down the hepatocyte lineage, it may function exactly the same way on the bone marrow precursor of the oval cell. If true, this would facilitate and even simpler method of obtaining cells for transplantation into the liver.

The clinical implications of this are astounding. It is known that hepatocyte transplantation only results in transient engraftment. Perhaps transplanting precursor cells might ensure prolonged engraftment. If Wnt1 signaling truly initiates hepatocyte differentiation while not inhibiting proliferation, treatment of oval cells or bone marrow precursor cells might even cause an intrahepatic expansion of the transplanted cells along with directed hepatocyte differentiation. Essentially, the engrafted cells are directed down a hepatic lineage and allowed to proliferate, which would increase the numbers of engrafted cells and, therefore, enlarge the size of the graft without having to increase the number of transplanted cells.

6.2.2 Disregulation of Wnt1 Signaling and Cancer Induction

6.2.2.1 Atypical ductular proliferation after Wnt1 shRNA exposure i*n vivo*

It is evident that without Wnt1 signaling oval cells cannot differentiate down the hepatic lineage. Every animal exposed to the Wnt1 shRNA had developed severe atypical ductular hyperplasia globally throughout the liver after 21 days. These foci were even undergoing potentially preneoplastic changes. Nuclear pleomorphisms and squamous or columnar metaplasia was evident in numerous of these foci in various animals. These findings indicate that oval cells must receive a distinct pattern of signals to undergo hepatocyte differentiation. Without Wnt1 signaling they "defaulted" to a biliary lineage. The dual differentiation potential of the oval cell has been well documented, but until now no one has shown that without stimulus to become a hepatocyte, oval cells revert to a biliary lineage. Also Wnt1 is the only signal preventing the severe atypical ductular hyperplastic phenotype. This suggests that tight control of oval cells is required and without tight control there are drastic consequences.

Although the study only went for 21 days after PHx, this potentially preneoplastic state strongly aids the oval cell theory of cholangiocarcinoma. If all it takes to push oval cells down a cancerous road is the lack of one growth factor, then it is no wonder that they have the potential to create liver tumors of hepatocyte and/or biliary origin. Extension of the study will determine if these foci of atypical ductular hyperplasia spontaneously resolve or if they undergo true transformation into a tumor of a biliary origin.

Use of the Wnt1 shRNA 2AAF/PHx protocol could provide a very fast method for forming repeatable tumors in a very rapid manner. Assuming the foci develop into true cancerous nodules within another month of the study, this would result in a cholangiocarcinoma model executable in only 2 months from initiation of the protocol (2AAF implantation) and tumor development (8-9 weeks). That is definitely faster than the standard protocols utilized in the literature.

6.2.2.2 Use of Wnt1 in preneoplastic foci

Conceivably Wnt1 exposure might reverse the changes seen during Wnt1 shRNA and 2AAF/PHx protocol. If so then this could be utilized to reverse preneoplastic changes initiated by disregulation of hepatic stem cells. Only studies that replace the Wnt1 protein levels after shRNA could determine the efficacy of this technique, but if Wnt1 protein does "rescue" this phenotype, it could lead to therapies in the early stages of cancer or preneoplastic changes seen in massive, chronic hepatic damage.

Increasing the understanding of the regulation of stem cells can only aid in our understanding of the things that can potentially go wrong during initiation and promotion of tumors. It may be that Wnt1 is the only signal preventing oval cells from becoming cancerous during stem cell based liver regeneration. This is possibly why oval cells are rarely seen in human livers. The need for oval cells must be so great as to risk the potential damage they could inflict if tight control on them is not maintained. This risk need not be taken in normal situations as hepatocytes have the immense capacity for proliferation necessary to resolve most hepatic injuries. Perhaps oval cells are only seen in humans when hepatocyte function is beyond repair and the need outweighs the potential for damage induced by disregulation of the hepatic stem cell.

6.3 Future Studies

6.3.1 Continuation of the Wnt1 shRNA 2AAF/PHx Protocol

Extending the shRNA studies will elucidate the question of whether the changes seen within the foci of atypical ductular hyperplasia are truly preneoplastic or benign. Resolution of these foci is possible and is seen in the DDC diet in mice. Remove the stimulus (DDC) and the oval cell numbers decline and the sites of atypical ductular hyperplasia regress. If the foci present 21 days after PHx in the Wnt1 shRNA treated animals do not regress but maintain themselves or

progress into neoplastic lesions, then the functions of Wnt1 in oval cells must truly be discovered. Knowledge of one growth factor having such control over normal function or tumorgenic changes would greatly advance the fields of stem cell and tumor biology.

6.3.2 Exposure of Oval Cells to Wnt1

Isolation of oval cells and exposure of them to Wnt1 *in vitro* may facilitate oval cell engraftment in oval cell transplantation. It also may induce hepatocyte differentiation in culture faster than the current differentiation protocols. Currently Wnt1 is not available in a palmitolated form. However, the same isolation procedure employed by Nusse *et al.* for Wnt3a, Wnt5a, Wnt5b, and Wnt7a (currently all sold by R and D Systems) could be easily employed. Furthermore, portal vein injections of Wnt1 protein during 2AAF/PHx protocol might increase the rate by which oval cells regenerate the liver. Use of a retrovirus containing the Wnt1 gene could also be utilized to expose the infiltrating oval cells to an increase in Wnt1 signaling during 2AAF/PHx.

6.3.3 Wnt1 Conditional Knockout Animal

Changes in Wnt levels during embryogenesis results in severe and drastic malformations of numerous tissues and/or failure of the embryo to fully develop, therefore development of a Wnt1 conditional knockout could further define the role of Wnt1 in liver regeneration. Controlling Wnt1 with a Tet on/off system and the albumin promoter would result in a conditional knockout that would only be active in the liver when desired, i.e. during oval cell activation protocols. This knockout would confirm the results seen in this study and provide alternative methods for looking at the role of Wnt1 in the liver.

6.3.4 Summary of Proposed Experiments

Each of these experiments would confirm the results found in this study while enhancing the knowledge of Wnt1's role in oval cell based liver regeneration and normal liver function.

Complete understanding of Wnt1's functions during these processes is essential for the understanding of oval cell based liver regeneration. This study has demonstrated the crucial role Wnt1 plays in initiation of oval cell hepatocyte differentiation, as well as how disregulation of Wnt1 creates a potentially preneoplastic state in oval cells.

LIST OF REFERENCES

1. Desmet,V.J. The liver: biology and pathobiology. Arias,I.M. & Boyer,J.L. (eds.), pp. 3-15, Raven Press, New York (2001).

2. Crawford,J.M. Robbins and Cotran: Pathologic Basis of Disease. Kumar,V., Abbas,A. & Fausto N. (eds.), pp. 877-938, Elsevier Saunders, Philadelphia (2005).

3. Cunningham,C.C. & Van Horn,C.G. Energy availability and alcohol-related liver pathology. *Alcohol Res. Health* **27**, 291-299 (2003).

4. Ross,M.H., Kaye,G.I. & Pawlina,W. Histology: a text and atlas. Lippincott Williams & Wilkins, Philadelphia, Pa (2003).

5. Fausto N. The Liver biology and pathobiology. Arias,I.M. & Boyer,J.L. (eds.), pp. 1501-1518, Raven Press, New York (1994).

6. Saxena,R., Theise,N.D. & Crawford,J.M. Microanatomy of the human liver-exploring the hidden interfaces. *Hepatology* **30**, 1339-1346 (1999).

7. Steer,C.J. Liver regeneration. *FASEB J.* **9**, 1396-1400 (1995).

8. Higgins,G.M. & Anderson R.M. Experimental pathology of the liver: Restoration of the liver of the white rat following partial surgical removal. *Arch Pathol* **12**, 186-202 (1931).

9. Bucher NLR. Regeneration of Mammalian Liver. *Int Rev Cytol* **15**, 245 (1963).

10. Michalopoulos,G.K. Liver regeneration: molecular mechanisms of growth control. *FASEB J.* **4**, 176-187 (1990).

11. Rabes,H.M. Kinetics of hepatocellular proliferation after partial resection of the liver. *Prog. Liver Dis.* **5**, 83-99 (1976).

12. Petersen,B.E. Hepatic stem cells and growth factor regulation in liver regeneration following toxic injury. 1996. Graduate School of Public Health, Dept. of Environmental and Occupational Health and Toxicology, University of Pittsburgh.
Ref Type: Thesis/Dissertation

13. Michalopoulos,G.K. & DeFrances,M.C. Liver regeneration. *Science* **276**, 60-66 (1997).

14. Badr,M.Z., Belinsky,S.A., Kauffman,F.C. & Thurman,R.G. Mechanism of hepatotoxicity to periportal regions of the liver lobule due to allyl alcohol: role of oxygen and lipid peroxidation. *J. Pharmacol. Exp. Ther.* **238**, 1138-1142 (1986).

15. Edwards,M.J., Keller,B.J., Kauffman,F.C. & Thurman,R.G. The involvement of Kupffer cells in carbon tetrachloride toxicity. *Toxicol. Appl. Pharmacol.* **119**, 275-279 (1993).

16. Lombardi,B. & Ugazio,G. Serum lipoproteins in rats with carbon tetrachloride-induced fatty liver. *J. Lipid Res.* **6**, 498-505 (1965).

17. Reid,W.D. Mechanism of allyl alcohol-induced hepatic necrosis. *Experientia* **28**, 1058-1061 (1972).

18. Fisher,R.A. & Strom,S.C. Human hepatocyte transplantation: worldwide results. *Transplantation* **82**, 441-449 (2006).

19. Matas,A.J. *et al.* Hepatocellular transplantation for metabolic deficiencies: decrease of plasms bilirubin in Gunn rats. *Science* **192**, 892-894 (1976).

20. Mito,M., Kusano,M. & Kawaura,Y. Hepatocyte transplantation in man. *Transplant. Proc.* **24**, 3052-3053 (1992).

21. Raper,S.E. *et al.* Safety and feasibility of liver-directed ex vivo gene therapy for homozygous familial hypercholesterolemia. *Ann. Surg.* **223**, 116-126 (1996).

22. Ambrosino,G. *et al.* Isolated hepatocyte transplantation for Crigler-Najjar syndrome type 1. *Cell Transplant.* **14**, 151-157 (2005).

23. Fox,I.J. *et al.* Treatment of the Crigler-Najjar syndrome type I with hepatocyte transplantation. *N. Engl. J. Med.* **338**, 1422-1426 (1998).

24. Horslen,S.P. & Fox,I.J. Hepatocyte transplantation. *Transplantation* **77**, 1481-1486 (2004).

25. Hughes,R.D., Mitry,R.R. & Dhawan,A. Hepatocyte transplantation for metabolic liver disease: UK experience. *J. R. Soc. Med.* **98**, 341-345 (2005).

26. Soriano,H.E. *et al.* Lack of C/EBP alpha gene expression results in increased DNA synthesis and an increased frequency of immortalization of freshly isolated mice [correction of rat] hepatocytes. *Hepatology* **27**, 392-401 (1998).

27. Strom,S.C. *et al.* Hepatocyte transplantation as a bridge to orthotopic liver transplantation in terminal liver failure. *Transplantation* **63** , 559-569 (1997).

28. Parkin,D.M., Bray,F., Ferlay,J. & Pisani,P. Global cancer statistics, 2002. *CA Cancer J. Clin.* **55**, 74-108 (2005).

29. Di Bisceglie,A.M., Rustgi,V.K., Hoofnagle,J.H., Dusheiko,G.M. & Lotze,M.T. NIH conference. Hepatocellular carcinoma. *Ann. Intern. Med.* **108**, 390-401 (1988).

30. Goodman,Z.D. Neoplasms of the liver. *Mod. Pathol.* **20 Suppl 1**, S49-S60 (2007).

31. Maximow A. Der Lymphozyt als gemeinsame Stammzelle der verschiedenen Blutelemente in der embryonalen Entwicklung und im postfetalen Leben der Säugetiere. *Folia Haematol. Int. Mag. Klin. Morphol. Blutforsch.* **8**, 125-141 (1909).

32. Buckner,C.D. *et al.* Allogeneic marrow engraftment following whole body irradiation in a patient with leukemia. *Blood* **35**, 741-750 (1970).

33. Osawa,M., Hanada,K., Hamada,H. & Nakauchi,H. Long-term lymphohematopoietic reconstitution by a single CD34-low/negative hematopoietic stem cell. *Science* **273**, 242-245 (1996).

34. Pappenheim,A. Morphologische Hämatologie. W. Klinkhardt, Leipzig (1919).

35. Magnuson,T., Epstein,C.J., Silver,L.M. & Martin,G.R. Pluripotent embryonic stem cell lines can be derived from tw5/tw5 blastocysts. *Nature* **298**, 750-753 (1982).

36. Evans,M.J. & Kaufman,M.H. Establishment in culture of pluripotential cells from mouse embryos. *Nature* **292**, 154-156 (1981).

37. Keller,G.M. In vitro differentiation of embryonic stem cells. *Curr. Opin. Cell Biol.* **7**, 862-869 (1995).

38. Martin,G.R. Isolation of a pluripotent cell line from early mouse embryos cultured in medium conditioned by teratocarcinoma stem cells. *Proc. Natl. Acad. Sci. U. S. A* **78**, 7634-7638 (1981).

39. Smith,A.G. Embryo-derived stem cells: of mice and men. *Annu. Rev. Cell Dev. Biol.* **17** , 435-462 (2001).

40. Kabrun,N. *et al.* Flk-1 expression defines a population of early embryonic hematopoietic precursors. *Development* **124**, 2039-2048 (1997).

41. Nishikawa,S.I., Nishikawa,S., Hirashima,M., Matsuyoshi,N. & Kodama,H. Progressive lineage analysis by cell sorting and culture identifies FLK1+VE-cadherin+ cells at a diverging point of endothelial and hemopoietic lineages. *Development* **125**, 1747-1757 (1998).

42. Robertson,S.M., Kennedy,M., Shannon,J.M. & Keller,G. A transitional stage in the commitment of mesoderm to hematopoiesis requiring the transcription factor SCL/tal-1. *Development* **127**, 2447-2459 (2000).

43. Schmitt,R.M., Bruyns,E. & Snodgrass,H.R. Hematopoietic development of embryonic stem cells in vitro: cytokine and receptor gene expression. *Genes Dev.* **5**, 728-740 (1991).

44. Faloon,P. *et al.* Basic fibroblast growth factor positively regulates hematopoietic development. *Development* **127**, 1931-1941 (2000).

45. Fehling,H.J. *et al.* Tracking mesoderm induction and its specification to the hemangioblast during embryonic stem cell differentiation. *Development* **130**, 4217-4227 (2003).

46. Huber,T.L., Kouskoff,V., Fehling,H.J., Palis,J. & Keller,G. Haemangioblast commitment is initiated in the primitive streak of the mouse embryo. *Nature* **432**, 625-630 (2004).

47. Lacaud,G. *et al.* Runx1 is essential for hematopoietic commitment at the hemangioblast stage of development in vitro. *Blood* **100**, 458-466 (2002).

48. Bautch,V.L. *et al.* Characterization of the vasculogenic block in the absence of vascular endothelial growth factor-A. *Blood* **95**, 1979-1987 (2000).

49. Kearney,J.B. *et al.* Vascular endothelial growth factor receptor Flt-1 negatively regulates developmental blood vessel formation by modulating endothelial cell division. *Blood* **99**, 2397-2407 (2002).

50. Roberts,D.M. *et al.* The vascular endothelial growth factor (VEGF) receptor Flt-1 (VEGFR-1) modulates Flk-1 (VEGFR-2) signaling during blood vessel formation. *Am. J. Pathol.* **164**, 1531-1535 (2004).

51. Zippo,A., De Robertis,A., Bardelli,M., Galvagni,F. & Oliviero,S. Identification of Flk-1 target genes in vasculogenesis: Pim-1 is required for endothelial and mural cell differentiation in vitro. *Blood* **103**, 4536-4544 (2004).

52. Maltsev,V.A., Rohwedel,J., Hescheler,J. & Wobus,A.M. Embryonic stem cells differentiate in vitro into cardiomyocytes representing sinusnodal, atrial and ventricular cell types. *Mech. Dev.* **44**, 41-50 (1993).

53. Hescheler,J. *et al.* Embryonic stem cells: a model to study structural and functional properties in cardiomyogenesis. *Cardiovasc. Res.* **36**, 149-162 (1997).

54. Banach,K., Halbach,M.D., Hu,P., Hescheler,J. & Egert,U. Development of electrical activity in cardiac myocyte aggregates derived from mouse embryonic stem cells. *Am. J. Physiol Heart Circ. Physiol* **284**, H2114-H2123 (2003).

55. Buttery,L.D. *et al.* Differentiation of osteoblasts and in vitro bone formation from murine embryonic stem cells. *Tissue Eng* **7**, 89-99 (2001).

56. Rohwedel,J. *et al.* Muscle cell differentiation of embryonic stem cells reflects myogenesis in vivo: developmentally regulated expression of myogenic determination genes and functional expression of ionic currents. *Dev. Biol.* **164**, 87-101 (1994).

57. Kramer,J. *et al.* Embryonic stem cell-derived chondrogenic differentiation in vitro: activation by BMP-2 and BMP-4. *Mech. Dev.* **92**, 193-205 (2000).

58. Dani,C. *et al.* Differentiation of embryonic stem cells into adipocytes in vitro. *J. Cell Sci.* **110 (Pt 11)**, 1279-1285 (1997).

59. Lumelsky,N. *et al.* Differentiation of embryonic stem cells to insulin-secreting structures similar to pancreatic islets. *Science* **292**, 1389-1394 (2001).

60. Hamazaki,T. *et al.* Hepatic maturation in differentiating embryonic stem cells in vitro. *FEBS Lett.* **497**, 15-19 (2001).

61. Chinzei,R. *et al.* Embryoid-body cells derived from a mouse embryonic stem cell line show differentiation into functional hepatocytes. *Hepatology* **36**, 22-29 (2002).

62. Gault,V.A. *et al.* Effects of Subchronic Treatment With the Long-Acting Glucose-Dependent Insulinotropic Polypeptide Receptor Agonist, N-AcGIP, on Glucose Homeostasis in Streptozotocin-Induced Diabetes. *Pancreas* **35**, 73-79 (2007).

63. Asahara,T. *et al.* Isolation of putative progenitor endothelial cells for angiogenesis. *Science* **275**, 964-967 (1997).

64. Ferrari,G. *et al.* Muscle regeneration by bone marrow-derived myogenic progenitors. *Science* **279**, 1528-1530 (1998).

65. Petersen,B.E. *et al.* Bone marrow as a potential source of hepatic oval cells. *Science* **284**, 1168-1170 (1999).

66. Bjornson,C.R., Rietze,R.L., Reynolds,B.A., Magli,M.C. & Vescovi,A.L. Turning brain into blood: a hematopoietic fate adopted by adult neural stem cells in vivo. *Science* **283**, 534-537 (1999).

67. Clarke,D.L. *et al.* Generalized potential of adult neural stem cells. *Science* **288**, 1660-1663 (2000).

68. Alison,M.R. *et al.* Hepatocytes from non-hepatic adult stem cells. *Nature* **406**, 257 (2000).

69. Theise,N.D. *et al.* Liver from bone marrow in humans. *Hepatology* **32**, 11-16 (2000).

70. Theise,N.D. *et al.* Derivation of hepatocytes from bone marrow cells in mice after radiation-induced myeloablation. *Hepatology* **31**, 235-240 (2000).

71. Krause,D.S. *et al.* Multi-organ, multi-lineage engraftment by a single bone marrow-derived stem cell. *Cell* **105**, 369-377 (2001).

72. Herzog,E.L., Chai,L. & Krause,D.S. Plasticity of marrow-derived stem cells. *Blood* **102**, 3483-3493 (2003).

73. Ianus,A., Holz,G.G., Theise,N.D. & Hussain,M.A. In vivo derivation of glucose-competent pancreatic endocrine cells from bone marrow without evidence of cell fusion. *J. Clin. Invest* **111**, 843-850 (2003).

74. Korbling,M. *et al.* Hepatocytes and epithelial cells of donor origin in recipients of peripheral-blood stem cells. *N. Engl. J. Med.* **346**, 738-746 (2002).

75. Jiang,Y. *et al.* Pluripotency of mesenchymal stem cells derived from adult marrow. *Nature* **418**, 41-49 (2002).

76. Horwitz,E.M. Stem cell plasticity: a new image of the bone marrow stem cell. *Curr. Opin. Pediatr.* **15**, 32-37 (2003).

77. Petersen,B.E. Hepatic "stem" cells: coming full circle. *Blood Cells Mol. Dis.* **27**, 590-600 (2001).

78. Petersen,B.E. & Terada,N. Stem cells: a journey into a new frontier. *J. Am. Soc. Nephrol.* **12**, 1773-1780 (2001).

79. Boyle,A.J., Schulman,S.P., Hare,J.M. & Oettgen,P. Is stem cell therapy ready for patients? Stem Cell Therapy for Cardiac Repair. Ready for the Next Step. *Circulation* **114**, 339-352 (2006).

80. Lindvall,O. & Kokaia,Z. Stem cells for the treatment of neurological disorders. *Nature* **441**, 1094-1096 (2006).

81. Sam,J., Angoulvant,D., Fazel,S., Weisel,R.D. & Li,R.K. Heart cell implantation after myocardial infarction. *Coron. Artery Dis.* **16**, 85-91 (2005).

82. Hollander,A.P. *et al.* Maturation of tissue engineered cartilage implanted in injured and osteoarthritic human knees. *Tissue Eng* **12**, 1787-1798 (2006).

83. Kuo,C.K., Li,W.J., Mauck,R.L. & Tuan,R.S. Cartilage tissue engineering: its potential and uses. *Curr. Opin. Rheumatol.* **18**, 64-73 (2006).

84. Cebotari,S. *et al.* Clinical application of tissue engineered human heart valves using autologous progenitor cells. *Circulation* **114**, I132-I137 (2006).

85. Atala,A., Bauer,S.B., Soker,S., Yoo,J.J. & Retik,A.B. Tissue-engineered autologous bladders for patients needing cystoplasty. *Lancet* **367**, 1241-1246 (2006).

86. Lindeman,B. *et al.* Alteration of G1 cell-cycle protein expression and induction of p53 but not p21/waf1 by the DNA-modifying carcinogen 2-acetylaminofluorene in growth-stimulated hepatocytes in vitro. *Mol. Carcinog.* **24** , 36-46 (1999).

87. Petersen,B.E., Zajac,V.F. & Michalopoulos,G.K. Hepatic oval cell activation in response to injury following chemically induced periportal or pericentral damage in rats. *Hepatology* **27**, 1030-1038 (1998).

88. Petersen,B.E., Goff,J.P., Greenberger,J.S. & Michalopoulos,G.K. Hepatic oval cells express the hematopoietic stem cell marker Thy-1 in the rat. *Hepatology* **27**, 433-445 (1998).

89. Petersen,B.E. *et al.* Mouse A6-positive hepatic oval cells also express several hematopoietic stem cell markers. *Hepatology* **37**, 632-640 (2003).

90. Corcelle,V., Stieger,B., Gjinovci,A., Wollheim,C.B. & Gauthier,B.R. Characterization of two distinct liver progenitor cell subpopulations of hematopoietic and hepatic origins. *Exp. Cell Res.* **312**, 2826-2836 (2006).

91. Guettier,C. Which stem cells for adult liver?. *Ann. Pathol.* **25**, 33-44 (2005).

92. Qin,A.L., Zhou,X.Q., Zhang,W., Yu,H. & Xie,Q. Characterization and enrichment of hepatic progenitor cells in adult rat liver. *World J. Gastroenterol.* **10**, 1480-1486 (2004).

93. Strain,A.J., Crosby,H.A., Nijjar,S., Kelly,D.A. & Hubscher,S.G. Human liver-derived stem cells. *Semin. Liver Dis.* **23**, 373-384 (2003).

94. Van Den Heuvel,M.C. *et al.* Expression of anti-OV6 antibody and anti-N-CAM antibody along the biliary line of normal and diseased human livers. *Hepatology* **33**, 1387-1393 (2001).

95. Kano,J., Noguchi,M., Kodama,M. & Tokiwa,T. The in vitro differentiating capacity of nonparenchymal epithelial cells derived from adult porcine livers. *Am. J. Pathol.* **156**, 2033-2043 (2000).

96. Roskams,T., De Vos,R. & Desmet,V. 'Undifferentiated progenitor cells' in focal nodular hyperplasia of the liver. *Histopathology* **28**, 291-299 (1996).

97. Yang,L., Faris,R.A. & Hixson,D.C. Characterization of a mature bile duct antigen expressed on a subpopulation of biliary ductular cells but absent from oval cells. *Hepatology* **18**, 357-366 (1993).

98. Yang,L., Faris,R.A. & Hixson,D.C. Long-term culture and characteristics of normal rat liver bile duct epithelial cells. *Gastroenterology* **104**, 840-852 (1993).

99. Zvibel,I., Fiorino,A.S., Brill,S. & Reid,L.M. Phenotypic characterization of rat hepatoma cell lines and lineage-specific regulation of gene expression by differentiation agents. *Differentiation* **63**, 215-223 (1998).

100. Engelhardt,N.V. *et al.* Common antigen of oval and biliary epithelial cells (A6) is a differentiation marker of epithelial and erythroid cell lineages in early development of the mouse. *Differentiation* **55**, 19-26 (1993).

101. Evarts,R.P., Hu,Z., Fujio,K., Marsden,E.R. & Thorgeirsson,S.S. Activation of hepatic stem cell compartment in the rat: role of transforming growth factor alpha, hepatocyte growth factor, and acidic fibroblast growth factor in early proliferation. *Cell Growth Differ.* **4**, 555-561 (1993).

102. Hixson,D.C. & Allison,J.P. Monoclonal antibodies recognizing oval cells induced in the liver of rats by N-2-fluorenylacetamide or ethionine in a choline-deficient diet. *Cancer Res.* **45**, 3750-3760 (1985).

103. Evarts,R.P., Nagy,P., Marsden,E. & Thorgeirsson,S.S. A precursor-product relationship exists between oval cells and hepatocytes in rat liver. *Carcinogenesis* **8**, 1737-1740 (1987).

104. Evarts,R.P., Nagy,P., Nakatsukasa,H., Marsden,E. & Thorgeirsson,S.S. In vivo differentiation of rat liver oval cells into hepatocytes. *Cancer Res.* **49**, 1541-1547 (1989).

105. Fausto,N. Protooncogenes and growth factors associated with normal and abnormal liver growth. *Dig. Dis. Sci.* **36**, 653-658 (1991).

106. Preisegger,K.H. *et al.* Atypical ductular proliferation and its inhibition by transforming growth factor beta1 in the 3,5-diethoxycarbonyl-1,4-dihydrocollidine mouse model for chronic alcoholic liver disease. *Lab Invest* **79**, 103-109 (1999).

107. Golding,M., Sarraf,C., Lalani,E. & Alison,M.R. Reactive biliary epithelium: The product of a pluripotential stem cell compartment? *Human Pathology* **27**, 872-884 (1996).

108. Sigal,S.H. *et al.* Evidence for Stem-Cells and Lineages in Embryonic and Adult Liver, A Tissue Assuming A Quiescent State. *Journal of Cellular Biochemistry* 268 (1993).

109. Evarts,R.P. *et al.* Cellular and molecular changes in the early stages of chemical hepatocarcinogenesis in the rat. *Cancer Res.* **50**, 3439-3444 (1990).

110. Lemire,J.M. & Fausto,N. Multiple alpha-fetoprotein RNAs in adult rat liver: cell type-specific expression and differential regulation. *Cancer Res.* **51**, 4656-4664 (1991).

111. Marceau,N., Grenier,A., Noel,M., Mailhot,D. & Loranger,A. Modulation of cytokeratin and actin gene expression and fibrillar organization in cultured rat hepatocytes. *Biochem. Cell Biol.* **70**, 1238-1248 (1992).

112. Petersen,B.E., Zajac,V.F. & Michalopoulos,G.K. Bile ductular damage induced by methylene dianiline inhibits oval cell activation. *Am. J. Pathol.* **151**, 905-909 (1997).

113. Lagasse,E. *et al.* Purified hematopoietic stem cells can differentiate into hepatocytes in vivo. *Nat. Med.* **6**, 1229-1234 (2000).

114. Deng,J., Steindler,D.A., Laywell,E.D. & Petersen,B.E. Neural trans-differentiation potential of hepatic oval cells in the neonatal mouse brain. *Exp. Neurol.* **182**, 373-382 (2003).

115. Lowes,K.N., Croager,E.J., Olynyk,J.K., Abraham,L.J. & Yeoh,G.C. Oval cell-mediated liver regeneration: Role of cytokines and growth factors. *J. Gastroenterol. Hepatol.* **18**, 4-12 (2003).

116. Kinosita,R. Studies on the cancerogenic chemical substances. *Transactions of the Japanese Pathological Society* 665-727 (1937).

117. Farber E. Similarities in the sequence of early histologic changes induced in the liver of the rat by ethionine, 2-acetylaminoflouorene, and 3'-methyl-4-dimethylaminoazbenzene. Cancer Res. 16, 142. 1956.
Ref Type: Journal (Full)

118. Leduc,E.H. & Wilson,J.W. Injury to liver cells in carbon tetrachloride poisoning; histochemical changes induced by carbon tetrachloride in mouse liver protected by sulfaguanidine. *AMA. Arch. Pathol.* **65**, 147-157 (1958).

119. Lemire,J.M., Shiojiri,N. & Fausto,N. Oval cell proliferation and the origin of small hepatocytes in liver injury induced by D-galactosamine. *Am. J. Pathol.* **139**, 535-552 (1991).

120. Price,J.M., Harman,J.W., Miller,E.C. & Miller,J.A. Progressive microscopic alterations in the livers of rats fed the hepatic carcinogens 3'-methyl-4-dimethylaminoazobenzene and 4'-fluoro-4-dimethylaminoazobenzene. *Cancer Res.* **12**, 192-200 (1952).

121. Wilson,J.W. &Leduc,E.H. Role of cholangioles in restoration of the liver of the mouse after dietary injury. *J. Pathol. Bacteriol.* **76**, 441-449 (1958).

122. Petersen,B.E. & Hatch,H.M. Methods of tissue engineering. Atala,A. & Lanza,R.P. (eds.), pp. 429-437 (Academic Press, San Diego, CA,2001).

123. Sell,S. Stem cell origin of cancer and differentiation therapy. *Crit Rev. Oncol. Hematol.* **51**, 1-28 (2004).

124. Farber,E. Hepatocyte proliferation in stepwise development of experimental liver cell cancer. *Dig. Dis. Sci.* **36**, 973-978 (1991).

125. Sell,S. & Pierce,G.B. Maturation arrest of stem cell differentiation is a common pathway for the cellular origin of teratocarcinomas and epithelial cancers. *Lab Invest* **70**, 6-22 (1994).

126. Dunsford,H.A., Karnasuta,C., Hunt,J.M. & Sell,S. Different lineages of chemically induced hepatocellular carcinoma in rats defined by monoclonal antibodies. *Cancer Res.* **49**, 4894-4900 (1989).

127. Dunsford,H.A. & Sell,S. Production of monoclonal antibodies to preneoplastic liver cell populations induced by chemical carcinogens in rats and to transplantable Morris hepatomas. *Cancer Res.* **49**, 4887-4893 (1989).

128. Van Eyken,P. *et al.* Cytokeratin expression in hepatocellular carcinoma: an immunohistochemical study. *Hum. Pathol* **19**, 562-568 (1988).

129. Denk,H., Krepler,R., Lackinger,E., Artlieb,U. & Franke,W.W. Biochemical and immunocytochemical analysis of the intermediate filament cytoskeleton in human hepatocellular carcinomas and in hepatic neoplastic nodules of mice. *Lab Invest* **46**, 584-596 (1982).

130. Hsia,C.C., Evarts,R.P., Nakatsukasa,H., Marsden,E.R. & Thorgeirsson,S.S. Occurrence of oval-type cells in hepatitis B virus-associated human hepatocarcinogenesis. *Hepatology* **16**, 1327-1333 (1992).

131. Vandersteenhoven,A.M., Burchette,J. & Michalopoulos,G. Characterization of ductular hepatocytes in end-stage cirrhosis. *Arch Pathol Lab Med.* **114**, 403-406 (1990).

132. Fausto,N. Oval cells and liver carcinogenesis: an analysis of cell lineages in hepatic tumors using oncogene transfection techniques. *Prog. Clin. Biol. Res.* **331**, 325-334 (1990).

133. Garfield,S., Huber,B.E., Nagy,P., Cordingley,M.G. & Thorgeirsson,S.S. Neoplastic transformation and lineage switching of rat liver epithelial cells by retrovirus-associated oncogenes. *Mol. Carcinog.* **1**, 189-195 (1988).

134. Marceau,N. Cell lineages and differentiation programs in epidermal, urothelial and hepatic tissues and their neoplasms. *Lab Invest* **63**, 4-20 (1990).

135. Gordon,M.D. & Nusse,R. Wnt signaling: multiple pathways, multiple receptors, and multiple transcription factors. *J. Biol. Chem.* **281**, 22429-22433 (2006).

136. Willert,K. *et al.* Wnt proteins are lipid-modified and can act as stem cell growth factors. *Nature* **423**, 448-452 (2003).

137. He,X. & Axelrod,J.D. A WNTer wonderland in Snowbird. *Development* **133**, 2597-2603 (2006).

138. Hinck,L., Nelson,W.J. & Papkoff,J. Wnt-1 modulates cell-cell adhesion in mammalian cells by stabilizing beta-catenin binding to the cell adhesion protein cadherin. *J. Cell Biol.* **124**, 729-741 (1994).

139. Nusse,R. & Varmus,H.E. Many tumors induced by the mouse mammary tumor virus contain a provirus integrated in the same region of the host genome. *Cell* **31**, 99-109 (1982).

140. Smalley,M.J. & Dale,T.C. Wnt signalling in mammalian development and cancer. *Cancer Metastasis Rev.* **18**, 215-230 (1999).

141. Wodarz,A. & Nusse,R. Mechanisms of Wnt signaling in development. *Annu. Rev. Cell Dev. Biol.* **14**, 59-88 (1998).

142. Borycki,A.G. & Emerson,C.P., Jr. Multiple tissue interactions and signal transduction pathways control somite myogenesis. *Curr. Top. Dev. Biol.* **48**, 165-224 (2000).

143. Church,V.L. & Francis-West,P. Wnt signalling during limb development. *Int. J. Dev. Biol.* **46**, 927-936 (2002).

144. Deardorff,M.A. & Klein,P.S. Xenopus frizzled-2 is expressed highly in the developing eye, otic vesicle and somites. *Mech. Dev.* **87**, 229-233 (1999).

145. Galli,L.M. *et al.* A proliferative role for Wnt-3a in chick somites. *Dev. Biol.* **269**, 489-504 (2004).

146. Hartmann,C. & Tabin,C.J. Dual roles of Wnt signaling during chondrogenesis in the chicken limb. *Development* **127**, 3141-3159 (2000).

147. Hartmann,C. & Tabin,C.J. Wnt-14 plays a pivotal role in inducing synovial joint formation in the developing appendicular skeleton. *Cell* **104**, 341-351 (2001).

148. Ikeya,M., Lee,S.M., Johnson,J.E., McMahon,A.P. & Takada,S. Wnt signalling required for expansion of neural crest and CNS progenitors. *Nature* **389**, 966-970 (1997).

149. Lee,S.M., Tole,S., Grove,E. & McMahon,A.P. A local Wnt-3a signal is required for development of the mammalian hippocampus. *Development* **127**, 457-467 (2000).

150. Sela-Donenfeld,D. & Kalcheim,C. Localized BMP4-noggin interactions generate the dynamic patterning of noggin expression in somites. *Dev. Biol.* **246**, 311-328 (2002).

151. Yamaguchi,T.P., Bradley,A., McMahon,A.P. & Jones,S. A Wnt5a pathway underlies outgrowth of multiple structures in the vertebrate embryo. *Development* **126**, 1211-1223 (1999).

152. Bienz,M. & Clevers,H. Linking colorectal cancer to Wnt signaling. *Cell* **103**, 311-320 (2000).

153. Kostakopoulou,K., Vogel,A., Brickell,P. & Tickle,C. 'Regeneration' of wing bud stumps of chick embryos and reactivation of Msx-1 and Shh expression in response to FGF-4 and ridge signals. *Mech. Dev.* **55**, 119-131 (1996).

154. Reya,T. *et al.* A role for Wnt signalling in self-renewal of haematopoietic stem cells. *Nature* **423**, 409-414 (2003).

155. Kioussi,C. *et al.* Identification of a Wnt/Dvl/beta-Catenin --> Pitx2 pathway mediating cell-type-specific proliferation during development. *Cell* **111**, 673-685 (2002).

156. Treier,M. *et al.* Multistep signaling requirements for pituitary organogenesis in vivo. *Genes Dev.* **12**, 1691-1704 (1998).

157. van de Wetering,M. *et al.* The beta-catenin/TCF-4 complex imposes a crypt progenitor phenotype on colorectal cancer cells. *Cell* **111**, 241-250 (2002).

158. Karim,R., Tse,G., Putti,T., Scolyer,R. & Lee,S. The significance of the Wnt pathway in the pathology of human cancers. *Pathology* **36**, 120-128 (2004).

159. Luo,J. *et al.* Wnt signaling and human diseases: what are the therapeutic implications? *Lab Invest* **87**, 97-103 (2007).

160. Torres,M.A. *et al.* Activities of the Wnt-1 class of secreted signaling factors are antagonized by the Wnt-5A class and by a dominant negative cadherin in early Xenopus development. *J. Cell Biol.* **133**, 1123-1137 (1996).

161. Monga,S.P., Pediaditakis,P., Mule,K., Stolz,D.B. & Michalopoulos,G.K. Changes in WNT/beta-catenin pathway during regulated growth in rat liver regeneration. *Hepatology* **33**, 1098-1109 (2001).

162. Thompson,M.D. & Monga,S.P. WNT/beta-catenin signaling in liver health and disease. *Hepatology* **45**, 1298-1305 (2007).

163. Cadoret,A. *et al.* Hepatomegaly in transgenic mice expressing an oncogenic form of beta-catenin. *Cancer Res.* **61**, 3245-3249 (2001).

164. Tan,X. *et al.* Epidermal growth factor receptor: a novel target of the Wnt/beta-catenin pathway in liver. *Gastroenterology* **129**, 285-302 (2005).

165. Benhamouche,S., Decaens,T., Perret,C. & Colnot,S. Wnt/beta-catenin pathway and liver metabolic zonation: a new player for an old concept. *Med. Sci. (Paris)* **22**, 904-906 (2006).

166. Benhamouche,S. *et al.* Apc tumor suppressor gene is the "zonation-keeper" of mouse liver. *Dev. Cell* **10**, 759-770 (2006).

167. Tsao,M.S., Smith,J.D., Nelson,K.G. & Grisham,J.W. A diploid epithelial cell line from normal adult rat liver with phenotypic properties of 'oval' cells. *Exp. Cell Res.* **154**, 38-52 (1984).

168. Muller-Borer,B.J. *et al.* Mechanisms controlling the acquisition of a cardiac phenotype by liver stem cells. *Proc. Natl. Acad. Sci. U. S. A* **104**, 3877-3882 (2007).

169. Couchie,D. *et al.* Expression and role of Gas6 protein and of its receptor Axl in hepatic regeneration from oval cells in the rat. *Gastroenterology* **129**, 1633-1642 (2005).

170. Zhong,X.G., He,S., Yin,W., Deng,J.Y. & Chen,B. Tropism of adult liver stem cells toward hepatocellular carcinoma cells in vitro. *Zhonghua Gan Zang. Bing. Za Zhi.* **13**, 644-647 (2005).

171. Muller-Borer,B.J. *et al.* Adult-derived liver stem cells acquire a cardiomyocyte structural and functional phenotype ex vivo. *Am. J. Pathol.* **165**, 135-145 (2004).

172. Couchie,D., Holic,N., Chobert,M.N., Corlu,A. & Laperche,Y. In vitro differentiation of WB-F344 rat liver epithelial cells into the biliary lineage. *Differentiation* **69**, 209-215 (2002).

173. Coleman,W.B. *et al.* Evaluation of the differentiation potential of WB-F344 rat liver epithelial stem-like cells in vivo. Differentiation to hepatocytes after transplantation into dipeptidylpeptidase-IV-deficient rat liver. *Am. J. Pathol.* **151**, 353-359 (1997).

BIOGRAPHICAL SKETCH

Jennifer Marie LaPlante was born in St. Louis, MO. She attended St. Elizabeth's of Hungary School until seventh grade (1990) when she moved to Woodstock, IL. Here she finished grade school at St. Mary's of Woodstock and completed high school at Marian Central Catholic High School. During high school she was actively involved in sports achieving varsity letters in volleyball, softball, and basketball. As editor in chief of the school newspaper, a member of the National Honor Society, the leader of academic clubs such as Math team and J.E.T.S., and a straight "A" student, she was rewarded with a Presidential Scholarship to Ohio Wesleyan University (OWU).

While attending OWU Jennifer was an active member of her sorority, Delta Delta Delta and involved in various choral groups. She was inducted into the Omicron Delta Kappa, Phi Beta Kappa, Phi Sigma, and Phi Sigma Iota Societies as well as a member of the Deans list. Jennifer was awarded honorary admission into the Sigma Xi society based on her senior thesis work sequencing the 16s rRNA isolated from the intestinal contents of the Licking County American Mastodont (*Mammut americanum*; NCBI Accession #s AF279699 and AF279699.1). During the semester of the fall of 1998, she studied abroad in Salamanca, Spain, and in 2000, Jennifer graduated with a Bachelor of Arts in Botany/Microbiology with a concentration in genetics and a minor in Spanish.

Jennifer was accepted into the University of Florida MD-PhD program beginning the fall of 2000. During her two years of didactic medical school work, Jennifer was active in numerous medical associations and volunteer organizations including the AMA-MSS, AMSA, and the student run Equal Access Volunteer Health Clinic. Jennifer served the AMA nationally in various positions including serving as the medical student liaison to the NBME for 3 years.

After completing her medical school didactic years as well as the USMLE step I exam, Jennifer began her graduate studies in the University of Florida Interdisciplinary Program. Jennifer studied under the tutelage of Dr. Bryon E. Petersen in the University of Florida Department of Pathology during her graduate work. Her project consisted of discerning the role of Wnt1 in oval cell based liver regeneration. Jennifer presented a portion of her research at the Washington, DC, 2006 national convention of the American Association for Cancer Research (AACR).

Jennifer then married Matthew James Williams on July 17th, 2006. She completed her dissertation requirements and returned to her clinical studies in order to complete her medical degree at the University of Florida.